Spin in fractional quantum Hall systems

Karel Výborný[*12]

[1] 1. Institut für Theoretische Physik, Universität Hamburg, Jungiusstr. 9, 20355 Hamburg, Germany

[2] Institute of Physics, Academy of Sciences of the Czech Republic, Cukrovarnická 10, 16253 Praha 6, Czech Republic

Key words fractional quantum Hall systems, quantum Hall ferromagnets, magnetic inhomogeneities

PACS 73.43.Cd,Nq, 71.10.-w, 75.30.-m

A system at filling factor $2/3$ could be a candidate for a quantum Hall ferromagnet at integer filling factor of composite fermions. Using exact diagonalization with electrons on a torus we study the transition from the singlet ground state to the polarized ground state at this filling and look for signatures of quantum Hall ferromagnetism. Differences between the fractional and corresponding integer systems are emphasised. Most interestingly, we find around the transition a low excited half-polarized state which might become the ground state in the thermodynamical limit. We study its structure and compare it to the singlet and polarized ground states. A new interpretation of the singlet state is suggested and comparison of the filling factors $2/3$ and $2/5$ is presented. Adding magnetic inhomogeneities into the system we investigate the stability of all the three involved states and the tendency to build up domains like in conventional ferromagnets.

Contents

[*] e-mail: vybornyk@fzu.cz, Phone: +420 220 318 459, Fax: +420 233 343 184

Similar to superconductivity, the *fractional quantum Hall effect* [14, 79] is a unique field, where correlations between electrons give rise to macroscopically well observable ground states which we would not expect on the level of a Hartree-Fock approximation. The correlations are introduced by interelectronic interaction and, contrary to atomic physics for instance, the quantization of single-electron energy levels is a consequence of the strong magnetic field (Landau levels) and of the suppressed motion in the direction of the field (quasi two-dimensional systems). The latter phenomenon leads to another unusual feature of the fractional quantum Hall systems: the many-electron states in a non-interacting system are highly (macroscopically) degenerate, since all electrons within one Landau level have the same energy. In particular, for filling factors below one, where it is useful to be restricted to the lowest Landau level, *all* many-electron states have the same energy. Now, the effect of interactions between electrons cannot be investigated by perturbation theory, as there is no single ground state to start with or, in other words, there is no small parameter in which we could expand the perturbation series. Since energy spacing between the many-body states is zero, the interaction is never a small perturbation, regardless of how weak it is. This fact renders the fractional quantum Hall systems unique from the theoretical point of view and makes completely novel types of quantum-mechanical ground states possible. The best known of these are the incompressible quantum liquids.

Quantum Hall ferromagnetism was one of the companions of the *integer* quantum Hall effect (Subsect. 1.6). The observed long-range spin order can be explained by exchange energy gain in the ferromagnetic state and hence Hartree-Fock models are sufficient to describe the ongoing physics. However, new experimental publications appeared in late nineties. Phenomena reminiscent of ferromagnetism have also been observed in the *fractional* quantum Hall regime, being most noticeable at filling factors $2/3$ and $2/5$ ([45, 15]). In this situation, the Hartree-Fock approximation is no longer acceptable, the spin-ordered states are highly correlated. This area is not very well explored. Instead of a lattice of spins which are all pointing in the same direction, here, we are dealing with itinerant electrons which are either in a fully polarized or in a spin singlet state (Subsect. 2.1). Although both states are incompressible, their structure is quite different [13].

How far can we extend the analogy between an Ising spin-lattice ferromagnet and fractional quantum Hall systems where two ground states with different spin order compete with each other? This was the central question of this thesis. There are several fundamental differences between these two systems. The latter one is itinerant and the liquid-like ground state is stable only owing to correlations while, in a spin-lattice, the electrons are spatially fixed and the ferromagnetism occurs also in classical systems with suitable site-to-site coupling. By observing e.g. hysteresis in magnetotransport, experimentators have provided a lot of evidence that the two phenomena are indeed very closely related [71, 70, 43], on the other hand, observations without an analogy to usual Ising systems have been reported too [46].

Before we start the theoretical introduction, let us summarize the basic experimental facts. At filling factors $2/3$ and $2/5$ two different ground states may appear. Depending on the ratio between the Zeeman to Coulomb energy, E_Z/E_C, it is the fully spin polarized ($E_Z/E_C \to \infty$) or the spin-singlet one ($E_Z/E_C \to 0$) [46]. This transition can be accomplished (a) by varying the electron density at a fixed filling factor [36], (b) by tilting the magnetic field [16, 21] or (c) by applying hydrostatic pressure which modifies the bulk g-factor [50].

When the two ground states are brought to degeneracy, transport experiments show hysteresis, time-dependent resistance with Barkhausen jumps [11] (see Refs. above) and huge longitudinal magnetoresistance [45] which is related to the spin polarization of the ion lattice of the hosting GaAs (NMR experiments [44, 19]). These could be related to formation of spatial domains of the two ferromagnetic ground states, even though surface acoustic wave experiments could not confirm this [20]. On the other hand, optical experiments [46, 24], suggest that a half-polarized ground state occurs near the transition.

1 Theoretical basics

1.1 One electron in magnetic field

When the mutual interactions are left aside, electrons in a plane subject to homogeneous perpendicular magnetic field B fill the macroscopically degenerate equidistant Landau levels (LLs) with energies $E = (n + \frac{1}{2})\hbar\omega$, $n = 0, 1, 2, \ldots$ The degeneracy of all the levels is the same, and it increases proportionally to the magnetic field. Therefore, occupancy of the Landau levels, the *filling factor*, depends both on the number of electrons N_e (per area L^2) and on B:

$$\nu = \frac{N_e/L^2}{eB/h} = \frac{N_e}{L^2/(2\pi\ell_0^2)} = \frac{N_e}{(BL^2)/(h/e)} = \frac{N_e}{\Phi/\Phi_0} = \frac{N_e}{N_m}\,. \tag{1}$$

Note that this ν, i.e. number of Landau levels occupied in the ground state is equal to the *inverse* number of magnetic flux quanta $\Phi_0 = h/e$ per electron in the system (the second last expression in (1).

These facts can easily be obtained by solving the single-electron Schrödinger equation with Hamiltonian

$$H_0 = \frac{1}{2m}(\mathsf{p} + e\mathsf{A})^2\,, \qquad \nabla \times \mathsf{A} = (0, 0, B)\,, \tag{2}$$

a particularly nice and understandable example of this calculation is given by Murthy and Shankar [56]. Suitable energy and length units are the cyclotron energy $\hbar\omega = \hbar eB/m$ and the magnetic length $\sqrt{\hbar/eB}$ denoted by ℓ_0.

Let us now focus on the lowest Landau level. There are $eB/h\cdot$ states per unit area having the same energy $\hbar\omega/2$ and infinitely many possibilities of constructing a basis of this space. Choosing the Landau (symmetric) gauge in (2) which is translationally symmetric in one direction (rotationally symmetric around the origin) we are lead to the following bases

$$\text{Landau: } \mathsf{A} = (0, Bx, 0)\,, \qquad \psi_{k_y}(x, y) = \exp(-ik_y y)\exp[-(x + k_y)^2/2\ell_0^2]\,, \qquad k_y/(2\pi/L) = 0, 1, 2, \ldots \tag{3}$$

$$\text{symmetric: } \mathsf{A} = \frac{1}{2}(y, -x, 0)\,, \qquad \psi_m(z) = z^m \exp(-|z|^2/4\ell_0^2)\,, \quad m = 0, 1, 2, \ldots \tag{4}$$

Especially for the latter basis, formulae are often more transparent if we use a complex variable $z = x + iy$ rather than x, y separately to address the points in the plane.

1.1.1 Magnetic translations

A plane with perpendicular homogeneous magnetic field is obviously translationally invariant. However, spatial translations applied to the Hamiltonian may alter the gauge even though they leave the magnetic field unchanged. Operators which conserve also the gauge (and which therefore commute with H_0) are the *magnetic translations* [83, 84]. These operators will thus replace the ordinary translations applicable to systems without magnetic field.

Magnetic translation operators depend on the choice of the gauge, in particular for the Landau gauge (3)

$$\mathsf{u} = (u_1, u_2)\,: \qquad T(\mathsf{u}) = \exp(-iu_x y/\ell_0^2)t(\mathsf{u})\,, \tag{5}$$

where $t(\mathsf{u})$ is the ordinary translation operator $\exp(i\mathsf{u}\cdot\mathsf{p}/\hbar)$. General explicit formula for any gauge can be found e.g. in the article of Haldane and Rezayi [32].

Note, that ordinary and magnetic translations (5) coincide for $u_x = 0$, exactly as a wavefunction in the form (3) remains unchanged up to a constant phase under the replacement $y \to y + u_y$. For $\mathsf{u} = (u_x, 0)$ this is not the case and that is why we must resort to *magnetic* translations.

1.2 What to do when Coulomb interaction comes into play

The quantum mechanical solution of one electron – or many non-interacting electrons in a plane subject to a perpendicular magnetic field is at the root of the integer quantum Hall effect. The basic fact is that for integer filling factors, *any*, even arbitrarily small excitation costs at least the energy $\hbar\omega$. This gap renders the ground state incompressible. The fractional quantum Hall effect cannot be explained in this picture. For instance at filling factor $\nu = 1/3$, a non-interacting system has a manyfold degenerate ground state, or, some excitations cost zero energy (those which involve only rearrangement of electrons within the lowest LL), and the ground state should be compressible. Today it is well established that the effect is due to electron-electron interactions which select among those states one special ground state and separate it by a gap from the excitations.

Now, the Hamiltonian of the many-electron system consists of two terms: the kinetic energy (leading to Landau level quantization) and the electron-electron interaction.

$$H = \sum_{i=1}^{N_e} \frac{\boldsymbol{p}_i^2}{2m} + \frac{e^2}{4\pi\varepsilon}\frac{1}{2}\sum_{i\neq j}\frac{1}{|\boldsymbol{r}_i - \boldsymbol{r}_j|} \tag{6}$$

Consider some particular filling factor, $\nu = 1/3$ for example, and let us vary the magnetic field. Since $\nu = n/(2\pi\ell_0^2) = n/(eB/\hbar)$, this implies changing the electron density n simultaneously. The kinetic energy will change proportionally to $\hbar\omega \propto B$. The interaction energy on the other hand scales with $1/a \propto \sqrt{B}$, as the mean electron-electron distance a is proportional to the magnetic length $a = \sqrt{1/n} = \sqrt{1/(\nu eB/\hbar)} \propto \ell_0$ (for a more thorough discussion see Yoshioka [79], Chap. 4)

In the high field limit we can therefore expect the Coulomb interaction to be a small perturbation which lifts the degeneracy of Landau levels. Looking for a (high-B) ground state at some particular $\nu < 1$ we can therefore omit the higher Landau levels and study only states *within the lowest Landau level*. This model gives qualitatively correct predictions (for high B) and the inclusion of the Landau level mixing leads only to quantitative corrections (e.g. in the ground state energy, see Chakraborty and Pietiläinen [14]).

1.2.1 Ground states: analytical many-body wavefunctions

It is very surprising that even though we now handle a *many-body* Hamiltonian (6), there are still *analytic* (correlated) wavefunctions which describe the ground state at some special filling factors. The best known example was suggested by R. B. Laughlin [48] earning him the Nobel Prize:

$$\Psi_L(z_1, \ldots, z_n) = \exp\big(-(|z_1|^2 + \ldots + |z_n|^2)/4\ell_0^2\big)\prod\nolimits_{i<j}(z_i - z_j)^3\,. \tag{7}$$

There are several beautiful physical arguments why this wavefunction must be the ground state at $\nu = 1/3$ (in fact, an excellent approximation to it, see Subsec. 1.3). These are explained in other more detailed publications [79] (Chap. 4), [14, 30]. Let us mention here only two basic ideas about the interpretation of Ψ_L.

First, the $(z_i - z_j)^3$ term makes the Laughlin wavefunction isotropic and translationally invariant. More detailed studies (density-density correlations, see Subsec. 2.1) suggest that it resembles a liquid. Second, Ψ_L resembles Ψ_1, the wavefunction of completely occupied lowest Landau level which is the same as (7), only with $(z_i - z_j)^3$ replaced by $(z_i - z_j)$. In fact,

$$\nu = 1\text{, GS: } \Psi_1 \propto \prod_{i<j}(z_i - z_j) \overset{\times\Pi_{i<j}(z_i - z_j)^2}{\longrightarrow} \nu = \tfrac{1}{3}\text{, GS: } \Psi_L \propto \prod_{i<j}(z_i - z_j)^3\,.$$

Now consider a single electron in a state $\psi_m(z) \propto z^m$ (4). If we pierce the system by an infinitely thin solenoid at z_0 and pass two magnetic flux quanta adiabatically through it, this state will evolve into

$\psi_m(z)(z-z_0)^2$. This leads to the following interpretation. The Laughlin state is just the completely filled lowest Landau level, but the constituent particles are electrons with two attached magnetic flux quanta rather than bare electrons.

So far we have only spoken about the filling factor $\nu = 1/3$ and fully spin-polarized electrons. Generalizations of these concepts are possible also to systems where electrons are not fully spin polarized. Halperin proposed the following WFs [35]

$$\Phi_{mm'n}[z] = \prod_{i<j\leq N_\uparrow} (z_i - z_j)^m \prod_{k<l\leq N_\downarrow} (z'_k - z'_l)^{m'} \prod_{\substack{i\leq N_\uparrow \\ k\leq N_\downarrow}} (z_i - z'_k)^n \prod_{i,j} \exp(-|z_i|^2/4\ell_0^2) \exp(-|z'_j|^2/4\ell_0^2) \tag{8}$$

with m, m' odd. The state assumes $N_\uparrow$ ($N_\downarrow$) particles with spin up (down) and z_i (z'_j) describe their positions. The filling factors of the two components are

$$\nu_\uparrow = \frac{m'-n}{mm'-n^2}\,, \qquad \nu_\downarrow = \frac{m-n}{mm'-n^2}\,.$$

Thus, they describe a state at filling $\nu = \nu_\uparrow + \nu_\downarrow$ and polarization $p = (\nu_\uparrow - \nu_\downarrow)/\nu$. For example, the choice $m = m' = 3$ and $n = 2$ leads to the total filling factor $2/5$ and zero spin polarization ($\nu_\uparrow = \nu_d n$).

These analytical results will always be a good starting point for investigations going to regions where only numerical methods are possible. Before continuing, however, it must be emphasised, that wavefunctions in (7,8) are not the only analytical trial wavefunctions known in the lowest Landau level. A more detailed review can be found in [17] (MacDonald and Girvin).

1.3 Other types of electron-electron interactions

A model of *short-range interaction* (SRI) in fractional quantum Hall systems is the main issue of this section. We will explain how a general interaction $V(r)$ between two particles within the lowest Landau level (LL) can be represented by a set of *Haldane pseudopotentials* $\{V_m\}$ [30] and show how this concept makes it easier to study different classes of interaction. In particular, this discussion will unveil under what conditions the Laughlin wavefunction (7) becomes the exact many-body ground state.

1.3.1 Two particles, magnetic field and a general isotropic interaction

Let us consider two negatively charged particles in a plane subjected to a perpendicular magnetic field B. Assume that their interaction is described by a potential (energy) $V(r)$ which depends only on their mutual distance. Classically, when starting from rest, the particles would move along a straight line towards or away from each other were it not for the magnetic field. The Lorentz force bends their trajectories and makes them orbit around their centre-of-mass on a circular trajectory. In quantum mechanics, this circular motion is quantized just as in case of an electron orbiting around a hydrogen nucleus. *Roughly speaking*, only discrete separations r_m between the two particles are allowed. Interaction energies $V(r_m) = V_m$ rather than the full form $V(r)$, $r \in (0;\infty)$ fully determine the spectrum of a many-body system of particles interacting via $V(r)$.

Let us now follow this idea in more detail and derive the precise claims. The Hamiltonian for two particles reads

$$H = \frac{1}{2m}(\boldsymbol{p}_1 + |e|\boldsymbol{A}_1)^2 + \frac{1}{2m}(\boldsymbol{p}_2 + |e|\boldsymbol{A}_2)^2 + V(|\boldsymbol{r}_1 - \boldsymbol{r}_2|)\,. \tag{9}$$

Following Laughlin [49], we write it as a sum of the centre-of-mass (CM) and relative parts [$\boldsymbol{r}_{CM} = (\boldsymbol{r}_1 + \boldsymbol{r}_2)/2$, $\boldsymbol{r}_{rel} = (\boldsymbol{r}_1 - \boldsymbol{r}_2)/\sqrt{2}$]. Without $V(r_{rel})$, both parts will be equivalent to a single particle in

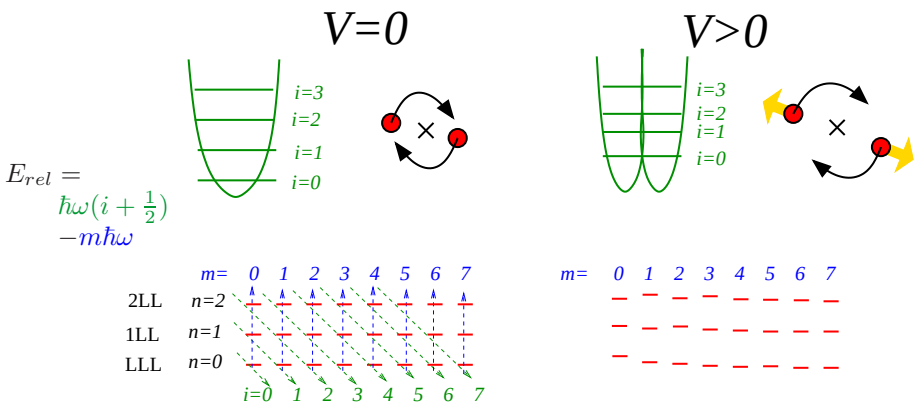

Fig. 1: Spectrum of one particle confined to a plane subject to a perpendicular magnetic field or, equivalently, the spectrum corresponding to the relative motion of two particles (H_{rel}). *Left:* without particle-particle interaction, the two terms, 'harmonic oscillator' (quantum number i) and 'angular momentum' (quantum number m) combine into degenerate Landau levels (quantum number n). *Right:* interaction lifts the degeneracy. If the interaction potential is small compared to the harmonic oscillator term (i.e. $\langle V\rangle \ll \hbar\omega$), Landau levels are roughly preserved. The energy levels V_m *within* the lowest Landau level (sorted according to $m = \langle L_z/\hbar\rangle$) are then the Haldane pseudopotentials.

a plane in magnetic field. Hence, a Landau level index ($N = n_{CM}$, $n = n_{rel}$) and an angular momentum ($M = m_{CM}$, $m = m_{rel}$) will be attributed to both parts. Out of these, N is fixed to zero (two-particle state within the lowest LL) and M is unimportant as it is merely tantamount to fixing the CM to some particular position in the plane. Eigenstates of the relative part will be sorted as shown in Fig. 1 on the left.

With $V(r_{rel})$ included, the relative part reads

$$H_{rel} = \underbrace{\frac{p_{rel}^2}{2m} + \frac{1}{8}\hbar\omega(r_{rel}/\ell_0)^2 - \frac{1}{2}\omega L_{rel}^z}_{H_{rel,kin}} + V(|r_{rel}|) \tag{10}$$

with L_{rel}^z denoting the (z-component of relative) angular momentum. This is the well known Fock-Darwin form, the standard usage of which is to describe one particle in a magnetic field and confining potential V. However, we will use it in a different way here: we consider $V(r)$ to be weak, and for example a repulsive $\propto 1/r$ potential, compared to the parabolic term in $H_{rel,kin}$. It is only our initial assumption that the interaction is much weaker than the cyclotron energy, $E_C \ll \hbar\omega$ (Subsec. 1.2).

Owing to $[H_{rel}, L_{rel}^z] = 0$, the eigenstates of H_{rel} can still be classified by angular momentum. Moreover, assuming the states of the lowest LL to have no admixtures from higher LLs ($E_C \ll \hbar\omega$), the eigenstates

$$\psi_{rel}^m(r,\varphi) = \exp(-im\varphi)\, r^m \exp(-r^2/4\ell_0^2)\,. \tag{11}$$

will not depend on $V(r_{rel})$ at all. This is a combined effect of the L_z symmetry and the requirement of analyticity (confinement to the lowest LL): angular part of the form $\exp(-im\varphi)$ implies $\psi^m(z) \propto z^m$.

On the other hand, energies of these states will shift differently for different m's (Fig. 1, right). The energy shift due to the interaction between particles is $V_m = \langle\psi_{rel}^m|V|\psi_{rel}^m\rangle$ in a state with relative angular momentum m. Since $r_m = \langle\psi_{rel}^m|r|\psi_{rel}^m\rangle = \ell_0\sqrt{2m+1}$ we can *roughly* estimate V_m to be $V(r_m)$.

The operator of any weak ($E_C \ll \hbar\omega$) interaction (in the lowest Landau level) can be then written in terms of its spectral decomposition

$$V(r_{rel}) = \sum_{m=0}^{\infty} |\psi_{rel}^m\rangle V_m \langle\psi_{rel}^m|\,.$$

The spectrum and eigenstates of a *many-body* system confined to the lowest Landau level and *interacting* by $V(r_{rel})$ is thus completely determined by the discrete set of numbers $\{V_m\}$.

The quantities $\{V_m\}$ are called *Haldane pseudopotentials*. They were first introduced in [30] in the context of interacting electrons on a sphere. Finally, we add two remarks.

Fermions and bosons. A careful reader may have noticed that we have spoken just about two *particles* so far. An additional constraint that e.g. (spatial part of the) wavefunction should be antisymmetric implies

$$\psi_{rel}(\mathsf{r}_1, \mathsf{r}_2) = -\psi_{rel}(\mathsf{r}_2, \mathsf{r}_1) \qquad \Rightarrow \qquad \psi_{rel}(r, \varphi) = -\psi_{rel}(r, -\varphi)\,.$$

Therefore, only the states with m odd (11) are allowed in the case of two electrons with the same spin (where a symmetric spinor part implies an antisymmetric orbital part of the wavefunction). In other words: only the values of $V_1, V_3, \ldots$ are needed when we describe motion of fully spin polarized electrons.

Uniqueness. If $V(r)$ is given, the pseudopotentials V_m are determined uniquely. However, the opposite is not true: knowing only the values of V_m, we cannot reconstruct the full form of $V(r)$.

1.3.2 Particular values of Haldane pseudopotentials for the Coulomb interaction

The ideas above are not valid exclusively for the lowest Landau level.

Let us consider a numerical example for electrons in a plane, one of them located in *arbitrary* Landau level n_1 and another in n_2. Their relative angular momentum be m. Given these three numbers, the state is uniquely defined, up to the center-of-mass part of the wavefunction, as we have already stated. Assuming interaction of the form $V(q)$ (in the Fourier space), their interaction energy can be written as [60]

$$V_m^{n_1,n_2} = \int_0^\infty q\mathrm{d}q V(q) L_{n_1}(q^2/2) L_{n_2}(q^2/2) L_m(q^2) \exp(-q^2)\,. \tag{12}$$

The *Laguerre polynomials* are defined by $L_n(x) = (1/n!)[x^n e^{-x}]^{(n)} e^x$. For the case of Coulomb interaction, $V(q) = \alpha/|q|$, the integrals in (12) can be evaluated (easily and) analytically. Figure 2 shows their values for the cases (a) both particles in the Lowest Landau level ($n = 0$), (b) both particles in the first Landau level ($n = 1$) and (c) one in the lowest and one in the first Landau level.

For $n_1 = n_2 = 0$ the coefficients V_m decay monotonically with increasing m, exactly as the Coulomb energy does with increasing distance. The non-monotonic structure of V_m for the case of particles in the first Landau level is due to the additional structure of wavefunctions in higher Landau levels (e.g. a node at $r = 0$ for $n = 1$).

1.3.3 Model interactions: hard core, hollow core

Why is a hard-core interaction (*short-range interaction*) important for the physics of the lowest Landau level?

There are three reasons: (i) it is the strongest part of the Coulomb interaction, (ii) the Laughlin wavefunction is an exact (zero energy) gapped ground state for this interaction and (iii) the ground state changes only little if the other terms of the Coulomb interaction are considered.

Let us discuss this in more detail. For the purposes of this paper, the short-range interaction (SRI) for *spin polarized electrons* is defined by the Haldane pseudopotentials

$$\text{short-range int. (spin polarized electrons): } \{V_1, V_3, V_5, \ldots\} = \{1, 0, 0, \ldots\}\,. \tag{13}$$

For the *Coulomb* interaction, Fig. 2a, V_1 is indeed the strongest pseudopotential.

On the other hand, considering the Laughlin wavefunction of N particles (7), any pair of electrons in it is in a state with relative angular momentum $m = 3$: owing to factors $(z_i - z_j)^3$. As there are no pairs

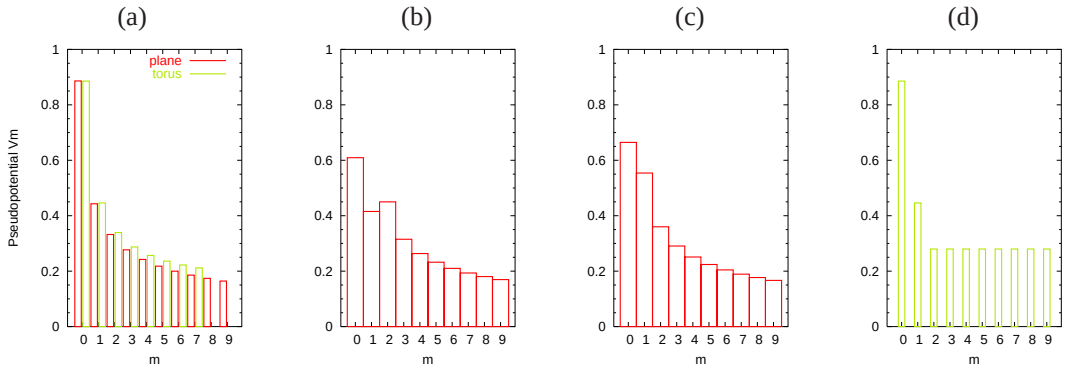

Fig. 2: Values of Haldane pseudopotentials V_m for Coulomb-interacting electrons (a-c): between two particles (a) both in the lowest Landau level, $(n_1, n_2) = (0, 0)$, (b) both in the first Landau level, $(n_1, n_2) = (1, 1)$, and (c) one in the lowest and the second in the first Landau level, $(n_1, n_2) = (1, 0)$. The pseudopotentials referring to electrons in a plane (a,b,c) are 'universal', those related to electrons on a torus (a,d) depend on its size (here $N_m = 30$, Subsec. 1.5.1). Values of $\{V_m\}$ chosen for as a model for short-range interaction in this work are shown in (d).

with angular momentum $m = 1$, the total energy of this state will be $V_1 \cdot 0 + V_3 \cdot N(N-1)/2 = 0$ for SRI. Also, this state is rigid: any excitation of this state must remove the triple zero from some of the electrons (leaving only a single zero required by antisymmetry) thereby creating some pairs with $m = 1$. This implies a finite excitation gap.

These are analytical results. A surprising numerical result is that the many-body ground state changes only slightly if other pseudopotentials $V_3, V_5, \ldots$ are 'turned on' up to their Coulomb values (Fig. 2a). This has been confirmed by Haldane and Rezayi [33] (later also by others, e.g. [23]) by calculating the overlap between the real ground state and the Laughlin state for different sets of V_m. It is also shown in [33] that if V_1 is lowered beyond some critical value (while keeping other pseudopotentials on their Coulomb values), the gap collapses rendering the ground state compressible. These observations have been systematised by Wójs and Quinn [75]: they argued that both Coulomb and short-range (13) interactions belong to the same class of *superharmonic* pseudopotentials where particles try to avoid low m pair states, implying the Laughlin ground state. A drastic change in the ground state occurs first when we leave the mentioned class of interactions. The 'superharmonicity' means roughly that V_m decays fast enough with growing m [75]. The aforementioned collapse of the gap is then no longer surprising as the decreased value of V_1 will eventually violate potentials superharmonicity between $m = 1$ and 3.

An advantageous property of the interaction (13) is that it is effectively non-parametric, the only present parameter V_1 determines only the overall scaling of the energy scale within the lowest Landau level.

These results can be summarized by stating that the short-range interaction is the component of a realistic interaction which determines almost completely the properties of the $\nu = 1/m$ spin-polarized ground states.

Obviously, for non-fully spin polarized systems it is not possible to keep $V_1 \neq 0$ only. Electrons with equal spin are still closest in the state $m = 1$ (with energy V_1), electrons of unlike spin however are closest in the state $m = 0$ with energy V_0. Such a model is obviously not as elegant as in the former case, it contains two parameters V_0, V_1 whose ratio cannot be factored out of the Hamiltonian. An alternative might be the potential

$$\{V_0, V_1, V_2, \ldots\} = \{\infty, 1, 0, 0, 0, \ldots\}\,. \tag{14}$$

Another typical model potential presented by Haldane and Rezayi [34] was inspired by the low value of V_0 in the first Landau level compared to the lowest Landau level (Fig. 2). They suggested the hollow-core

	V_0	V_1	V_2	V_3	V_4	V_5
q^0 $(k=0)$	$1\cdot 2^0$	0	0	0	0	0
q^2 $(k=1)$	$1\cdot 2^1$	$-1\cdot 2^1$	0	0	0	0
q^4 $(k=2)$	$2\cdot 2^2$	$-4\cdot 2^2$	$2\cdot 2^2$	0	0	0
q^6 $(k=3)$	$6\cdot 2^3$	$-18\cdot 2^3$	$18\cdot 2^3$	$-6\cdot 2^3$	0	0
q^8 $(k=4)$	$24\cdot 2^4$	$-96\cdot 2^4$	$144\cdot 2^4$	$-96\cdot 2^4$	$24\cdot 2^4$	0

Table 1: Values of Haldane pseudopotentials corresponding to particle-particle interactions of the type $V(q)=q^{2k}$. These values are additive, e.g. $V(q)=-\frac{1}{2}q^2+1$ corresponds to the 'hollow core interaction': $\{V_m\}=\{0,1,0,0,0,\ldots\}$.

potential

$$\text{hollow-core interaction: } \{V_0,V_1,V_2,\ldots\}=\{0,1,0,0,0,\ldots\}\,.$$

and tried to explain the even-denominator fractional quantum Hall effect at $\nu=\frac{5}{2}$ using this interaction.

1.3.4 An alternative definition of Haldane pseudopotentials

Haldane introduced the quantities V_m originally for interacting electrons on a sphere [30]. In that case, or for electrons in a plane, m can be identified with the relative angular momentum of the electron pair, having in mind that m is closely related to the average separation between the particles increases. In contrast to that, rotational symmetry of the configuration space is lost on a torus and angular momentum is no longer a good quantum number. Here we will introduce an alternative definition of Haldane pseudopotentials which is applicable also for particles on a torus [74].

First, recall that matrix elements of the *Coulomb* interaction on a torus can be conveniently evaluated in Fourier space (Subsec. 1.5.3) where

$$V(\boldsymbol{r})=e^2/|\boldsymbol{r}| \qquad \Rightarrow \qquad V(\boldsymbol{q})=e^2/|\boldsymbol{q}|\,.$$

Second, consider a general (radial, bounded) interaction with its Fourier transforms $V=V(|\boldsymbol{q}|)$ and expand $V(|\boldsymbol{q}|)$ into a Taylor series. Owing to $V(\boldsymbol{r})=V(-\boldsymbol{r})=V(|\boldsymbol{r}|)$, the series will be free of odd powers q^{2k+1}. Now, go back to the direct space and use $\mathcal{F}[f(r)]^{(k)}=(iq)^k\mathcal{F}f(r)$

$$V(q)=\widetilde{v}_0+\widetilde{v}_2q^2+\widetilde{v}_4q^4+\ldots \qquad \Rightarrow \qquad V(r)=\widetilde{v}_0\delta(r)-\widetilde{v}_2\nabla^2\delta(r)+\widetilde{v}_4\nabla^4\delta(r)-\ldots\,. \quad (15)$$

The coefficients $\widetilde{v}_i$ now fully characterize the particle-particle interaction. In an extension to the article of Trugman *et al.* [74], let us show how to translate them into V_m's, i.e. interaction energy of the two-particle state in a plane (or on a sphere) with relative angular momentum m.

For the evaluation of $V_m=\langle\psi_m|V(r)|\psi_m\rangle$, let us take the functions ψ^m_{rel} from the planar system, (11) plus normalization. If $V(q)=q^{2k}$ then

$$V_m=(-1)^k\int \mathrm{d}r^2\psi_m\psi_m^*\nabla^{2k}\delta(\boldsymbol{r})=\frac{(-1)^k}{2^m m!}\left[\left(\frac{1}{r}\frac{\mathrm{d}}{\mathrm{d}r}r\frac{\mathrm{d}}{\mathrm{d}r}\right)^k r^{2m}e^{-r^2/2}\right]_{r=0} \quad (16)$$

This is a unique prescription of how an interaction of the type $V(q)=q^{2k}$ can be transcribed into the terms of V_m. Table 1 contains these coefficients for several lowest powers of q. Note that $V_m=0$ for $m>k$.

In conclusion, an interaction potential defined by some particular set of values of Haldane pseudopotentials V_m can be recalculated into the coefficients $\widetilde{v}_i$ in (15) (Taylor series of $V(q)$) using Table 1 or, more generally using (16).

Again, several remarks should be made.

(1) The expansion in (15), being first suggested by Trugman and Kivelson [74], looks unusual. In the distributional sense, we say that a non-zero ranged potential $V(r)$ can be written as a sum of terms with 'zero range'.

Instead of a δ-function imagine rather a sharp peaked function δ_b, a Lorentzian of width b, for instance. Functions $\nabla^{2k}\delta_b(\boldsymbol{r})$ will then have 'the longer the range the higher the k is': it is instructive to draw a sketch of the first few functions $(\delta_b)^{(2k)}$ and consider as 'range' the position of the local extreme which is the most distant from the origin. In this sense, (15) is an expansion of $V(q)$ in terms of 'increasing ranges'.

(2) When calculating the Coulomb matrix elements for particles on a torus (Subsec. 1.5.3), we do not use the full function $V(q)$ but only its values in discrete 'lattice' points $\boldsymbol{q}$. This is obviously due to the periodic boundary conditions. In particular, $\boldsymbol{q} = 0$ is missing among these points.

Thus, we need not worry about the long-rangedness of the Coulomb potential, $V(q \to 0) \to \infty$ which renders it unexpandable into a power series of q. Instead of $1/q$ we may imagine to have considered any other polynomial in q which matches the values of $1/q$ at the 'lattice' points. Both interactions must lead to the same results.

(3) *Example:* consider two electrons in the lowest Landau level interacting via $V(q) = \alpha q^2$. Eigenstates sorted according the to increasing value of the particle-particle distance $\langle r\rangle$ may be indexed by an integer, say m. The state $m = 0$ will have an energy of $-\alpha$, the state $m = 1$ will have an energy of α and all other states (with larger interparticle separation) will have zero energy.

The state with $m = 0$ will have a symmetric wavefunction and will be thus prohibited for electrons with equal spins. Thus there will be only one state with non-zero energy for this case and it is the state with the lowest interparticle separation. The potential $V(q) = \alpha q^2$ defines therefore a hard-core interaction.

1.3.5 Short-range interaction on a torus

The decomposition of the Coulomb interaction (in the lowest LL) into the set of Haldane pseudopotentials has already been shown in Fig. 2. This is also the spectrum of two Coulomb-interacting particles on a sphere.

Let us now consider a pair of particles on a torus, Fig. 2a. The index m is no longer the angular momentum of the pair as this is not a good quantum number. The wavefunctions $\psi^m_{rel}(z) \propto z^m \exp(-|z|^2/4\ell_0^2)$ in (11) must be modified, in order to comply with the periodic boundary conditions.

In Fig. 3 we show some of the wavefunctions corresponding to the relative motion on a torus of size $N_m = 30$ ($= ab/2\pi\ell_0^2$, Subsec. 1.5.1). We will denote them simply by ψ^m, $m = 0, 1, \ldots, m_{max}$ and skip all other indices which would be appropriate, e.g. to indicate that they depend on the size of the torus ($a \times a$). Even though these states are more complicated than those in (11), they can still be sorted according to growing values of $r_m = \langle\psi^m|r|\psi^m\rangle$. It is not surprising that the states ψ^m for low m ($\ll N_m$), Fig. 3b, look very similar to the eigenstates of angular momentum m for infinite systems (11). First when r_m becomes comparable to the system size, deviations from the circular form of $|\psi|^2$ occur (middle column of Fig. 3b). It is an intriguing property of the periodic boundary conditions that the states with very high m look very similar to those with very low m. If we fix one electron to $\boldsymbol{r} = (0, 0)$, then the second electron orbits around $(0, 0)$ at a distance r_m in the state ψ^m, whereas in the state $\psi^{m_{max}-m}$ it orbits around $(a/2, a/2)$ at the same distance. This can be seen by comparing the left and right columns of Fig. 3b.

Now, with ψ^m, as a substitute for the relative angular momentum eigenstates, we can define Haldane pseudopotentials on a torus by $V_m = \langle\psi^m|V(r_{rel})|\psi^m\rangle$. Their values (Fig. 3a) are almost equal to V_m in a plane, as long as ψ^m is not affected by the periodic boundary conditions (Fig. 2a) i.e. for small values of m.

A reasonable model mimicking the short-range interaction keeps the first two energies of the spectrum in Fig. 2, i.e. the pseudopotentials V_0, V_1 at their 'Coulomb' values while setting the other ones to zero.

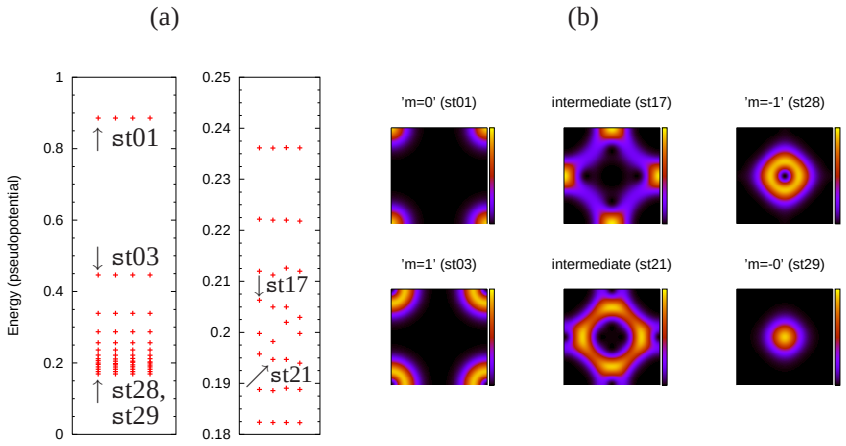

Fig. 3: Two-particle eigenstates of Coulomb-interacting particles in the lowest LL confined to a torus. States are shown irrespective of the symmetry or antisymmetry of the wavefunction. *Left:* spectrum (horizontal axis has no meaning: levels are 'randomly' distributed into four groups in order to show degeneracies). *Right:* relative part of the wavefunction, $|\psi^m(r_{rel})|^2$, for several states. Here, $r_{rel} = 0$ corresponds to the corner of the square (the four corners are identical due to periodic boundary conditions). Some of these states resemble the eigenstates of relative angular momentum, see text.

Table 1 gives a prescription how to encode such an interaction into $V(q)$. We thus arrive at an interaction potential defined by $V(q) = 0.34q^2 - 1.51$ which is used throughout this work to model a short-range interaction unless something else is explicitly stated.

1.4 Composite fermion theories

Let us recall the observation from Subsec. 1.2: three zeroes are bound to each electron in the Laughlin state Ψ_L. A good way to see this is to fix the positions of $z_2, \ldots, z_n$ and use the last 'free' coordinate z_1 to inspect (the zeros of) the wavefunction. One zero is required by the Pauli principle (when $z_1 = z_2$, the wavefunction must vanish), the others are 'voluntary'.

Whenever an electron goes once around a zero in Ψ_L, the wavefunction acquires a phase equal to the Aharonov-Bohm phase corresponding to one magnetic flux quantum. From this point of view, the Laughlin state can be interpreted as the $\nu = 1$ state where two magnetic flux quanta are attached to each electron. These objects (electron dressed by two flux quanta) are called *composite fermions* (CF). Note however that the precise definition of a composite fermion may vary in different theories as will be explained below.

Intuitively, this concept explains the existence of a gapped ground state at filling factor $\nu = 1/3$. Originally, there are *three* flux quanta per electron (1) and the huge Hilbert space of many-electron states in the lowest Landau level is completely degenerate without interaction. In other words, we expect no gap without interaction. If we now assume, that the Coulomb interaction leads to the formation of composite objects, an electron and *two* flux quanta, then there remains only *one* free flux quantum per CF. This in turn implies the filling factor of $\nu_{CF} = 1$ for CF (1). We know that in this case the ground state of particles obeys Fermi statistics (see comment [1]) and is gapped. If a Landau level is completely filled, then any, even infinitesimal, excitation requires promoting at least one CF into a higher CF Landau level which costs the finite energy $\geq \hbar\omega_{CF}$. Now let us describe some of the current composite fermion theories in a little more detail.

1.4.1 Chern-Simons transformation

Looking at the Laughlin wavefunction in the way sketched above, we might find it reasonable to incorporate the flux attachment into the Hamiltonian.

The Chern-Simons (CS) transformation is just a gauge transformation of the magnetic field

$$\mathsf{a}_{CS}(\mathsf{r}) = \alpha\Phi_0 \int \mathrm{d}^2 r_1 \frac{\mathsf{e}_z \times (\mathsf{r} - \mathsf{r}_1)}{|\mathsf{r} - \mathsf{r}_1|^2} \Psi^\dagger(\mathsf{r}_1)\Psi(\mathsf{r}_1)\,. \tag{17}$$

It does not change the magnetic field ('gauge transformation') felt by the electrons only owing to the fact that two electrons cannot be simultaneously on the same place (see comment [2]). The price for this is that the transformation is singular, a_{CS} diverges for $\mathsf{r} = \mathsf{r}_i$. The objects $\Psi^\dagger(\mathsf{r})$ are the one-electron field operators and α is the number of attached magnetic fluxes.

After this transformation the full Hamiltonian

$$H = \frac{1}{2m} \int \mathrm{d}^2 \mathsf{r}\, \Psi^\dagger(\mathsf{r}) \left[-i\hbar\nabla_r + e\mathsf{A}(\mathsf{r}) - e\mathsf{a}_{CS}(\mathsf{r})\right]^2 \Psi(\mathsf{r}) \tag{18}$$

contains – apart from one-particle terms – two-particle terms (those containing a_{CS}) and also three-particle terms $\Psi^\dagger(\mathsf{r})\Psi(\mathsf{r})\Psi^\dagger(\mathsf{r}_1)\Psi(\mathsf{r}_1)\Psi^\dagger(\mathsf{r}_2)\Psi(\mathsf{r}_2)$ (they originate from a_{CS}^2). The CS transformation alone thus does not really simplify the original Hamiltonian.

A mean field approximation can be made at this point where the density operator $\Psi^\dagger(\mathsf{r}_1)\Psi(\mathsf{r}_1)$ in a_{CS} is replaced by the mean value n_S. We arrive at a single particle problem with an effective magnetic field $B_{CF} = B - \alpha\phi_0 n_S$. In illustrative terms:

	CS transf.		mean field	
a many-body system at $\nu = 1/3$	$\longrightarrow$	a very complicated many-body problem at $\nu = 1/3$	$\longrightarrow$	a simple one-particle problem at $\nu = 1$

The final one-particle problem at $\nu = 1$ has a non-degenerate ground state, the lowest Landau level fully occupied by CF. By means of this procedure we thus circumvented the original problem that the Coulomb interaction must select the ground state out of the vast number of degenerate many-body $\nu = 1/3$ states within the lowest LL.

A mean field approximation is not the only possible treatment of the Hamiltonian (18). However, theories beyond the mean field i.e. those treating fluctuations of the gauge field, are very complex [51].

Using the CS transformation we attach $2s = \alpha$ vortices (not zeroes) to each electron. In the mean field approximation the problem is equivalent to non-interacting particles in reduced magnetic field B_{CF} which then corresponds to a filling factor ν_{CF}. It turns out that many of the experimentally observed fractions ν (exceptions see in [59]) correspond to integer ν_{CF}. Let us conclude with an overview of relations between quantities referring to electrons and to CF, cf. (1).

$$B_{CF} = B(1 - 2s\nu) = B - 2sn_S\Phi_0\,, \qquad \ell^* \equiv \ell_{CF} = \frac{\ell_0}{\sqrt{1 - 2s\nu}}\,, \tag{19}$$

$$\frac{1}{\nu_{CF}} = \frac{1}{\nu} - 2s\,, \qquad \nu = \frac{p}{2sp+1}\,,\ (p, s \text{ integer}).$$

1.4.2 Composite fermions *à la* Jain

Compared to the Chern-Simons transformation, Jain chooses to go in some sense the same path but in the opposite direction [38, 39]. It starts with a wavefunction of particles (fermions) at integer filling $\nu_{CF} = p$, attaches s zeroes (*not* vortices) to each particle and, after projection into the lowest Landau level, it presents the result as a trial wavefunction for the ground state at filling $\nu = p/(2sp+1)$ (19). This procedure

$p_\uparrow$	1	2	3	-2	...	1	2	2	-1
$p_\downarrow$	0	0	0	0		1	1	2	-1
$p = p_\uparrow + p_\downarrow$	1	2	3	-2		2	3	4	-2
$\nu = p/(2sp+1)$	$\frac{1}{3}$	$\frac{2}{5}$	$\frac{3}{7}$	$\frac{2}{3}$		$\frac{2}{5}$	$\frac{3}{7}$	$\frac{4}{9}$	$\frac{2}{3}$
$S/\frac{n}{2}$	1	1	1	1		0	$\frac{1}{3}$	$\frac{1}{2}$	0

Table 2: The scheme of construction of Jain's wavefunctions for CF with two flux quanta attached: examples of composite fermion filling factors ($p_\uparrow$, $p_\downarrow$ are numbers of fully occupied spin up and spin down CF-Landau levels) and corresponding electronic filling factors.

reproduces exactly the Laughlin wavefunction and at other fractions it gives wavefunctions with very high overlap with ground states calculated numerically by exact diagonalization.

There are two central reasons why this approach is very popular. On one hand, it gives a simple single-particle picture of what is going on in the highly correlated many-body problem. On the other hand, it offers explicit formulae to work with since it is easy to write down a wavefunction of p full Landau levels. A very pleasant feature of this approach is that it allows to incorporate the spin of electrons easily [77]. Take $p_\uparrow$ of full Landau levels with spin up and $p_\downarrow$ of full Landau levels with spin down. These Landau levels are then called *composite fermion Landau levels*. The magnetic field felt by the CF, i.e. the field corresponding to filling factor $\nu_{CF} = p$ is called *effective magnetic field* B_{eff}. It is weaker than magnetic field B corresponding to the electronic state at ν (19).

Note, that the filling factors in (19) are all in range $\nu < \frac{1}{2}$. For $\frac{1}{2} < \nu < 1$, Jain *et al.* [77] suggest the idea of *antiparallel flux attachment*: the effective field B_{eff} is antiparallel to the real field B, however, the additional flux quanta are added in parallel to B i.e. antiparallel to B_{eff}. In terms of (19) this means $p \to -p$ or $\nu = p/(2sp-1)$.

An example of candidates for ground states and their polarization provided by Jain's composite fermion theory is given in Tab. 2 (see Chakraborty [13] for a review regarding ground states with various spins).

1.4.3 Composite fermions *à la* Shankar and Murthy (Hamiltonian theory)

The Hamiltonian theory of FQHE (Shankar and Murthy [56]) builds on previous works of Jain and those concerning the CS transformation, quoting words of its authors, it combines the strengths of the both theories.

It provides a projected Hamiltonian of the lowest Landau level which scales only with the Coulomb interaction. In addition to each electron a new independent object is introduced: a pseudovortex. Its definition on the level of commutation relations (Eq. 129 in [56]) assures, that if an electron goes around a pseudovortex, it picks up the phase of $2\pi\, 2s$ i.e. it has the same effect as an insertion of $2s$ flux quanta. Note however that it is *not* a zero of the wavefunction. The projected Hamiltonian is written in coordinates which are a combination of the electron and pseudovortex position (Eq. 138 in [56]). This combination is then called *composite fermion coordinate*.

For this Hamiltonian an ansatz for a ground state can be written down. At filling $\nu = p/(2sp+1)$, it is p Landau levels filled with CF. It is then possible to evaluate their Hartree-Fock energies.

The first substantial success of this theory is that it produces the correct scaling of spectra within the lowest Landau level ($\propto \sqrt{B}$). Compared to Jain's theory, it keeps track of the fact that the two fluxes (which sit exactly at each electron in the Laughlin state) can be only loosely bound to electrons. This is owing to the dynamical degree of freedom given to the pseudovortices. On the other hand, the electronic coordinates are actually the only really independent ones, for instance in the Laughlin wavefunction, all the zeroes

$(z_i - z_j)$ are expressed in terms of electronic coordinates. Thus, the price we must pay for the extension of the Hilbert space is that we must perform a projection to the space of physical states at the end.

Nevertheless, this does not seem to be a substantial problem and thus the Hamiltonian theory is probably the most advanced achievement in an effort to understand the many-body physics in the FQHE.

1.5 How to test the CF theory?

The concept of flux attachment (Sec. 1.4) provides a well-understandable model of the FQHE. However transparent it seems at the first look, predictions based on it must be tested against a model which contains less approximations. Exact diagonalization (ED) is a good choice for this purpose. In exchange for extensive numerics to perform, the only substantial approximation of the method is to take a finite instead of an infinite system.

The main part of this Section concerns the exact diagonalization (ED) [14]. It is definitely not the only numerical method used in the context of the FQHE. Some numerics is at the end of nearly any method as soon as many-body problems are concerned, be it a Hartree-Fock treatment of CFs or Monte Carlo simulations of the Laughlin state mapped onto a one-component plasma. O

We take the complete many-body Schrödinger equation but confine the interacting electrons moving actually in an infinite plane onto a compact (i.e. finite-sized) surface, possibly without edges. The standard choices are a sphere [30], a torus (square with periodic boundary conditions) [80] and a disc [48] (see Yoshioka [79] for an overview). Although these manifolds are locally flat and therefore with growing system size a convergence towards infinite-plane results can be expected, they all break some of the symmetries of the infinite plane. For instance, the sphere keeps the angular momentum while the torus retains the translational symmetry. In any case, the hope is that effects inflicted by the finite size can be separated from those generic to a two-dimensional electron gas. Another usual yet not necessary approximation is to neglect Landau level mixing, i.e. restriction to the lowest Landau level only. Also note, that there is a long way from an ideal 2D system which study here, to the experimental reality (impurities, effective mass approximation, finite thickness of the 2D electron gas etc.).

1.5.1 Torus boundary conditions

One possibility to model an infinite plane by a finite manifold without edges is a rectangle with area $a \cdot b$ with periodic boundary conditions (PBC). Topologically, this is the same as a torus, although it is better to stay with the former picture for the sake of twisted PBC, even if we sometimes use the word 'torus' as a shortcut for this model.

What are the single particle states of the lowest Landau level in this case? Recall (3) where single-particle states complying with translational symmetry along y are given

$$\psi_{0,k'_y}(x', y') = \exp(-ik'_y y') \exp[-(x' + k'_y)^2/2] \,,$$

primed variables are in units of magnetic length, $x' = x/\ell_0$, $k' = k\ell_0$. Periodic boundary conditions along y admit only discrete values of $k'_y = (2\pi\ell_0/b)j$ with j integer. The wavefunction is centered in the x-direction around $X_j = k_y\ell_0^2$ and if we require X_j to lie within $[0; a)$, we have $0 \leq -k'_y < a/\ell_0$. Thus, up to a sign,

$$0 \leq j < \frac{ab}{2\pi\ell_0^2} \equiv m \,. \tag{20}$$

Equation (1) with $L^2 = ab$ implies that $ab/2\pi\ell_0^2$ is equal to the number of magnetic flux quanta (Φ/Φ_0) which pass through the rectangle and by virtue of (20) it must be an integer. This brings us to the central insight that *there is only a finite number $m = N_m$ of states in a square with periodic boundary conditions*

(subject to magnetic field and discarding all but the lowest Landau level) and that the size of the torus (area in units of ℓ_0^2) can be measured by the number of magnetic flux quanta N_m penetrating the torus: $ab = 2\pi\ell_0^2 N_m$.

States $\psi_{0,k'_y}(x', y')$ shown above are not periodic in the x direction and this can be accomplished by periodic continuation: $\psi(x, y) \to \psi(x, y) + \psi(x + a, y) + \dots$. The (non-normalized) single particle states we will be dealing with are thus [80, 78, 81]

$$\varphi_j(x', y') = \sum_{k=-\infty}^{\infty} \exp\left[iy'(\frac{j}{m} + k)\zeta - \frac{1}{2}\left(x' - (\frac{j}{m} + k)\zeta\right)^2\right], \quad \zeta = \sqrt{\frac{a}{b} \cdot 2\pi m}\,, \quad j = 0, 1, 2, \dots, m-1\,. \tag{21}$$

These states constitute the single-particle basis of the lowest Landau level.

Twisted boundary conditions

Consider what happens if we require the modulus of ψ rather than ψ itself to be periodic, similar to Bloch's theorem. Thus, the wavefunction may acquire a non-trivial phase when going once around the torus. Mathematically, this can be described using the magnetic translation operators (5)

$$T(a\mathbf{e}_x)\psi = \exp(i\phi_x)\psi\,, \qquad T(b\mathbf{e}_y)\psi = \exp(i\phi_y)\psi\,. \tag{22}$$

Fixing phases ϕ_x, ϕ_y, the correct (non-normalized) periodic single particle states are

$$\varphi_j(x, y) = \sum_{k=-\infty}^{\infty} \underbrace{\exp(ik\phi_x)t(ka\mathbf{e}_x)}_{T(ka\mathbf{e}_x)} \exp(-iX_j y/\ell_0^2 + i\phi_y y/b) \exp[-(x - X_j)^2/2\ell_0^2]\,, \quad X_j = \frac{j}{m}a\,, \quad j = 0, 1, \dots, m-1\,, \tag{23}$$

where $t(\xi\mathbf{e}_x)$ is an ordinary translation, i.e. an operator transforming $\psi(x, y)$ into $\psi(x+\xi, y)$. For $\phi_x, \phi_y = 0$ the original result (21) is recovered. This choice of ϕ_x, ϕ_y is also used throughout this work.

Interpretation of ϕ_x, ϕ_y. By imposing the PBC we arrived at the statement that wavefunctions must be centered (along x) at $X_j = (a/m) \cdot j$, $j = 0, 1, \dots$ There is no *a priori* reason for the point $x = X_0 = 0$ to be more important than $x = X_{0.5} = (a/m) \cdot 0.5$ which is not among the just mentioned X_j's. By varying ϕ_x, the set $\{X_0, X_1, \dots\} = (a/m)\{0, 1, \dots\}$ is transformed into $(a/m)\{0 + \phi_x/2\pi, 1 + \phi_x/2\pi, \dots\}$. Thus, sweeping ϕ_x from 0 to 2π, we probe all points between 0 and a in the x direction. Independently on this, we may sweep through all k_y points in the interval $[0; 2\pi/b]$ by changing ϕ_y. Thus, ϕ_x and ϕ_y are analogous to lattice wavevectors within the first Brillouin zone in an ordinary periodic system defined by ordinary rather than magnetic translations.

In summary, by considering only a finite system, we have only m states to probe the whole plane (i.e. $[0, a]$ in x and $[0, 2\pi/b]$ in y). Sweeping ϕ_x, ϕ_y from 0 to 2π we can access an arbitrary point in the plane.

Another interpretation of ϕ_x, ϕ_y was given by Tao and Haldane [73] in terms of additional magnetic fluxes. These come from two ideal anuloids (closed solenoids): one goes inside the torus and another around the torus outside. $(h/e)(\phi_{x,y}/2\pi)$. It was also shown [32, 37] that ϕ_x increasing linearly in time acts as a homogeneous electric field in x direction.

General basis of single-particle states on a torus: complex coordinates

A precise discussion of one-particle states on a torus including the phases ϕ_x, ϕ_y was first given by Haldane and Rezayi [32]. They showed that the most arbitrary state is

$$\psi(x,y) = \exp(-\tfrac{1}{2}x^2) \cdot \underbrace{\exp(ikz) \prod_{l=1}^{m} \vartheta_1\left(\pi(z-z_l)/b|i\right)}_{\text{analytic}}, \qquad z = x+iy \tag{24}$$

where $\vartheta_1(u|\tau)$ is an elliptic theta function ([29], p. 921), k is a real number in the range $|k| < \pi m/b$ and z_i are some fixed complex numbers within the rectangle $[0,a] \times [0,b]$. In the terminology of (23), these states correspond to any j and any ϕ_x, ϕ_y. The most important things to know about the theta functions are that it is analytic, that $\vartheta_1(z-z_l|i) \propto z - z_l$ for $|z-z_l| \to 0$ and that z_l is its only zero in the rectangle. In this form, it is also clear that m is equal to the number of flux quanta in the elementary cell (the rectangle). Going once around the rectangle, the wavefunction gathers a phase of $2\pi\times$ number of zero points inside. That number is just m, each factor in (24) contributes by a single zero.

By choosing fixed ϕ_x, ϕ_y, there arise m possible choices for the values of k and $z_0 = \sum_l z_l$, say $j = 0, 1, \ldots, m-1$. For each pair (k, z_0) we can construct one function of the form (24) and the resulting m functions will constitute a basis of the lowest Landau level, just as the basis in (23). There is naturally a large freedom in choosing one particular basis. This happens by choosing some particular position of the zero points z_l's while observing the constraint on z_0. The basis in (23) can be obtained from (24) by putting the zeroes on a line, $z_l = i \cdot bl/m + j/ma$ and choosing $k = (2\pi/b)j$ for the state φ_j with $\phi_x = \phi_y = 0$. Even though it is by far not obvious in (23), Fig. 4 shows a 2D plot of one of such functions.

In principle, the wavefunctions in (24) are very similar to those obtained in the circular gauge (4) except for substituting z by $\vartheta_1(z|i)$. This is a manifestation of the fact, that even on a torus, circular symmetry is approximately preserved at short distances and deviations occur first when $\vartheta_1(z|i)$ deviates from z at larger distances. One could say, $\vartheta_1(z|i)$ is the function $f(z) = z$ adapted to the torus i.e. deformed to comply with periodic boundary conditions.

On the other hand contrary to the infinite plane, each single-electron wavefunction on a torus has as many zeroes as there are flux quanta passing through the torus.

1.5.2 Many-body symmetries on a torus

Center-of-mass

What changes if we consider n-body states instead of single-particle ones [32]? Given the considered Hamiltonian (33), the most obvious symmetry is the separation of center-of-mass and relative part of the wavefunction

$$\Psi(z_1, \ldots, z_n) = \Psi_{CM}(Z)\psi_{rel}\,, \qquad Z = z_1 + \ldots + z_n\,. \tag{25}$$

The center-of-mass part is just a one-particle wavefunction. Hence it must have the form shown in (24). Haldane and Rezayi [32] showed that it has q zeroes in the region $[0;a] \times [0;b]$ for filling factor $\nu = N_e/(qN_e)$. Again as for single-particle states, there are q basis states for Ψ_{CM}. Since the energy does not depend on the center-of-mass position in a homogeneous system, these three states will lead to degenerate many-body states, provided ψ_{rel} remains the same.

This introduces a delicate topic. The electron density in a given state depends on the center-of-mass part of the wavefunction. Different choices of bases in the q-fold i.e. threefold for $\nu = 1/3$, degenerate space of center-of-mass wavefunctions may lead to a q-tuple of states with practically homogeneous density in some cases or with quite strongly varying density in other cases (Fig. 5). This is true in spite of that we always describe the same ground state subspace. Even worse, in homogeneous systems we often want to

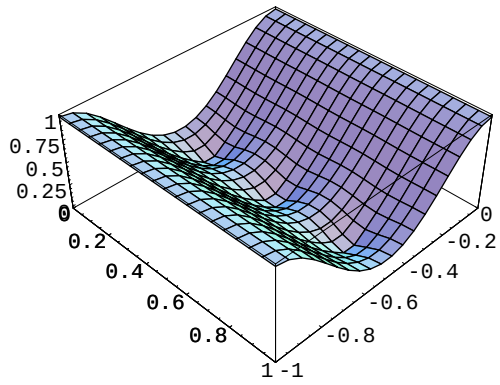

(a) Modulus.

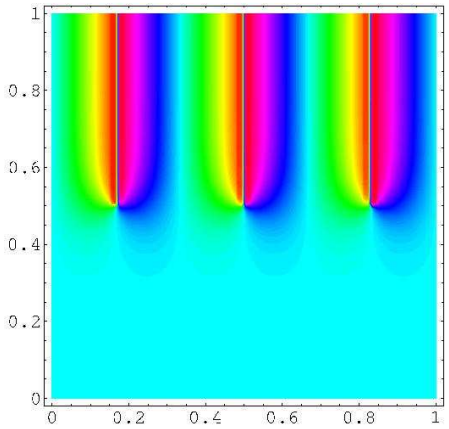

(b) Phase.

Fig. 4: One possible one-particle state on a torus pierced by three flux quanta (i.e. $m = 3$).

study only the relative part of the wavefunction, which must be the same in all cases. If it is for example the Laughlin wavefunction, we know that it leads to a homogeneous density. The central trouble is then that the Hamiltonian eigenstates obtained by exact diagonalization contain Ψ_{CM}.

Relative-motion part of the wavefunction

The discussion in the previous paragraph is based on (magnetic) translations of the center-of-mass $T_{CM}(u)$. In an n-body state, the translation of a single (i-th) particle (Subsect. 7.2 in [14]), $t_i(v)$, can be split into a

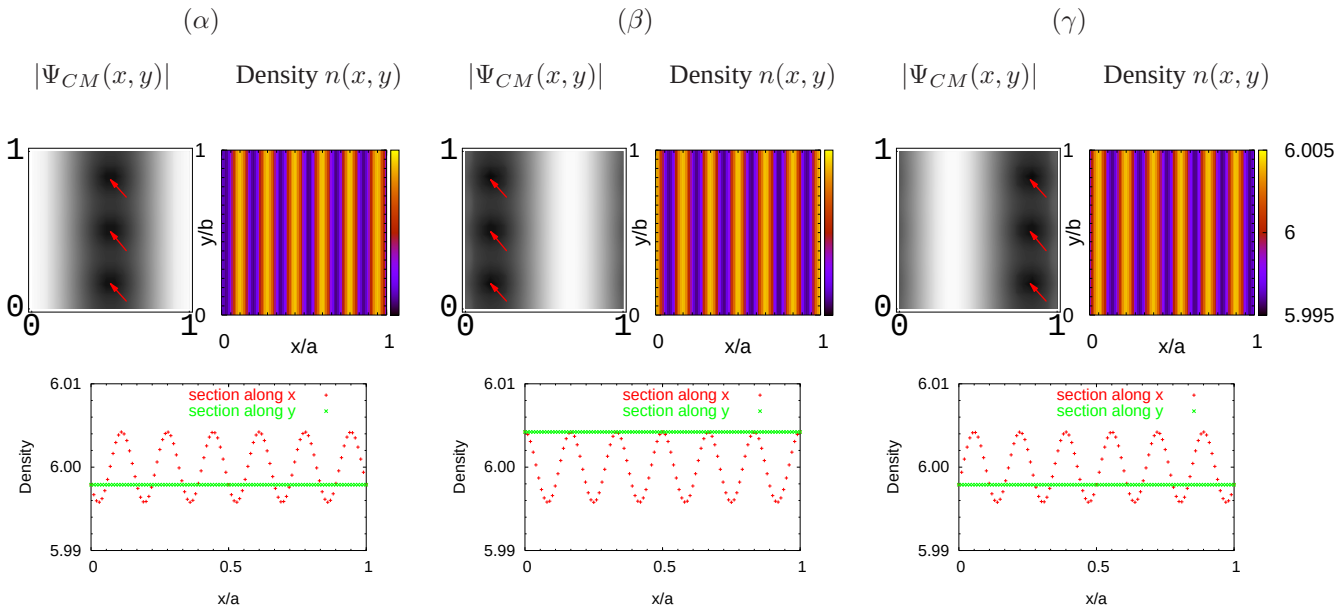

(a) A basis leading to more inhomogeneous densities.

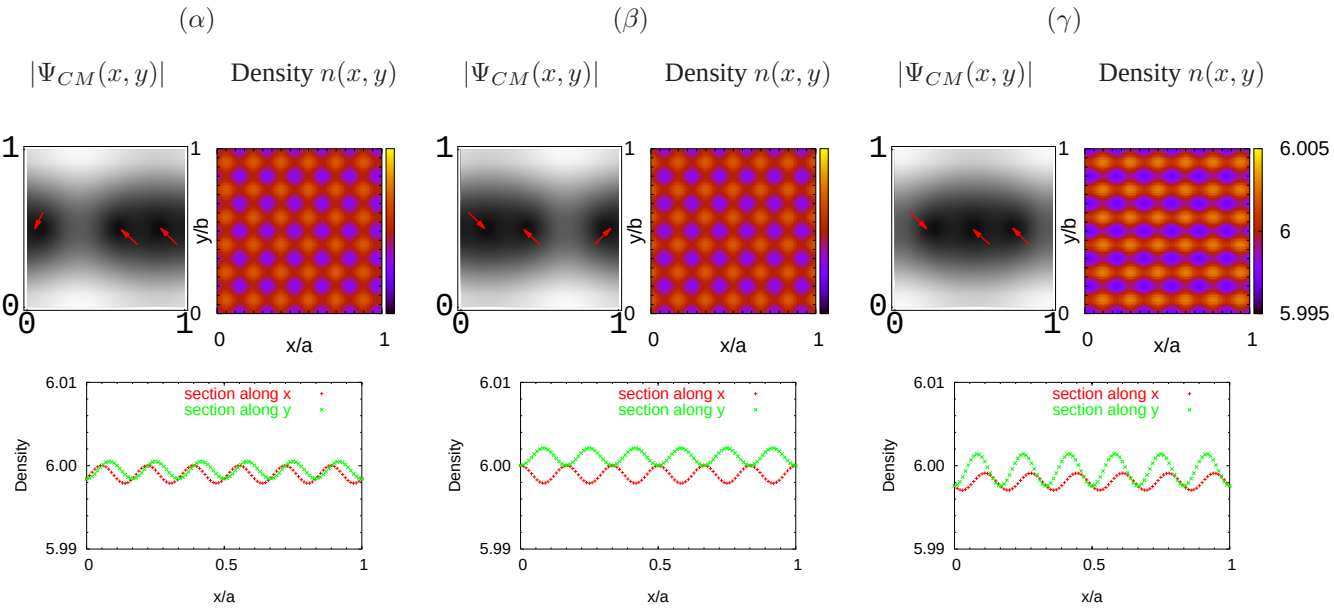

(b) A basis leading to less inhomogeneous densities.

Fig. 5: Two different bases for Ψ_{CM}, (a) and (b). At filling $\nu = 1/3$ there are three allowed CM states on a torus. They are labeled α, β, γ in this figure. For each element of each basis we show the modulus of Ψ_{CM}, the density of the corresponding Laughlin state with six electrons, i.e. the state $\Psi_{CM}\Psi_L$, and section of the density along x and along y. Note the positions of the three zeroes in different Ψ_{CM}'s (marked by the red arrows).

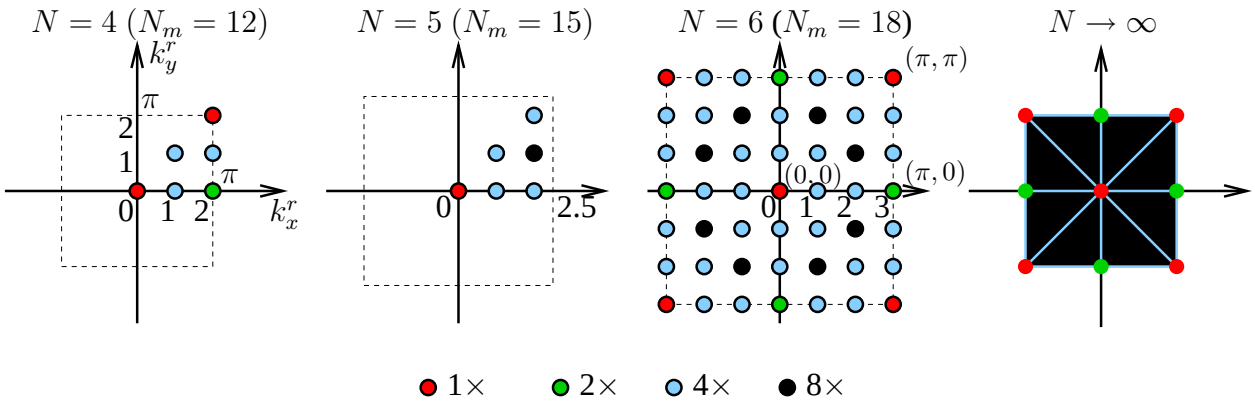

Fig. 6: The first Brillouin zone for relative translations on the torus (square with periodic boundary conditions). Its size depends on the number of particles in the system, cf. (27). At filling factor $\nu = p/q$ with $N_e = Np$ particles (and $N_m = Nq$ fluxes), number of allowed k^r-points is N^2 and the upper right corner has $k^r = \gamma(\pi, \pi)$, $\gamma = \sqrt{N/2\pi q}/\ell_0$. Different colours indicate points of different symmetry (or degeneracy number of a state with this k^r in a homogeneous system), the rightmost figure shows the limit of large N.

translation of the center of mass $T_{CM}(\frac{1}{n}v)$ and a relative translation $T_{rel,i}(v - \frac{1}{n}v)$. Owing to the indistinguishability of particles, the effect of the relative translation $t_i(v)$ on a particular many-particle state is the same for any i. We may thus omit the index and imagine $i = 1$, for instance.

Again, as in Bloch's theorem, wavevector k^r can be attributed to these relative translations [31]

$$T_{rel}(v)\psi = \exp(ik^r \cdot v)\psi\,. \tag{26}$$

Since $T_{rel}(v)$ commutes with the Hamiltonian (33), the Hamiltonian eigenstates can be sorted according to values of k^r. In Bloch's theorem, the allowed translations are given by an arbitrary lattice vector v. Not all of them are allowed for T_{rel} though [31].

This concept is very similar to a single particle in a periodic potential. However, there is no real periodic potential in an infinite plane and we introduced one particular period artificially. The largest period possible within our model is the size of the rectangle.

The Brillouin zone for k^r is rectangular (Fig. 6) and its *size* grows with the size of the elementary cell. For filling factor $\nu = p/q$ (p, q with no common divisor > 1) and number of flux quanta per cell $N_s = Nq$, the allowed values of k^r are

$$k^r\ell_0 = \sqrt{\frac{2\pi}{N_s\lambda}}(s, t)\,, \qquad |s|, |t| \le N/2 \text{ and integer.} \tag{27}$$

The quantity λ is the aspect ratio. For the sake of comparison between systems of different sizes we will sometimes use size-independent units for k^r, where $\widetilde{k}^r = (\pi, \pi)$ means the upper right corner of the Brillouin zone, i.e. $s = t = N/2$.

It can be verified ([14], p. 169), that application of the operator

$$\text{CDW: } \sum_j \exp(iq \cdot r_i)\,, \text{ or} \qquad \text{SDW: } \sum_j S_j^+ \exp(iq \cdot r_i) \tag{28}$$

to an arbitrary state corresponding to k^r increases its wavevector k^r by q. On the other hand, the operator (28) generates a charge-density wave (spin-density wave) with wavevector q, as can be best verified by the simple example of the Fermi gas. Isotropic states are supposed to have $k^r = 0$.

The wavevector $\boldsymbol{k}^r$ for states on a torus is also related to the angular momentum of the corresponding states on a sphere or on a disc, $|\boldsymbol{k}^r| = (|\boldsymbol{L}|/\hbar)/R$, where R is radius of the sphere [30, 14]. The direction of $\boldsymbol{L}$ (or alternatively L_z, for instance) is related to the direction of $\boldsymbol{k}^r$: for example a plane wave going around the equator specified by the wavevector $\boldsymbol{k}^r$ will have $\boldsymbol{L}$ pointing to the pole and $L_z = \hbar|\boldsymbol{k}^r|R$. This correspondece allows to directly compare spectra for FQH states obtained for different boundary conditions [33] and this, in turn, helps to sort out the finite size effects.

Momentum

So far, we have introduced two sorts of translational symmetries of states on a torus. One of the center-of-mass part of the wavefunction and another of the relative part. Since the corresponding magnetic translation operators commute with the homogeneous Hamiltonian, it would, in principle, be possible to split the basis of the whole lowest Landau level into several smaller bases and diagonalize in the subspaces separately. Each basis would be characterized by a particular value of $\boldsymbol{k}_{CM}$ and $\boldsymbol{k}^r$.

This procedure can help to treat larger systems but it costs some extra effort to implement it and moreover it is only possible in homogeneous systems. We will now discuss another of Hamiltonian's symmetries, described by a new quantum number J, which is a combination of the previous two. This symmetry is preserved with a certain class of inhomogeneities and it can be implemented straightforwardly. When constructing the basis for a particular value of J, we only have to select the matching Slater determinants (31) rather than to construct linear combinations of them.

The homogeneous Hamiltonian in the Landau gauge (i is the particle index, V_{int} is the Coulomb interaction between particles)

$$H = V_{int} + \sum_i H_0^i\,, \qquad H_0 = \frac{1}{2}\hbar\omega\left[-\frac{\partial^2}{\partial x'^2} + \left(-i\frac{\partial}{\partial y'} + x'\right)^2\right], \qquad (x', y') = (x/\ell_0, y/\ell_0)$$

conserves the total momentum in y direction. Due to the periodic boundary conditions allowed values of k_y are $(2\pi/b)j$, $j = 0, 1, \ldots, m-1$. In an n-body state constructed as a Slater determinant of single-electron states φ_{j_i} (21), the total momentum along y is

$$(b/2\pi)K_y = (b/2\pi)\sum_{i=1}^{n} k_y^i = j_1 + \ldots + j_n (\mathrm{mod}\; m) \equiv J\,. \qquad (29)$$

Values of J thus range for instance from 0 to $m-1$. It is useful to keep in mind, that j_i is (up to the factor) the point in x-direction at which φ_{j_i} is centered, $X_{j_i} = (j_i/m)a$. Thus, J can also be interpreted as the x-coordinate of the center-of-mass of the n-electron state.

Without proof, let us now present the precise connection between J and the wavevectors following from T_{CM} and T_{rel} (i.e. $\boldsymbol{k}_{CM}, \boldsymbol{k}^r$). Let $\nu = p/q$ (p, q with no common divisor > 1) and $m = Nq$ the number of flux quanta per cell. An arbitrary J can be decomposed into two parts

$$J = J_{CM}\cdot N + J_{rel}\,, \quad |J_{rel}| \le N/2\,,\ J_{CM} \text{ integer}, \qquad (30)$$

i.e. J_{rel} is J modulo N and J_{CM} is J divided by N. The quantity J_{rel} is directly the y-component of $\boldsymbol{k}^r$, more precisely, $J_{rel} = t$ or $J_{rel} = N/2 - t$ in (27), the former for $pq(n-1)$ even, the latter for $pq(n-1)$ odd [14].

J_{CM} distinguishes states which differ *only* in the center-of-mass coordinate. By a successive application of T_{CM} to one state Ψ we can go through all possible values of $J_{CM} = 0, 1, \ldots, q-1$.

Each subspace with definite J contains states of all different k_x^r. Since T_{rel} by allowed translation vectors commute with the total momentum along y, it is in principle possible to split a basis corresponding to a particular J into subspaces with $k_x^r\ell_0\sqrt{N/2\pi} = -N/2, \ldots N/2$. However, the basis state will no longer have the simple form of antisymmetrized product states of φ_j (21).

1.5.3 Exact diagonalization

Many interacting electrons in a rectangle with periodic boundary conditions can be described in the following way.

- Choose the number of flux quanta penetrating the rectangle (m). All allowed single-particle states φ_j are those written in (21) or (23) for nontrivial boundary-condition phases ϕ_x, ϕ_y. Their number is m.
- Construct all possible linearly independent n-particle states (for the given number of flux quanta m). Most conveniently, these can be antisymmetrized products (Slater determinants) of n states φ_{j_i}, denote them by

$$|j_1 \dots j_n\rangle = a^\dagger_{j_1} \dots a^\dagger_{j_n} |0\rangle \,. \tag{31}$$

- The filling factor is then $\nu = n/m$, cf. (1).
- Take an arbitrary many-body Hamilton operator and calculate its matrix elements in the basis $|j_1 \dots j_n\rangle_k$, $k = 1, \dots, N$. The dimension of the matrix is $N = \binom{n}{m}$.
- Diagonalize the Hamilton matrix. Eigenvalues are the total energies E_i, eigenvectors $\mathsf{v}_i = (v_i^1, \dots, v_i^N)$ are related to the many-body eigenstates by

$$H|\psi_i\rangle = E_i|\psi_i\rangle \,, \qquad |\psi_i\rangle = \sum_{k=1}^{N} v_i^k |(j_1 \dots j_n)_k\rangle \,. \tag{32}$$

This procedure is *exact* if we consider a system where electrons in the lowest Landau level form a periodic system. The approximation rests therefore in representing an infinite system by a periodic repetition of a representative finite cell, a procedure which has been very successfully applied in condensed matter theory. Formulated in other words: the Hamiltonian is exact and all approximations are implemented by the choice of the basis. The dimension of the matrix is finite by construction, no cutoff for one-particle states is needed.

In the rest of this Subsection we present the particular form of the Coulomb matrix elements ([80] or [14], Sect. 5.1).

The exact Hamilton operator in first and in second quantization is

$$\begin{aligned} H &= \frac{e^2}{4\pi\varepsilon} \sum_{i<j} V(|\mathsf{r}_i - \mathsf{r}_j|) \\ H &= \sum_j \mathcal{W} a^\dagger_j a_j + \sum_{\substack{j_1,j_2 \\ j_3,j_4}} \mathcal{A}_{j_1,j_2,j_3,j_4} a^\dagger_{j_1} a^\dagger_{j_2} a_{j_3} a_{j_4} \,, \end{aligned} \tag{33}$$

where $a^\dagger_j$ create single-electron states. The latter expression assumes already periodic boundary conditions. The first sum is the Madelung-type energy of the electron interacting with its own periodic images [12]

$$\mathcal{W} = -\frac{e^2}{4\pi\varepsilon\ell_0} \frac{1}{\sqrt{2\pi m}} \left[2 - \sum_{\substack{l_1,l_1 \\ (l_1,l_2)\neq(0,0)}} \varphi_{-\frac{1}{2}} \left(\pi(l_1^2\lambda + l_2^2/\lambda) \right) \right] , \qquad \varphi_n(z) \equiv \int_1^\infty \mathrm{d}t \, e^{-zt} t^n \,. \tag{34}$$

If only the electrons were considered, this energy would diverge at least as $\sum_n 1/n$. To keep it finite, a neutralizing positive background must be considered [12].

Choosing the single-electron basis according to (21) or (23), the interaction matrix elements are

$$\begin{aligned}\mathcal{A}_{j_1,j_2,j_3,j_4} &= \frac{1}{2}\int \mathrm{d}\boldsymbol{r}_1\mathrm{d}\boldsymbol{r}_2\varphi^*_{j_1}(\boldsymbol{r}_1)\varphi^*_{j_2}(\boldsymbol{r}_2)V(|\boldsymbol{r}_1-\boldsymbol{r}_2|)\varphi_{j_3}(\boldsymbol{r}_2)\varphi_{j_4}(\boldsymbol{r}_1) = \\ &= \frac{e^2}{4\pi\varepsilon\ell_0}\frac{1}{2m}\sum_{\substack{q_x=(2\pi/a)s\\ q_y=(2\pi/b)t\\ s,t\in\mathbb{Z}\\ (s,t)\neq(0,0)}} \delta'_{j_1+j_2,j_3+j_4}\delta'_{s,j_1-j_4}\frac{V(\boldsymbol{q})}{\ell_0}\exp\left[-\frac{1}{2}\boldsymbol{q}^2\ell_0^2\right]\times \\ &\qquad \times\exp\left[-2\pi i t(j_1-j_3)/m\right]\times\alpha(j_1+j_2-j_3-j_4,\phi_y)\,. \end{aligned} \tag{35}$$

with both integrals taken over the rectangle $[0;a]\times[0;b]$. Primed Kronecker δ compares the two arguments *modulo* m. The last factor α is solely due to the boundary condition phase ϕ_y

$$\alpha(\Delta J,\phi_y)=\delta_{J,0}+\delta_{\Delta J,m}\exp(i\phi_y)+\delta_{\Delta J,-m}\exp(-i\phi_y)\,,$$

and the matrix elements do not depend on ϕ_x, only the basis vectors $|j_1\ldots j_n\rangle_k$ do.
The periodic continuation of the Coulomb interaction in two dimensions is given by

$$\frac{4\pi\varepsilon}{e^2}V(\boldsymbol{r})=\left.\frac{1}{|\boldsymbol{r}|}\right|_{per}=\frac{1}{ab}\sum_{\boldsymbol{q}}\frac{2\pi}{|\boldsymbol{q}|}\exp(i\boldsymbol{q}\cdot\boldsymbol{r})\,,\qquad \boldsymbol{q}=\left(\frac{2\pi}{a}s,\frac{2\pi}{b}t\right)\,,\ s,t\in\mathbb{Z}\,, \tag{36}$$

hence the Fourier series of $V(\boldsymbol{r})$ used in (35) has $V(\boldsymbol{q})=1/|\boldsymbol{q}|$.
The Hamiltonian (33) assumes spin-polarized particles. Its extension to particles which may have different spin is straightforward, since the Coulomb interaction conserves spin [85],

$$H=\sum_j \mathcal{W}a^\dagger_j a_j+\sum_{\substack{j_1,j_2\\ j_3,j_4\\ \sigma,\sigma'}}\mathcal{A}_{j_1,j_2,j_3,j_4}a^\dagger_{j_1\sigma}a^\dagger_{j_2\sigma'}a_{j_3\sigma'}a_{j_4\sigma}\,. \tag{37}$$

operators $a^\dagger_{j\sigma}$ must be extended appropriately. They create a particle in state φ_j either with spin up or spin down.

1.5.4 Symmetries and choices of bases

Regarding the structure of the basis of our choice (31) there are two Hamiltonian symmetries which are easy to use: conservation of J, total momentum along y (29) and conservation of the z-component of the total spin S_z.
'Easy to use' means here that the basis of the whole lowest Landau level in the form of Slater determinants $|(j_1\sigma_1\ldots j_n\sigma_n)_k\rangle$ can be sorted into groups corresponding to particular values of J and S_z.
Sorting according to J splits the basis into m subspaces of approximately the same size $\approx\binom{m}{n}/m$. Utilisation of S_z brings a smaller profit, since the $S_z=0$ subspace is larger than the $S_z=n/2$ subspace by a substantial factor of about $\binom{n}{n/2}\approx 2^{n-1}/\sqrt{2\pi n}$. The size of the largest group is then not simply the number of all states divided by the number of subspaces.
Other symmetries of the homogeneous Hamiltonian would correspond to conservation of the total spin S^2 and conservation of k^r_x (Subsect. 1.5.2). The eigenstates of these operators, however, are generally not of the simple product form (31), but they are linear combinations of such states. More importantly, these symmetries are gone if inhomogeneous systems are considered. However, suitably chosen inhomogeneities can preserve the 'easy-to-use' symmetries mentioned previously (Subsect. 3.1) while still lowering the total symmetry of the Hamiltonian.
If the aim is to choose n as high as possible, then the largest accessible systems have about ten electrons. At filling $\nu=1/3$ with J symmetry employed and $S_z=n/2$, the basis counts 1 001 603 elements for $n=10$

and $J = 5$. The largest bases used in this work contained 5×10^6 elements, extremely elaborate programs can handle bases up to sizes about an order of magnitude larger [52]. An alternative to the classical exact diagonalization is presented in Subsect. 1.5.5

Particle-hole symmetry

Particle-hole symmetry provides a mapping between systems at fillings ν and $1-\nu$ (spinless electrons) or ν and $2-\nu$ (spinful electrons). The mapping is exact provided Landau level mixing is absent. As an illustrative example consider fully polarized electrons i.e. only the lowest LL with spin up is relevant, lowest LL spin down and all higher LLs are so far in energy that they can be neglected. The spectra of a $\nu = 1/3$ and $2/3$ systems are identical up to a constant shift and the corresponding wavefunctions are related by a simple transformation.

Think of the lowest Landau level as of a 1D chain. The Landau gauge is particularly illustrative for this as the one-electron states (3) are localised along x. The basic idea of the particle-hole symmetry is that two electrons at positions i and j feel the same repulsive force as two holes at the same positions, i.e. when the whole 1D chain is full and only at i and j electrons are missing.

Let us put this into mathematical terms. Let $a_j^\dagger$ be a creation operator of a single-electron state with momentum $k_y = 2\pi j/b$, being therefore localised in x-direction around $X_j = k_y \ell_0^2$ (3). Assuming that j can take values $0, \ldots, m-1$, particle-hole conjugated n-body states are

$$a_{j_1}^\dagger \ldots a_{j_n}^\dagger |0\rangle \text{ (particles)} \quad \longleftrightarrow \quad a_{j_1} \ldots a_{j_n} |1\rangle \text{ (holes)}, \tag{38}$$

where $|0\rangle$ is an empty Landau level (vacuum) while $|1\rangle \equiv a_0^\dagger \ldots a_{m-1}^\dagger |0\rangle$ is a completely filled Landau level. For example $a_0^\dagger a_2^\dagger |0\rangle \equiv |\bullet \cdot \bullet \cdots\rangle \longleftrightarrow |\cdot \bullet \cdot \bullet\bullet\bullet\rangle \equiv a_0 a_2 |1\rangle = a_1^\dagger a_3^\dagger a_4^\dagger a_5^\dagger |0\rangle$.

A straightforward calculation shows that matrices of a translationally invariant two-body operator $\hat{A}$ are the same (up to a multiple of identity matrix and complex conjugation) in an arbitrary n-particle basis and its conjugated $(m-n)$-electron basis. The only approximation we must concede is to neglect the Landau level mixing.

Result of the calculation is the following. The diagonal terms of an operator A in the particle basis and in the hole basis fulfil

$$\langle 1| a_{j_1}^\dagger \ldots a_{j_n}^\dagger \; A \; a_{j_n} \ldots a_{j_1} |1\rangle = \frac{m-2n}{m} \langle 1| \, A \, |1\rangle + \langle 0| a_{j_1} \ldots a_{j_n} \; A \; a_{j_n}^\dagger \ldots a_{j_1}^\dagger |0\rangle \tag{39}$$

and the off-diagonal terms remain the same up to the complex conjugation.

Two cases are worth of special attention:

The *spectra* of (fully polarized) systems at $\nu = n/m$ and $\nu = (m-n)/m$ are the same up to a shift

$$E_\nu^i = E_{1-\nu}^i + E_f \, (m-2n)/m \, , \tag{40}$$

where E_f is the energy of a completely filled (lowest) Landau level. This result does not depend on the form of the interaction $V(r)$. A nice demonstration of this formula is shown in Fig. 41b (see the comment [3]).

Conjugated states (38) may have different values of J (30). For instance: for $m = 4$, consider a three-electron state $|j_1 j_2 j_3\rangle = |013\rangle$ and its particle-hole conjugate $|j_1\rangle = |2\rangle$. The former has $J = 0$ while the latter has $J = 2$.

For the *density-density correlation function* $g_\Psi(r) = \langle \sum_{i<j} \delta(r - r_i + r_j) \rangle_\Psi$ we get

$$g_\Psi(r) = \frac{m-2n}{m} \big(1 - \exp(-r^2/2\ell_0^2)\big) + g_{\Psi'}(r) \, , \tag{41}$$

where Ψ and Ψ' are arbitrary particle-hole conjugated states. Note that $g_{\Psi'}$ refers to *electrons* in the 'hole' state. Correlations between holes in Ψ' are the same as those between electrons in Ψ.

Note, that $g(r)$ in (41) is *not* defined in the normalized form $\delta(r - r_i + r_j)/(n(n-1))$. Also $g(r)$ of a full Landau level may depend on system (finite-size) parameters, e.g. in a rectangle with periodic boundary conditions, it depends on aspect ratio.

Let us mention that densities of particle-hole conjugated states are related by $n_\Psi(r) = m - n_{\Psi'}(r)$, exactly as we expect from the picture of a hole as a missing particle. The plus sign in (41) might look puzzling. At the second glance, however, $g_\Psi = n \cdot n$ (schematically) and therefore $g_{\Psi'} = (1-n)\cdot(1-n) = 1 - 2n + g_\Psi$.

1.5.5 Density matrix renormalization group

Exact diagonalization as it has just been presented, boasts of taking the complete basis of the lowest Landau level on a torus. As long as the low-energy states are considered, many of the basis states will be almost absent in the product-state expansion (32). Especially those which place many electrons close to each other and thus contribute with a large Coulomb energy. Leaving out such states from the basis will not affect the calculated ground state noticeably while it reduces the matrix sizes.

Density matrix renormalization group (DMRG) is a systematic method to leave out irrelevant basis states. Roughly, its basic idea is to successively enlarge the considered system and to use only the most important n-particle states for calculating the $(n+1)$-particle ground state.

The idea was used originally for one-dimensional systems (a review in [64, 65]). Shibata and Yoshioka [66, 67, 68, 69, 82] noticed that the single-electron basis of the lowest Landau level *is* in principle one-dimensional (23) and adapted this method as an extension of the exact diagonalization for studies of the lowest Landau level. They were thus able to study systems with up to about 20 particles at fillings close to $\nu = 1/3$.

1.6 Quantum Hall Ferromagnets

Consider the situation $\nu = 1$ and vanishing Zeeman energy [26]. What is the ground state?

In the absence of Zeeman splitting, the lowest Landau levels ($n = 0$) for spin up and for spin down have the same energy, thus, without interaction, there are $2eB/h$ single-electron states available with energy $\hbar\omega/2$, which is the lowest energy an electron can have in the presence of a magnetic field B. Filling factor one means that only eB/h states (per unit area) are occupied. Hence there is a vast number of degenerate many-electron ground states without interaction.

One of these states has the form

$$\Psi_H = \Phi(z_1, \ldots, z_n)|\uparrow\uparrow \ldots \uparrow\rangle\,.$$

Antisymmetry of Ψ_H implies antisymmetry of Φ, or in other words Φ vanishes when any z_i approaches any z_j. Each particle is surrounded by a correlation hole, cf. (45). Moreover, the state Ψ_H is the only one (with $\nu = 1$ within the lowest Landau level) whose orbital part is fully antisymmetric, up to $SU(2)$ spin rotations. If we do *not* neglect the repulsive interaction between electrons, the 'optimal correlation hole' of the state Ψ_H will make its Coulomb energy lower than for any other $\nu = 1$ state and Ψ_H becomes the absolute ground state even at zero Zeeman energy. The long-range order in spins (all are pointing in the same direction) which are not localised at fixed positions, e.g. as it is in a spin lattice, renders Ψ_H an itinerant ferromagnetic state. In the absence of the Zeeman splitting the $\nu = 1$ quantum Hall system constitutes an example of a Heisenberg ferromagnet.

For Coulomb interaction, the energy cost of a single electron flip, which implies a violation of the antisymmetry of Φ, can be evaluated analytically: $E = (e^2/\varepsilon\ell_0)\sqrt{\pi/8}$ [26]. Quantitatively, this number is comparable to the cyclotron energy $\hbar\omega$ at magnetic fields in the range of few tesla in GaAs. The fully

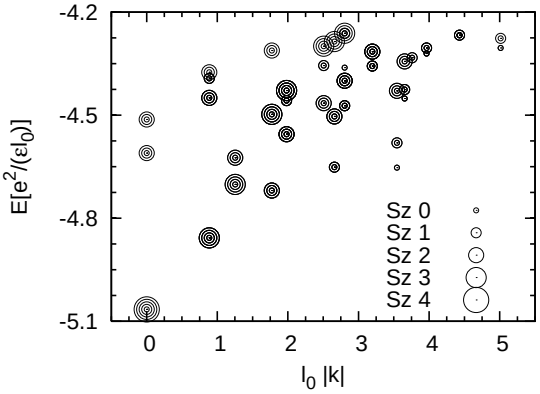

(a) The $\nu = 1$ QHF: $(0, \uparrow)$ and $(0, \downarrow)$ levels are active, the rest is empty. A Heisenberg ferromagnet. The $SU(2)$ spin symmetry is manifest in the degeneracy of all possible S_z states for one given S.

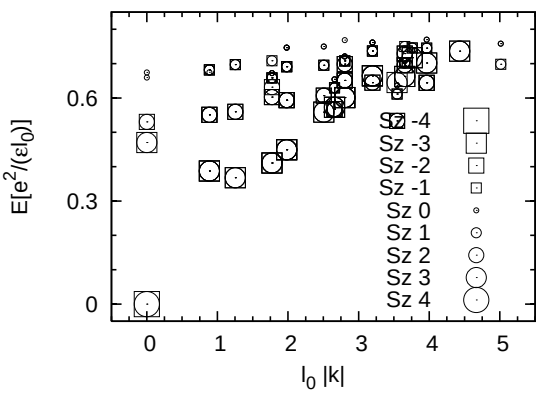

(b) The $\nu = 2$ QHF: $(0, \uparrow)$ and $(1, \downarrow)$ levels are active, $(0, \downarrow)$ is full and treated as inert, the rest is empty. An Ising ferromagnet. The Z_2 symmetry implies that only S_z and $-S_z$ levels are degenerate; S is no good quantum number. Ground state energy was shifted to zero.

Fig. 7: Spectra of two examples of quantum Hall ferromagnets (exact diagonalization, Coulomb interaction, eight electrons). The ferromagnetic ground state occurs in both cases at $k^r = 0$ which is a necessary condition for the state to be non-degenerate (in orbital degrees of freedom). See Fig. 8 for an explanation of the choice of Landau level indices and spins of involved levels (n, σ).

polarized state then becomes the ground state stabilized by the huge gain in exchange energy. A spectrum obtained by the exact diagonalization in a small system is shown in Fig. 7a. In agreement with the argumentation above, the ground state has $S = n/2$ and it is well separated from excited states.

For the Pauli principle to apply (Φ vanishes as $z_i \to z_j$), it is only important that all spins have the *same* direction, not that they are all pointing upwards. Thus, the $\nu = 1$ ground state is characterized by full spin polarization ($S = n/2$) and arbitrary S_z. All states $(S^-)^k \Psi_H$, $k = 0, 1, \ldots n$ are degenerate ground states. A finite Zeeman energy will lift this degeneracy and the $\nu = 1$ system will then have a nondegenerate ground state Ψ_H, e.g. $S_z = n/2$ for B pointing in the z-direction.

Other types of integer quantum Hall ferromagnets are possible, but they all share the common scheme: two degenerated Landau levels which provide $2eB/h$ 'free places' and only eB/h of them should be occupied. Depending on *which* two Landau levels are degenerate, different types of ferromagnets can follow. A classification of possible cases was given by Jungwirth and MacDonald [40].

Let us introduce one more example, the $\nu = 2$ QHF which turns out to be an Ising type ferromagnet (see also Jungwirth *et al.* [41]). By changing the ratio between Zeeman and cyclotron energy, $(n, \sigma) = (0, \uparrow)$ and $(1, \downarrow)$ Landau levels can be brought to coincidence (Fig. 8). Experimentally, this can be accomplished either by changing the g-factor (it decreases with pressure [15] or by tilting the magnetic field [18] (cyclotron energy depends only on the component perpendicular to the 2DEG plane, Zeeman energy depends on the total field). The low lying $(0, \downarrow)$ Landau level is fully occupied (eB/h states) and can be taken as inert. The remaining eB/h states (giving in total $\nu = 2$) can be distributed among the $2eB/h$ available places of the *two* crossing Landau levels (Fig. 8). Contrary to the $\nu = 1$ QHF, there are only two ground states now: either $(0, \uparrow)$ is full or $(1, \downarrow)$ is full (Fig. 7b). To obtain this result we should use the exact diagonalization because of the large degeneracy present when interaction is switched off. However, the fact that distributing the electrons between the $(0, \uparrow)$ level and the $(1, \downarrow)$ level costs extra energy (compared

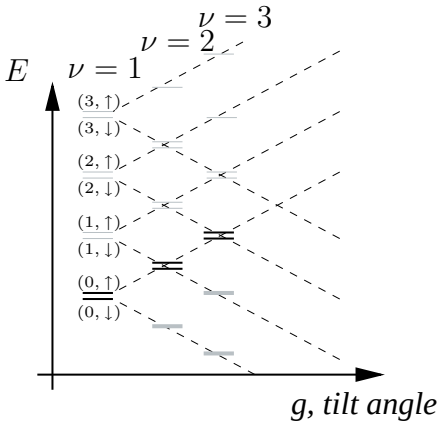

Fig. 8: Integer quantum Hall ferromagnets occur when two crossing Landau levels should be only half-filled ($2eB/h$ free states, eB/h electrons to occupy them). Thick (thin) grey levels indicate completely filled (empty) Landau levels, the pair of black levels are the 'active' ones. Despite the large number of possibilities of how to distribute electrons in the two levels, the Coulomb interaction selects (up to degeneracy in S_z) one state. Depending on which Landau level crossing is active, different types of ferromagnets occur: Heisenberg type for $\nu = 1$, Ising type for $\nu = 2, 3$.

to placing all electrons into one of the levels), is probably a consequence of the fact that spin up orbitals are not the same as spin down orbitals [40] as they lie in different Landau levels.

For a more detailed discussion of spectra of a Heisenberg and an Ising QHF (Fig. 7), see in Subsec. 2.3.3.

Quantum Hall ferromagnets which occur at integer filling factor have the advantage that they can often be well described by Hartree-Fock models, at least as far as the ground state is considered. Even here, exact diagonalization studies can sometimes unveil unexpected ground states, as shown by Nomura [58] in bilayer systems (spin degree of freedom is substituted by pseudospin which refers to the two layers).

The principial question which is addressed in this thesis is, whether quantum Hall ferromagnetism can also occur at fractional filling factors. Naively, one may expect that phenomena occuring for electrons (integer ν) would also occur for the CF (fractional ν). The Coulomb energy (of CF cyclotron energy) would take over the role of the cyclotron energy within the integer QHF. A pleasing fact is that now the ratio of the CF cyclotron energy and the Zeeman energy is B-dependent, so that the coincidence of the CF LL can be induced just by adjusting B at a given filling factor. Experimentally, there are strong hints on the existence of ferromagnetism even at fractional fillings [70, 22] and this work should contribute to the understanding of these phenomena from the side of theory.

2 Structure of the incompressible states and of the half–polarized states

2.1 Basic characteristics of the incompressible ground states

Being interested in phenomena occurring at the transition between two incompressible ground states, the spin-polarized and the singlet one, it is reasonable to get acquainted with these two ground states first.

In the very illustrative model of non-interacting composite fermions (NICF), introduced in Subsect. 1.4.2, the ground state at electronic filling factor $\nu = 2/3 = 2/(2 \cdot 2 - 1)$ corresponds to two completely filled composite fermion Landau levels (LL). If, in some particular situation, the CF cyclotron energy is smaller than the Zeeman splitting, these will be the $n = 0, \uparrow$, $n = 1, \uparrow$ CF Landau levels and the ground state will be fully spin polarized, Fig. 9a. If the ratio between Zeeman and CF cyclotron energies is reversed, the ground state has $n = 0, \uparrow$, $n = 0, \downarrow$ CF Landau levels filled and is therefore a spin singlet, cf. comment [4]. Here, the CFs are electrons with two flux quanta attached *antiparallel* to the effective magnetic field B_{eff} [77], which leads to a minus sign in the denominator of the CF filling factor (19).

A similar situation, i.e. occurrence of two incompressible ground states, the singlet and the polarized one, occurs also at filling factor $\nu = 2/5$. Here, the ground state can be interpreted as two filled CF LLs where the two flux quanta were attached *parallel* to B_{eff}. Thus, these ground states should be completely equivalent to the ground states at $\nu = 2/3$ within the NICF approximation.

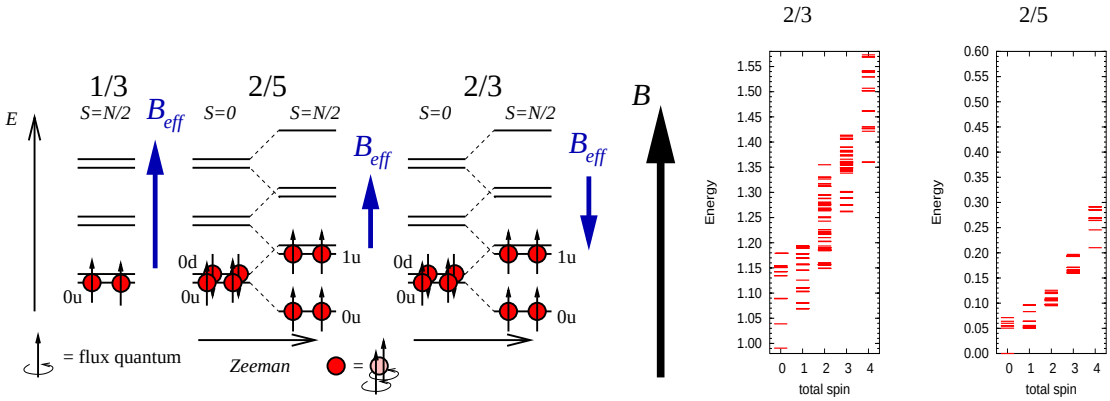

(a) Systems at filling factors $\nu = 1/3, 2/3$ and $2/5$ correspond to $\nu_{CF} = 1, 2$ and 2 within the non-interacting CF picture. The composite fermions (CF) are electrons with two magnetic flux quanta attached parallel (for $\nu = 1/3, 2/5$) or antiparallel (for $\nu = 2/3$) to the effective magnetic field B_{eff} (but always parallel to the real external field B). When Zeeman splitting is increased, crossings between CF Landau levels occur and spin polarization of the ground state changes.

(b) Energy levels of 8 particles on a torus at filling factors $2/3$ and $2/5$ without Zeeman splitting (short-range interaction, see Subsec. 1.3). Note the large excitation energies (related to the incompressibility gaps) for the ground states at $S = 0$ and $S = 4$, as compared to other inter-level separations.

Fig. 9: Ground states at filling factors $1/3$, $2/5$ and $2/3$ from the point of view of a composite fermion picture and the exact diagonalization.

Let us compare this picture of an infinite two-dimensional system with a finite system treated exactly. Looking at the exact spectra of a $\nu = 2/3$ and a $\nu = 2/5$ finite system, Fig. 9b, we readily recognize ground states in the $S = 0$ and the $S = N/2$ sector which are well separated from excited states, as compared to the typical level separation within the excitation spectrum or in subspaces with other values of the total spin. Also, as the NICF model predicts, the spin singlet ground state ($n = 0, \uparrow$, $n = 0, \downarrow$) has a lower energy $E(S = 0)$ than the polarized one ($n = 0, \uparrow$, $n = 1, \uparrow$), $E(S = N/2)$ if the Zeeman energy is set to zero. Both ground states have $k^r = (0, 0)$ which corresponds to $L = 0$ in a system with circular symmetry, Subsect. 1.5.2. Angular momentum equal to zero is in turn a property inevitable in any state with no partially filled Landau levels, corresponding argumentation is analogous to the comment [4].

It should be emphasised at this place that however strong support for the NICF model these findings provide, they cannot be taken as a proof of its complete correctness. The interacting electrons can*not* be exactly mapped to *non-interacting* CFs and even the quality of the approximation is hard to control. Although the NICF model gives correct answers to questions indicated above, there is no guarantee of correct answers in other cases, especially at other filling factors. In the following, we will continue discussing properties of both incompressible states at $\nu = 2/3$ and of those at $\nu = 2/5$ as calculated by exact diagonalization and we will occasionally mention links to composite fermion theories.

2.1.1 Densities and correlation functions

Having computed a many-particle wavefunction numerically usually does not automatically mean that we can say much about the nature of the state it describes. Very often, the only statement to be made is that the state is highly correlated, or entangled. By this we mean that the state cannot be written as a single Slater determinant [5], not even approximately, and thus its description goes far beyond any Hartree-Fock model.

In order to learn more about the state it is apt to evaluate expectation values of observables such as density or density-density correlation functions. In the first quantization formalism these are the following

operators

$$n(\boldsymbol{r}) = \sum_i \delta(\boldsymbol{r} - \boldsymbol{r}_i)\,, \qquad g(\boldsymbol{r}) = \frac{1}{N_e(N_e-1)} \sum_{i\neq j} \delta\big(\boldsymbol{r} - (\boldsymbol{r}_i - \boldsymbol{r}_j)\big)\,, \tag{42}$$

summations running over all particles in the system. For inhomogeneous systems it is also useful to consider an unaveraged density-density correlation operator

$$g(\boldsymbol{r}'', \boldsymbol{r}') = \frac{1}{N_e(N_e-1)} \sum_{i\neq j} \delta(\boldsymbol{r}' - \boldsymbol{r}_i)\delta(\boldsymbol{r}'' - \boldsymbol{r}_j)\big)\,,$$

where an average over $\boldsymbol{r}''$ gives (42). This is the probability density of finding a particle at place $\boldsymbol{r}'$ provided there is a particle at place $\boldsymbol{r}''$. The function $g(\boldsymbol{r})$ is just $g(\boldsymbol{r}+\boldsymbol{r}', \boldsymbol{r}')$ averaged over all $\boldsymbol{r}'$, hence $g(\boldsymbol{r}) \propto g(\boldsymbol{r}+\boldsymbol{r}', \boldsymbol{r}')$ for homogeneous systems, i.e. both quantities are the same up to a proportionality constant.

For not fully spin polarized states it is also useful to watch quantities $n_\uparrow(\boldsymbol{r})$ or $g_{\uparrow\downarrow}(\boldsymbol{r})$ and its analogues with other spin indices. For example

$$g_{\uparrow\downarrow}(\boldsymbol{r}) = \frac{1}{N_e(N_e-1)} \sum_{i\neq j} \delta_{\sigma_i\uparrow}\delta_{\sigma_j\downarrow}\delta\big(\boldsymbol{r} - (\boldsymbol{r}_i - \boldsymbol{r}_j)\big)\,. \tag{43}$$

The normalization of density and density-density correlation functions we chose in (42,43) is the following:

$$\int \mathrm{d}\boldsymbol{r}\, n(\boldsymbol{r}) = N_e\,, \qquad \int \mathrm{d}\boldsymbol{r}\, g(\boldsymbol{r}) = 1\,, \qquad \int \mathrm{d}\boldsymbol{r}\, g_{\sigma\sigma}(\boldsymbol{r}) = \frac{N_\sigma(N_\sigma-1)}{N_e(N_e-1)}\,,\ \sigma \in \{\uparrow,\downarrow\}\,, \tag{44}$$

where integrals are taken over the whole system i.e. elementary cell.

As long as homogeneous systems are concerned we naturally expect density and also polarization to remain constant. For the incompressible states this is true only up to finite size effects. The density shows a slight modulation which decays rapidly as the system size is increased. Discussion of these effects which have no relevance for the real infinite 2D system will be presented later, Subsec. 2.1.4.

In the following, by $g(r)$ we mean $g(\boldsymbol{r})$ with $r = |\boldsymbol{r}|$ for isotropic and homogeneous systems. Also, whenever we will speak about 'correlation functions' we mean equal time density-density correlation functions.

Fully occupied Landau levels

The density-density correlation function can be analytically evaluated for a state with $\nu = n$ fully occupied Landau levels [42]. This is the ground state of non-interacting electrons at integer filling factor. For the spin polarized case,

$$g(r) = 1 - \frac{1}{n^2}\exp(-[(rk_F)^2/4n]) \left[L^1_{n-1}\left(\frac{(rk_F)^2}{4n}\right)\right]^2\,. \tag{45}$$

Here $L^\alpha_n(x)$ are the associated Laguerre polynomials [6, 29]. In particular,

$$\nu = 1:\quad g_{\nu=1}(r) = 1-\exp(-r^2/2\ell_0^2)\,, \qquad \nu = 2:\quad g_{\nu=2}(r) = 1-\exp(-r^2/4\ell_0^2)\cdot\frac{1}{4}[2-r^2/4\ell_0^2]^2\,. \tag{46}$$

The Fermi wavevector k_F for a system subjected to a perpendicular magnetic field is defined as k_F in exactly the same system (i.e. the same areal density of electrons) just with magnetic field switched off. In this scheme

$$(k_F\ell_0)^2 = 2\nu\,, \text{ or} \qquad k_F = \sqrt{2\nu}\ell_0^{-1}\,. \tag{47}$$

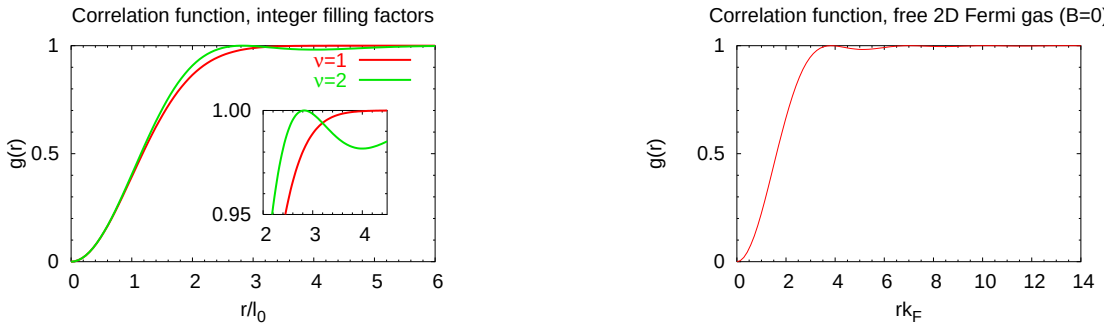

Fig. 10: Density-density correlation in a free 2D electron gas and in magnetic field at integer filling factors (spin-polarized electrons).

It is a pleasant news that by taking the limit $\nu = n \to \infty$ in (45) we obtain

$$g_{FS}(r) \quad = \quad 1 - \left[\frac{2}{k_F r} J_1(k_F r)\right]^2 , \tag{48}$$

which is the correlation function of free electrons in two dimensions (Fermi sea). It should not be anything else because $\nu \to \infty$ with k_F kept constant means that B is decreased to zero at a given areal density of electrons.

Filling factor $\nu = 1/3$

Provided Landau level mixing is absent and considering only the short-range interaction between particles (Sec. 1.3), the ground state at filling factor $\nu = 1/3$ is described by the Laughlin wavefunction $\Psi_L(z_1, \ldots, z_n)$, (7). Up to my knowledge, no *closed* [7] analytical expression of the correlation function in this state is available. Only the short range behaviour can be determined analytically. For $(z_1 - z_2) \to 0$, $|\Psi_L|^2$ vanishes proportional to $(z_1^* - z_2^*)^3 (z_1 - z_2)^3 = |z_1 - z_2|^6$, hence $g(r) = cr^6 + o(r^6)$ for $r \to 0$. Numerically, $\langle \Psi_L | g(r) | \Psi_L \rangle$ can be evaluated by various Monte Carlo techniques, Fig. 11. These results are closer to the thermodynamic limit, referring to larger numbers of particles, than $g(r)$ which can be obtained from exact diagonalization, Fig. 12. This is however only because we know an analytic WF of the GS for arbitrarily large systems in this case, Ψ_L. Exact diagonalization can be performed only for systems with $N_e \lesssim 10$ electrons, but it is not necessary to know anything about the ground state in advance apart of that it lies in the lowest Landau level. Therefore, exact diagonalization provides us a way to confirm that Ψ_L is indeed the ground state or a good approximation to it, e.g. for Coulomb-interacting electrons. Note also that Figs. 12 refer to electrons on torus whereas Fig. 11 refers to the disc geometry. Indeed, the correlation functions are very similar in both geometries, compare Fig. 12(b) and Fig. 11. This fact supports the hypothesis that the corresponding states, Ψ_L on a disc and those on tori, are universal and hence basically the same as the ground state in an infinite 2D system.

The correlation function $g(r)$ in Fig. 12 is rather isotropic, at least on distances smaller than $a/2$. This distinguishes the Laughlin state from a Wigner crystal (Subsect. 2.4.1) or a unidirectional charge density wave in which some special directions exist, Subsect. 2.1.3. This fact motivates also the incompressible *liquid* terminology. Regarding the distinction between liquids and gases, the difference is the strength of interparticle interaction. Whereas negligible in gases, the interaction in liquids is strong compared to kinetic energy. In the lowest Landau level, kinetic energy is zero, or better a constant $\hbar\omega/2$.

The first maximum in $g(r)$ occurs at $r_1 \approx 4.4\ell_0$, Fig. 12b, and this separation can be taken as a typical interparticle distance in the Laughlin state. This distance lies close to the mean interparticle distance determined by the filling factor, $r_{mean}/\ell_0 = \sqrt{2\pi/\nu} \approx 4.35$ (1).

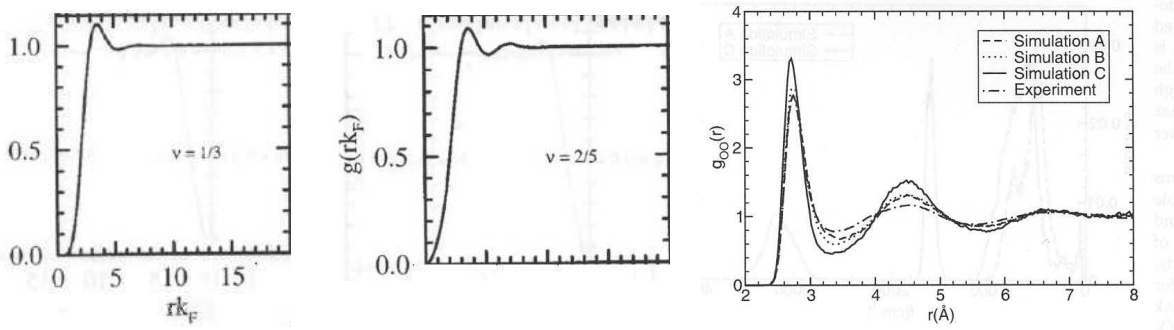

$\nu = \frac{1}{3}$ $\nu = \frac{2}{5}$ Water

Fig. 11: *Left and middle:* Correlation functions of the ground states of 50-60 particles at filling factors $1/3$ and $2/5$ of the principal Jain's sequence, $\nu = p/(2p+1)$ (cf. Subsect. 1.4.2). The wavefunctions (WF) predicted by composite fermion theory were taken (for $\nu = 1/3$ this is identical with the Laughlin WF) and $g(r)$ was calculated by a Monte Carlo method. Taken from Ref. [42]. *Right:* correlation function between oxygen atoms in liquid water as an example of a density-density correlation function in a well-known liquid (see text on p. 30). Results of both numerical simulation and experiments are shown, see the original paper by Allesch *et al.* [9] for details.

After r_1, oscillations in $g(r)$ decay rapidly. The overall form of $g(r)$ in the Laughlin state clearly differs from the correlation function of a free 2D Fermi gas (48). We will emphasise three aspects.

(i) Laughlin state, Fig. 12b: the first peak of $g(r)$ is relatively high, measured for instance by ratio $g(r_1)/g(a/\sqrt{2}) \gtrsim 1.1$. Here $a/\sqrt{2} \approx 10\ell_0$ is the maximum interparticle distance in the considered finite system.

2D Fermi gas, Fig. 10: the first structure of $g(r)$ is about ten times weaker. Here, it is more appropriate to watch the depth of the first minimum, see (ii).

(ii) 2D Fermi gas: all maxima (at r^i_{FS}) of $g(r)$ have the same value, $g(r^i_{FS}) = 1$. Laughlin state: the first maximum $g(r_1) \approx 1.1$ (for $N_e \to \infty$) is much higher than other maxima.

(iii) 2D Fermi gas: $g(r) \propto r^2$ for $r \to 0$. This is purely the effect of Pauli exclusion principle. Mathematically, it comes from the antisymmetry of the wavefunction Ψ, in other words, Ψ is a Slater determinant. Laughlin state: $g(r) \propto r^6$. This is a manifestation of correlations in the state, i.e. of the fact that Ψ_L cannot be written as a single Slater determinant. $g(r) \propto r^6$ also means that any two electrons avoid being close to each other very efficiently and this helps to minimize the Coulomb energy which is high at short inter-particle distances [33], Subsect. 1.3.3.

Just as an illustration, a correlation function $g(r)$ of liquid water is shown in Fig. 11, right. Of course, it is not possible to directly compare water and a 2D electron gas in the fractional quantum Hall regime. Nevertheless, the pronounced structures in $g(r)$ beyond the correlation hole in the Laughlin state, Fig. 11 left, are definitely more similar to $g(r)$ of *liquid* water, Fig. 11, right, rather than to $g(r)$ of a 2D Fermi *gas*, Fig. 10.

The Laughlin state, Fig. 12b, also differs from integer filling factor states apparently, Fig. 10. The latter ones ($i = 1, 2, \ldots$) namely have always $g_{\nu=i}(r) \propto r^2$ at $r \to 0$. Also $g_{\nu=i}(r)$ has exactly $i-1$ maxima, i.e. $g_{\nu=1}(r)$ is free of maxima.

This demonstrates the fact, that in the $\nu_{CF} = 1$ composite fermion (CF) state, which is the model of the $\nu = 1/3$ electronic ground state (Sect. 1.4), the *electron-electron* correlations are different to those in a $\nu = 1$ electronic state. This is a bit counterintuitive, since the CFs were created by adding two zeroes to electrons *in the* $\nu = 1$ *state* and we could have therefore expected that the electrons 'remained at their original positions' under this transformation. Figures 12b and 10 however show that even though the CF density equals the electronic one the electron-electron *correlations* are different in both states.

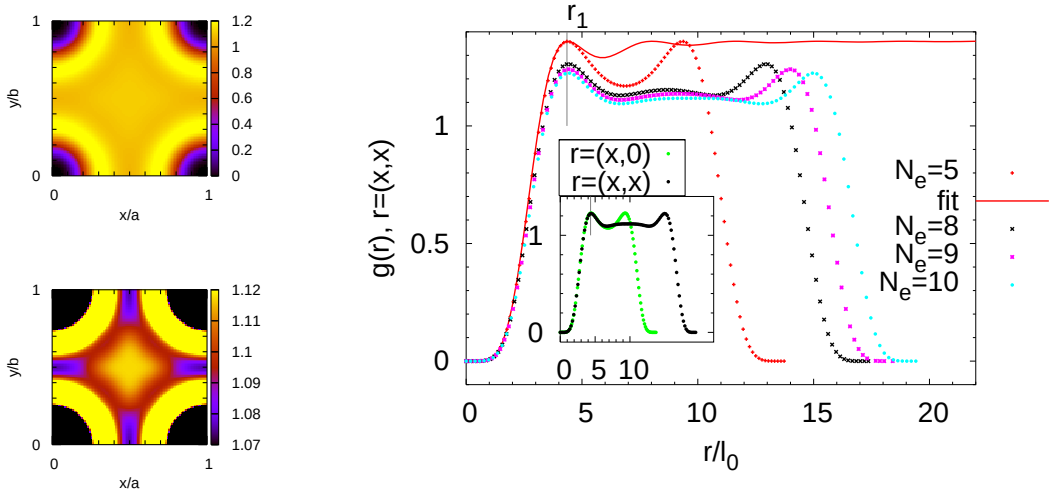

(a) $N_e = 10$. Due to the absence of circular symmetry on the torus, $g(\boldsymbol{r})$ is in general not only a function of $r = |\boldsymbol{r}|$. For $|\boldsymbol{r}| \ll a$, $g(\boldsymbol{r})$ is however quite isotropic, Fig. 12b inset. The first electron is sitting at the corner, the four corners are identical owing to the periodicity. The lower plot differs from the upper one only by a finer z-scale which highlights the structures in $g(\boldsymbol{r})$ at larger distances.

(b) Section of $g(\boldsymbol{r})$ for $N_e = 5, 8, 9, 10$-electron ground states along $\boldsymbol{r} = (x, x)$; the perfectness of match to $g(r)$ in Fig. 11 gives us a feeling how little the ground state is affected by the finiteness of the system. It is noteworthy that $g(r)$ can be astonishingly well fitted by the $[g_{FS}(r)]^3$ (48) up to distances beyond the first maximum (up to vertical scaling, only k_F must be fitted, see the text). *Inset:* sections along diagonal and side of the square, i.e. $g(x/\sqrt{2}, x/\sqrt{2})$ and $g(x, 0)$ for the $N_e = 10$ system. The good match of the two curves as far as well beyond the first maximum ($\approx 6\ell_0$) indicates that the isotropy on length scales $< 6\ell_0$ is not much affected by the rectangular geometry (periodic boundary conditions).

Fig. 12: Correlation functions in the ground state of N_e electrons on a torus (square, length of sides $a = b$, with periodic boundary conditions) at filling factor $\nu = 1/3$. The function $g(\boldsymbol{r})$ gives the probability of finding an electron at position $\boldsymbol{r} = (x, y)$ provided there is an electron sitting at $\boldsymbol{r}' = (0, 0)$. For a homogeneous system the choice of $\boldsymbol{r}'$ does not influence the probability distribution of finding the second electron.

On 'intermediate length scales' (1 to 5 magnetic lengths), the correlation function of the Laughlin state $g(r)$ in Fig. 12b can be strikingly well fitted by

$$c \cdot [g_{FS}(r)]^3 \,, \tag{49}$$

where $g_{FS}(r)$ is the correlation function of a free 2D Fermi gas, (48). Herefore, we put $k_F \approx 0.874\ell_0^{-1}$ which is only by about 7% more than what we would expect for filling factor $\nu = 1/3$, (47).

The quality of the match relies on the choice of $m = 3$ for the exponent in Expr. 49 (for $r \to 0$) and on the fitting constants c and k_F (around $r \approx r_1$). The surprising fact is therefore only the good match *between* $r = 0$ and $r = r_1$. Also note that long-range ($r \gg r_1$) behaviour of expression (49) and of $g(r)$ of the Laughlin state are different. This again emphasises the differences between the Laughlin state and the Fermi gas. Expression (49) provides therefore only another representation of the exchange hole, parallel to approximate formulae given e.g. by Girvin [25].

In conclusion, we have seen that the correlation function of the correlated $\nu = 1/3$ ground state (Fig. 11) has a strong first maximum (near to $4.4\ell_0$) and an unusual exchange hole $g(r) \propto r^6$. These features distinguish the $1/3$ state from both free 2D Fermi gas and completely filled Landau levels and indicate the *liquid-like* and *correlated* nature of the Laughlin state.

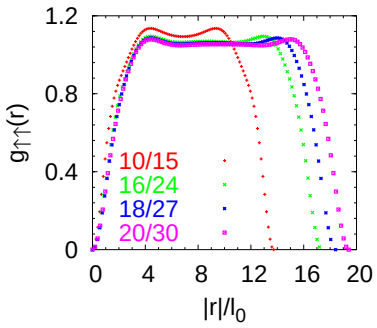

(a) The polarized state.

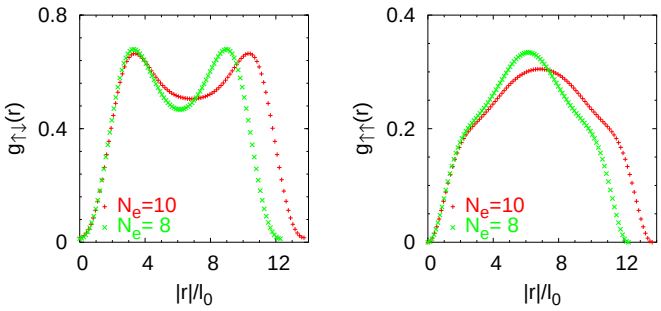

(b) The spin-singlet state: correlation between unlike spins (*left*) and like spins (*right*).

Fig. 13: The $\nu = 2/3$ ground states shown in their correlation functions. Section along the diagonal of the square elementary cell is shown, i.e. $g(r) = g(x/\sqrt{2}, x/\sqrt{2})$ and systems of different sizes are compared.

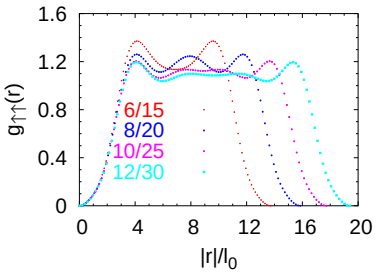

(a) The polarized state.

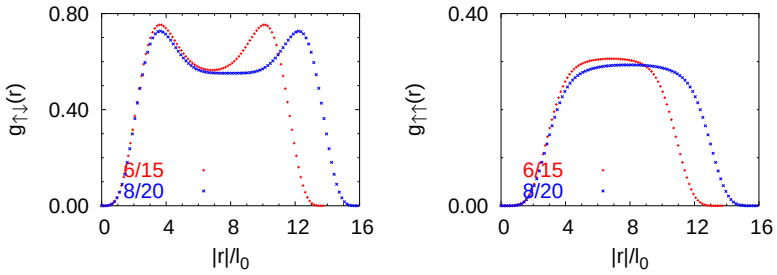

(b) The spin-singlet state: correlation between unlike spins (*left*) and like spins (*right*).

Fig. 14: The $\nu = 2/5$ ground states, correlation functions $g(r) = g(x/\sqrt{2}, x/\sqrt{2})$. Note the good match of peak positions in systems of different sizes.

Filling factor $\nu = 2/3$

Provided the Landau level mixing is absent, the particle-hole symmetry in one Landau level gives a direct relation (isomorphism) between Hilbert subspaces of fully polarized states at $\nu = 2/3 = 1 - 1/3$ and $\nu = 1/3$, Subsect. 1.5.4. Owing to this relation eigenvectors of any radial two-particle interaction are exactly the same[1] in both spaces and corresponding eigenvalues are identical up to a constant shift.

The correlation function in the *fully polarized* $\nu = 2/3$ ground state, Fig. 13a, is thus linked to the one of the Laughlin WF by an analytical formula (41). For a system with N_m flux quanta, i.e. having an area of $2\pi\ell_0^2 N_m$, it reads

$$2/3N_m(2/3N_m - 1)g_{\nu=2/3}(r) = 1/3N_m(1/3N_m - 1)g_{1/3}(r) + 1/3N_m^2 g_{\nu=1}(r)\,. \tag{50}$$

The $g(r) \propto r^6$ short range behaviour is thus obscured by the second term.

[1] In the following sense: Take an eigenvector for $\nu = 1/3$. This is a linear combination of Slater determinants from the $\nu = 1/3$ space. Replace each of them by its particle-hole counterpart and the resulting state from the $\nu = 2/3$ space is an eigenstate.

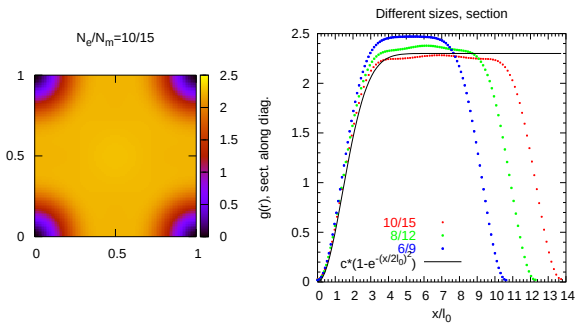

Fig. 15: Different density-density correlation functions in the $\nu = 2/3$ singlet state seem to be related to each other: $g_{\uparrow\downarrow}(r)+g_{\uparrow\uparrow}(r)$ (properly normalized, see text) is very similar to the function $1 - \exp(-r^2/4\ell_0^2)$, the density-density correlation in a full Landau level with $\ell_0\sqrt{2}$ in the place of ℓ_0.

The *spin singlet* ground state at $\nu = 2/3$ has a different character. Here, we can distinguish between correlation functions for electrons of like spin, $g_{\uparrow\uparrow}(r)$, and for electrons of opposite spin, $g_{\uparrow\downarrow}(r)$, Fig. 13. Neither of them bears any apparent resemblance to either the $\nu = 2/3$ or $\nu = 1/3$ polarized ground states. We should like to point out some of their particular features.

(i) The ring-like form of $g_{\uparrow\downarrow}(r)$ suggests that the state consists of pairs of particles with opposite spin with average separation $r_{\uparrow\downarrow} \approx 3.3\ell_0$.

(ii) There is a deep hole in $g_{\uparrow\downarrow}(r)$ around zero. This can*not* be due to Pauli exclusion principle which applies only to electrons of like spin, but rather solely due to Coulomb repulsion. As a check (not presented here), a comparison between $g_{\uparrow\downarrow}(r)$ in Fig. 13 and the 'lowest LL Pauli hole' $g_{\nu=1}(r)$ (46) reveals that their forms are indeed different. Also note that the value of $g_{\uparrow\downarrow}(0)$ is not exactly zero, it is several percent of the maximal value of $g_{\uparrow\downarrow}(r)$, Subsect. 2.1.2.

(iii) There is a well pronounced shoulder in $g_{\uparrow\uparrow}(r)$ around $r \approx 2\ell_0$. It is very suggestive, how well this shoulder can be fitted by the correlation function of a full lowest LL, $g_{\nu=1}(r)$, i.e. the lowest LL exchange hole (46). This is shown in Fig. 16a.

This feature reminds of the relation between $1/3$ and $1 - 1/3$ systems (50). This is also supported by the fact, that after the shoulder is subtracted [$g_{\nu=1}(r)$ times a constant], the remaining part of $g_{\uparrow\uparrow}(r)$ is $\widetilde{g}(r) \propto r^6$ at short distances (Fig. 16a), just as it is the case in the $1/3$ Laughlin state. However, particle-hole conjugation between filling factors $1/3$ and $2/3$ is applicable only for spin-polarized states.

(iv) The sum of $g_{\uparrow\uparrow}(r)$ and $g_{\uparrow\downarrow}(r)$ properly scaled for $N_e \to \infty$ lies very close to $g_{\nu=1}(r)$ with ℓ_0 substituted by $\ell_0\sqrt{2}$, Fig. 15. Proper scaling means that $g_{\uparrow\uparrow}(r)$ and $g_{\uparrow\downarrow}(r)$ should have the same norm, e.g. equal to one, in sense of (44). With the current notation (43) this is true only for $N_e \to \infty$.

Therefore, if spin is disregarded, the singlet ground state at $\nu = 2/3$, created by magnetic field B, strongly resembles the state of a completely filled lowest LL at magnetic field $B/2$.

Summary: the *polarized* ground state at $\nu = 2/3$ is the particle-hole conjugate of the Laughlin state at $\nu = 1/3$. The electronic correlation function of the $2/3$ state reproduces the liquid-like maximum at $r_1 \approx 4.4\ell_0$ but the $\nu = 1/3$ broad exchange hole with $g(r) \propto r^6$ is hidden behind the lowest LL exchange hole, $g_{\nu=1}(r)$.

The *singlet* GS seems to consist of pairs of spin up and spin down electrons with characteristic size of $3.3\ell_0$. Together with the sum rule, point (iv) above, this could be interpreted as that N_e electrons in the singlet GS form $N_e/2$ pairs, each with total $S_z = 0$ and these pairs form the same state as $N_e/2$ fermions at $\nu = 1$ in the ground state.

In particular, it should be emphasised that the singlet state can*not* be described as a mixture of two mutually uncorrelated $\nu = 1/3$ Laughlin liquids, one with spin up, another with spin down, as we could wrongly infer from the picture of non-interacting composite fermions, see comment [8].

Filling factor $\nu = 2/5$

This filling factor should be the counterpart to $\nu = 2/3$ within the CF picture. The two magnetic fluxes are attached parallel rather than antiparallel to the effective magnetic field and in both cases the CF filling is two (Sect. 1.4). In spite of this relation the density-density correlations between electrons show significant differences.

The correlation hole of the *polarized* ground state (Fig. 14a or Fig. 11, middle) is much broader for $\nu = 2/5$. The first maximum occurs in both systems ($2/5$ and $2/3$) at about the same distance $\approx 4.1\ell_0$, it is however much better pronounced in the $2/5$ system and also more structure is present beyond the first maximum here. Around $r = 0$ both systems follow $g(r) \propto r^2$. However, whereas $g(r)$ for $\nu = 2/3$ is dominated by the 'exchange hole', i.e. $g_{\nu=1}(r)$, cf. (50), the $2/5$ state has a much broader minimum around $r = 0$.

These findings are not unexpected. Consider two systems of the same area $2\pi\ell_0 N_m$, one at fillings $2/3$ and $2/5$, respectively. The latter will be more diluted ('emptier'), since it contains only $2/5N_m$ electrons, compared to $2/3N_m$ in the $\nu = 2/3$ system (1). Therefore, the correlation hole in $g(r)$ can be broader in the $2/5$ system. This conclusion is not a controversy of the CF picture, rather, it is a warning. By far not all claims which are true for electronic Landau levels (e.g. $\nu = 2$ state remains the same regardless of the direction of the magnetic field) are true for composite fermions as well (it matters whether B_{eff} is pointing parallel and antiparallel to the attached flux quanta).

There is also a close relation between the polarized $2/5$ GS and the Laughlin $1/3$ state according to the CF picture. The latter one corresponds to filling factor one, the former one to filling factor two of composite fermions. Comparing these two states, we find a bit stronger structures in the density-density correlation of the $\nu = 2/5$ GS and also the first maximum shifts to smaller distances ($4.4\ell_0$ at $\nu = 1/3$ and $4.1\ell_0$ at $\nu = 2/5$). Both effects are quite similar to what happens when going from $\nu = 1$ to $\nu = 2$, cf. Figure next to (46). Comparing the $\nu = 2$ and $2/5$ systems, we again (cf. $\nu = 1$ and $1/3$) find much stronger structures of $g(r)$ in the latter case, just as we expect for a liquid state.

Some marked differences occur also in the *singlet ground states* at both filling factors. At $2/5$, correlation functions $g_{\uparrow\uparrow}(r)$ as well as $g_{\uparrow\downarrow}(r)$ seem to be quite flat beyond $r_m \approx 6\ell_0$. We may speculate that the same is true for the filling $2/3$, Fig. 14 (the shoulder in $g_{\uparrow\uparrow}$ would probably have to be subtracted first), but then the plateau would occur first beyond some larger distance r_m which is not accessible by exact diagonalization.

It is remarkable that after subtracting the shoulder from $g_{\uparrow\uparrow}(r)$ of the $2/3$ singlet state (point (iii) in the discussion of $2/3$), the rest $\widetilde{g}(r)$ is $\propto r^6$ near to $r = 0$. This is the same behaviour as we find in $g_{\uparrow\uparrow}(r)$ of the $2/5$ singlet state, see Fig. 16.

Correlations of unlike spins exhibit one clear maximum which is, as compared to $2/3$, slightly but perceptibly shifted to a bit larger $r_{\uparrow\downarrow} \approx 3.7\ell_0$. This agrees with the above argument that $2/5$ systems are more diluted than the $2/3$ ones, but quantitatively this shift is too small. It is only $\approx 30\%$ of what we would naively expect from comparing the areal electron densities.

Finally, the $r \to 0$ behaviour of the $2/5$ singlet state, $g_{\uparrow\downarrow}(r) \propto r^4$ and $g_{\uparrow\uparrow}(r) \propto r^6$, matches the behaviour of the $\{3, 3, 2\}$-Halperin wavefunction (8) and this $\Phi_{332}[z]$ is in turn identical with the ground state wavefunction proposed by Jain's theory, Subsect. 1.4.2. This is because $\Phi_{nn'm}[z]$ lies completely in the lowest LL and thus the last step of Jain's procedure, namely the projection to the LLL, is out of effect. Seen from the opposite direction: the singlet $2/5$ state corresponds to filling only the lowest CF LL spin up and spin down.

Summary: From the viewpoint of composite fermion theories, the *polarized* $2/5$ state ($p = 2$), Tab. 2, is related both to the $1/3$ Laughlin state ($p = 1$) and $2/3$ polarized ground state ($p = -2$). The electron-electron correlations in exactly diagonalized systems clearly support the former relation, the latter one ($2/5$ with $2/3$) is however far from being obvious in this way.

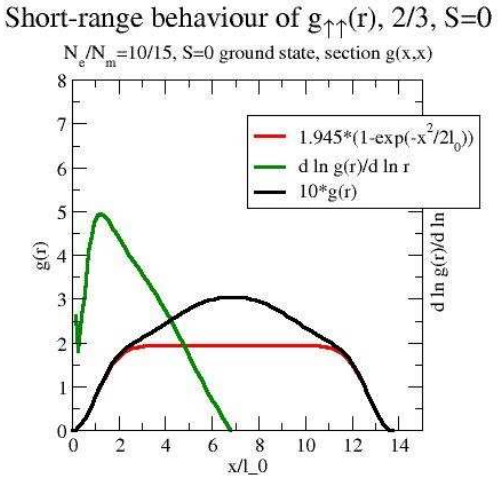

(a) Filling factor $2/3$. The shoulder at $r \approx 2\ell_0$ is apparently caused by a term proportional to $1 - \exp(-r^2/2\ell_0^2)$, i.e. $g_{\nu=1}(r)$, cf. (46), which contributes to the total $g_{\uparrow\uparrow}(r)$. After this term was subtracted, a local power analysis of $g_{\uparrow\uparrow}(r)$ has been performed.

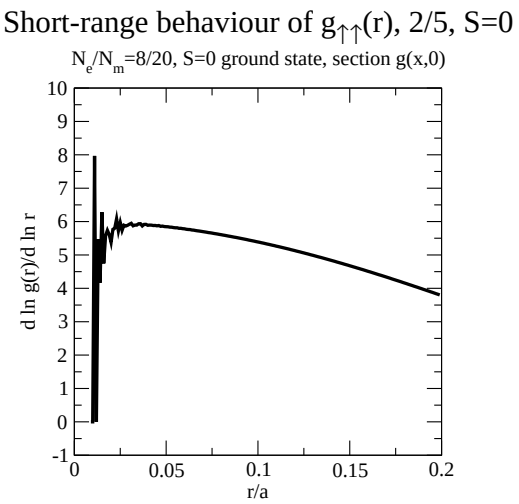

(b) Filling factor $2/5$. Local power analysis near to $r = 0$. Noise at very small distances is purely due to numerical inaccuracies: values of $g(r)$ are already very small there.

Fig. 16: Correlation of like spins, $g_{\uparrow\uparrow}(r)$, of the singlet ground states at filling factors $2/3$ and $2/5$. Local power analysis (51) shows, that both correlation functions are $\propto r^6$ for $r \to 0$; however, the shoulder in the state at filling factor $2/3$ has to be subtracted first.

Neither is the analogy between $2/5$ and $2/3$ apparent for the *singlet* ground state. Although similarities exist, perhaps most importantly pairing between electrons of unlike spin, short range behaviour of correlation functions is very different.

2.1.2 Ground state for Coulomb interaction and for a short-range interaction

Short-range interactions as they were introduced in Section 1.3 have a special significance for the FQHE. It has been repeatedly emphasised that the Laughlin WF is on one hand an *extremely good* approximation of the ground state of a Coulomb-interacting (CI) system while on the other hand, it is the *exact* ground state of electrons feeling only a short-range mutual interaction (SRI) as it was defined in section 1.3. Consequently, it is very popular to say that a short-range interaction Hamiltonian captures the essential physics of the FQHE by inducing the correct correlations in the ground state. By the correct correlations we mean the $\Psi \propto (z_i - z_j)^3$ behaviour when two particles approach each other.

The SRI was used in most of the calculations presented in this work. This choice has been made for two reasons. It brings better chances in finding analytical results like the Laughlin WF. Moreover we may hope that the results in finite systems converge faster to the thermodynamical limit ($N \to \infty$) because the electrons see only as far as their interaction reaches and thus – sooner than for a long-range interaction – they will not 'realize' anymore that they live on a torus and not in an infinite plane. Aim of the following section is to show and discuss how the ground states at $\nu = 2/3$ change if the character of the interaction changes.

The ground state energies for CI and SRI are naturally quite different. This is however for the largest part only an unessential shift, a part of it is the missing Madelung constant (34). Under SRI an electron of

course cannot interact with its own image in the neighbouring primitive cell. More importantly, the gap energies are quite similar in both cases, Subsect. 3.2.1.

Since the density of the incompressible ground states should always be constant, up to finite size effects to be discussed later, let us now focus on correlation functions. The three plots in Fig. 18 show $g_{\uparrow\uparrow}(r)$ and $g_{\uparrow\downarrow}(r)$ of the singlet state and $g(r)$ of the polarized state. In all three cases, the correlation functions of the CI state and the SRI state are quite similar. Most apparent differences appear at large distances. On a torus, the largest possible separation between two electrons is $r = a/\sqrt{2}$. On the other hand, the correlation functions are very precisely identical for small r. This shows that, e.g. in the polarized GS, the wavefunction contains the factor $(z_i - z_j)^3$ for CI as well as for SRI. In other words, the Laughlin state (as the GS for SRI) describes *exactly* the short-range behaviour of an incompressible state of even long-range interacting electrons. Fig. 18 demonstrates that this is true (at least in a very good approximation) also for other ground states where the analytical wavefunction is not available (e.g. the singlet GS).

In fact, for the singlet GS there is a tiny but perceptible difference in $g_{\uparrow\downarrow}(0)$ for the two types of interaction. Since $g_{\uparrow\downarrow}(0)$ is almost zero, this observation suggests that a yet modified interaction might lead to analytical results, $\{V_0, V_1, \ldots\} = \{\infty, \alpha, 0, 0, \ldots\}$ in terms of pseudopotentials, Sect. 1.3. Such an interaction enforces $g_{\uparrow\downarrow}(0) = 0$, which is anyway almost fulfilled for the current SRI, and on the other hand it retains the pleasant property of SRI in polarized systems, i.e. it is one-parametric.

There is yet another significant difference between SRI and CI which is not obvious in Fig. 18 at first glance. The difference concerns the placement of zeroes in the wavefunction and we will concentrate on the $\nu = 1/3$ ground state now (see Sec. 1.3).

In a general fermionic state, there must always be a zero bound to each electron in order to fulfil the Pauli exclusion principle: two electrons (of the same spin) cannot be at the same point in space simultaneously, *ergo* if $z_1 = z_i$ then the wavefunction must vanish. Factors $(z_i - z_j)^3$ in the Laughlin state mean that there are two extra zeroes exactly at the position of each electron. That is why $g(r) \propto r^6$ for small r's, Fig. 17, right and (51). For CI, the Laughlin WF is only an *approximation* to the ground state. In the real ground state, the one obligatory zero is still sitting on each electron and the two others are only near rather than exactly on the top of the electron. In Fig. 17 we can even see how far they are on average. These two extra zeroes are now mobile and their position depends on the position of all other electrons. Note that this distance depends on the system size [53].

Local power analysis

A comment is due on the way how the plots in Figs. 17,16 were obtained. It is basically a section of $g(r)$ along one straight line going through $r = 0$. This function was then transformed by

$$g(r) \;\longrightarrow \frac{\mathrm{d}\ln g(r)}{\mathrm{d}\ln r} \tag{51}$$

which gives a local degree of the polynomial behaviour. Let us give an two examples. If $g(r)$ were αr^n then $\mathrm{d}\ln g(r)/\mathrm{d}\ln r = n$. If $g(r) \propto (r - r_0)^n$ then $\mathrm{d}\ln g(r)/\mathrm{d}\ln r = nr/(r - r_0) \to n$ for $r \gg r_0$. In other words, if there is a dominant r^n term in $g(r)$, the quantity plotted in Fig. 12(b) gives the exponent. Of course, it is only approximate except for the case $g(r) = \alpha r^n$ but it is quite easy to evaluate and moreover it gives a global property of the wavefunction as compared to fixing electron positions $z_2, \ldots, z_n$ and examining the WF as a function of z_1 where results depend on where we fix the electrons $z_2, \ldots, z_n$.

2.1.3 Some excited states

There is a rich variety of excitations to the incompressible FQH states. For instance quasiholes, excitons (quasihole-quasielectron pairs), charge density waves (CDW) or spin density waves (SDW), all of them can be described analytically (at least to some extent), and then of course all the rest of excitations which

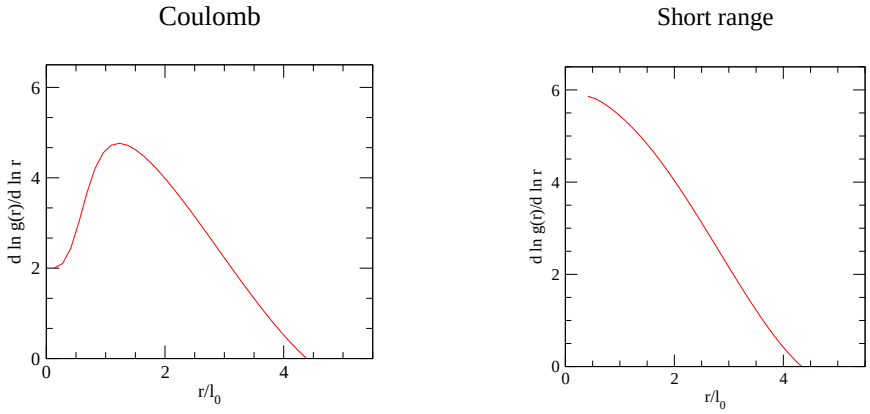

Fig. 17: The incompressible ground state at $\nu = 1/3$ (with ten electrons), Coulomb interaction (left) and a short-range interaction (right). Section through the density-density correlation function $g(r)$ along $r = (x, x)$ is taken and the 'local degree' of the polynomial behaviour is determined (see the text). While the local behaviour around $r = 0$ is $g(r) \propto r^6$ for the SRI, indicating that there is exactly a **triple** ($6 = 2 \cdot \mathbf{3}$) zero of the wavefunction on on each electron, we can clearly see only **one** zero at each electron's position for the Coulomb interaction, $g(r) \propto r^2$ and $2 = 2 \cdot \mathbf{1}$. However, going away from $r = 0$, the 'local degree' grows and beyond $\approx 1.5\ell_0$ it approaches the curve of the SRI state. The conclusion is that one zero (the obligatory Pauli exclusion principle zero) is fixed to each electron ($r = 0$) in the Coulomb state and the other two zeroes are only loosely bound to the electron. First from distances $\gtrsim 1.5\ell_0$ this compound object looks like an electron with two attached flux quanta.

has not been understood up to now. Following the introduction given around (28), we will now demonstrate how to identify some of these excitations in spectra obtained by exact diagonalization at the example of $\nu = 1/3$.

Charge density waves

CDWs can be excited for example in the liquid GS at $\nu = 1/3$. Disregarding the possibility of spin flips (as it may be reasonable when Zeeman energy is too high), it turns out that these are the lowest excitations.

In Fig. 19 spectra of several short-range-interacting $\nu = 1/3$ systems (tori of different sizes) are presented. The horizontal axis is modulus of k^r, i.e. the 'crystallographic k-vector' described in Subsec. 1.5.2. The Laughlin state has $k^r = 0$ and a CDW of wavevector Q excited from this state has $k^r = Q$. Beware however, that not every state which has $k^r \neq 0$ must be a charge density wave! Apart from other possible periodic excitations, there are also basically nonperiodic excitations (e.g. quasiholes) and such states are forced into periodicity only 'artificially' by the periodic boundary conditions imposed in our exact diagonalization model.

The lowest excitations in Fig. 19 form a well developed branch $E(k^r)$, which is usually called *magnetoroton branch*, and other excited states form a quasicontinuum. The dispersion of the magnetoroton branch can be calculated analytically in the single mode approximation. The original calculation by Girvin *et al.* [27] for *Coulomb* interacting systems at $\nu = 1/3$ showed a well pronounced minimum in $E(|k^r|)$ of the magnetoroton branch at $k^r\ell_0 \approx 1.4$. In a short-range interacting system, shown in Fig. 19, the situation is slightly different. Having reached its minimum value, $E(|k^r|)$ remains constant beyond $k^r\ell_0 \approx 1.4$.

A point worth of emphasis is that the magnetoroton branch in Fig. 19 contains points (energies) from exactly diagonalized systems of *different* sizes. This confirms our hope that these states are not bound to some particular geometry of the elementary cell and that they appear also in an infinite system.

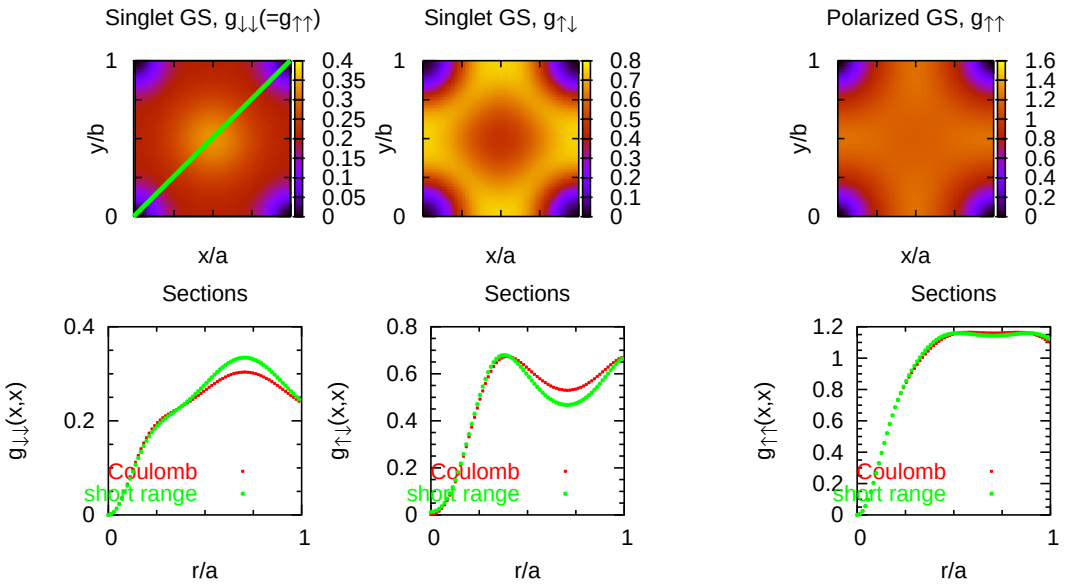

Fig. 18: Correlation functions of the singlet and polarized ground states at $\nu = 2/3$: comparison between the Coulomb and short-range interaction. The curves are identical for small r and slight deviations occur at longer scales. This is another way to demonstrate that it is sufficient to consider short-range interaction in order to get (almost) correct ground states under FQHE conditions.

Dealing with finite systems, we will always have only a finite, and usually quite small, number of allowed values for k^r (27). On the other hand, the more points in k^r-space we can access, the better we can recognise modes in exact diagonalization spectra, just like the magnetoroton branch in Fig. 19. Note also the large space between $k^r = 0$ and the next smallest $|k^r| \approx 0.5\ell_0^{-1}$ in Fig. 19 which corresponds to the longest wavelength compatible with the periodic boundary conditions.

The traditional way to improve these limits (few k^r-points, too large smallest $|k^r| > 0$) is to study larger systems. This is however prohibitively difficult with exact diagonalization. An alternative approach may be to study systems with aspect ratios $\lambda = a : b$ slightly deviating from one. This allows us to deform the lattice of allowed k^r-points continuously (27 contains λ), and on the other hand, we can expect that the states will not suffer from the *slight* asymmetry in $a : b$ in line with the argument that these states are not bound to any particular geometry of the elementary cell. This method is demonstrated in Fig. 19 by the blue points. The aspect ratio was varied from one up to 1.3. Since the energies of the CDW states still lie well on the magnetoroton branch, we can conclude that this variation was still only a small perturbation, i.e. acceptable for studying this branch. A more reliable critierion would be to check overlaps of wavefunctions at $a : b = 1$ and $a : b > 1$.

Correlation functions of several states in the magnetoroton branch (Fig. 19) are shown in Fig. 20. The first look at $g(r)$ (upper row in Fig. 20) may be sometimes not enough to distinguish their charge density wave nature. The CDW is superimposed on the structure of the mother Laughlin state, which these states are an excitation of. The periodic structure of $g(r)$ is thus more clear if we subtract the corresponding correlation function of the Laughlin state first, Fig. 20 lower row. We can find three periods in y direction (horizontal waves at $x = 0, 0.3$ and 0.6) in the state A or 4 periods in y and one period in x in the state C, in agreement

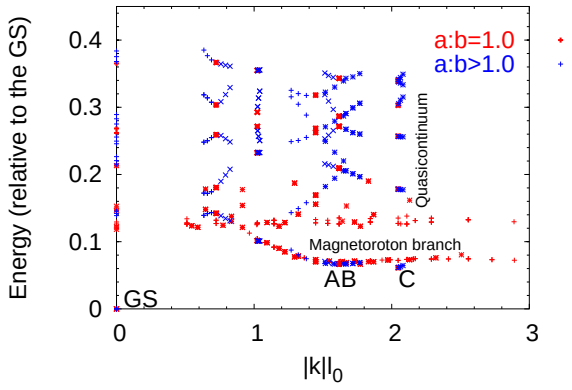

Fig. 19: The ground state (at $k = 0$) and low excitations in SRI fully polarized $\nu = 1/3$ systems of different sizes (4-10 electrons). Energy plotted against the $|k^r|$, see Sec. 1.5.2. To be able to study more points in k space, systems of different sizes are compared and also systems with aspect ratios slightly varying from one, see text. Note the well pronounced magnetoroton branch. Note that energies calculated in systems of *different* sizes lie on the *same* branch indicating that these states are not much system-size-dependent (and therefore relevant even in infinite systems). The correlation functions for three states lying on this branch (A,B,C) are depicted in Fig. 20.

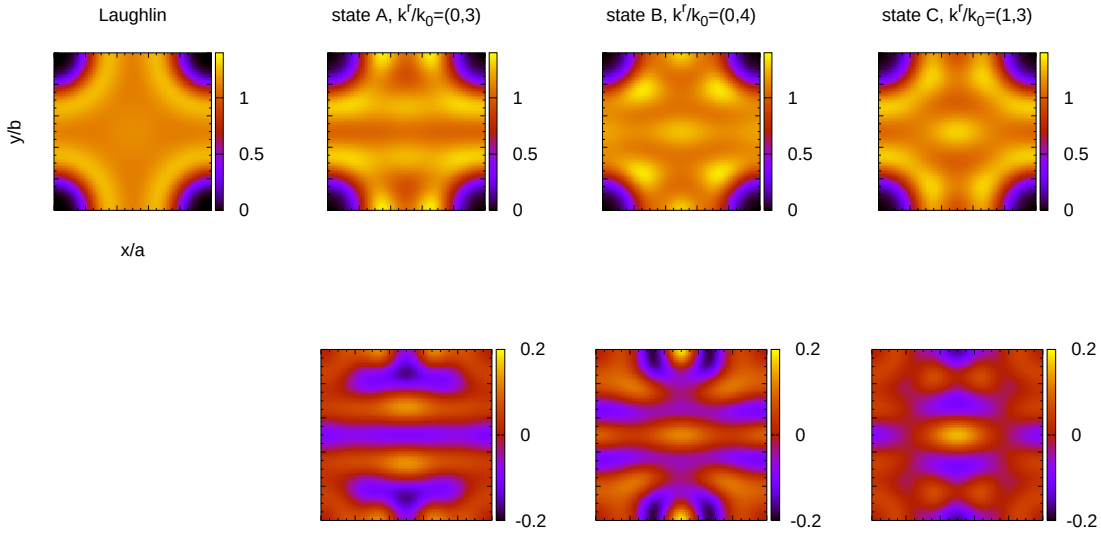

Fig. 20: Correlation functions of the ground state (Laughlin) and several CDW states which lie on the magnetoroton branch of a $\nu = 1/3$ system with short-range interaction (eight electrons). *Upper row:* correlation functions $g(r)$, *lower row:* $g(r)$ of the CDW states from which the Laughlin state $g(r)$ has been subtracted.

with their values of $\widetilde{k}^r/k_0 = \widetilde{k}^r/(N_m\pi/6)$. Note, that it is harder to distinguish the periodic structure in the $\widetilde{k}^r = (0, \pi)$ state (B), which may be partly because this is a point of high symmetry in $\widetilde{k}^r$-space, Fig. 6. In conclusion, we have shown how (the best known type of) charge density wave states on a torus can be identified in the exact diagonalization spectra and in correlation functions. Generally, we can expect that charge density waves excited from incompressible liquid states will form branches in $E(|k^r|)$, provided of course that their energy is not hidden in a quasicontinuum of other excited states. Correlation functions show indeed the expected periodicity of a CDW superimposed on the structure of the ground state.

2.1.4 Finite size effects

Consider a $\nu = 1/3$ system with its exact GS written as Ψ_L, the Laughlin wavefunction (WF), see (7). Particle density in the state Ψ_L is very precisely constant provided we stay within the disc of radius $\ell_0\sqrt{2\pi \cdot 3N}$. The first striking observation is that the density of the ground state obtained from exact

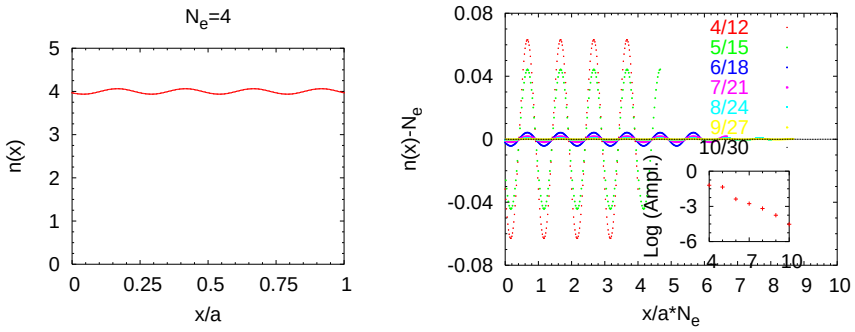

(a) Inhomogeneous density in an $N_e = 4$ system.

(b) Comparison between systems of different sizes. Note the scaling of the x axis.

Fig. 21: Density of the $\nu = 1/3$ incompressible ground state as obtained in torus geometry for different system sizes. The oscillations can be traced back to the centre-of-mass part of the wavefunction. As far as this effect is considered, differences between Coulomb interaction and short-range interaction are small.

diagonalization varies quite strongly, Fig. 21. At the same time we notice that the ground state, which is claimed to be incompressible, hence non-degenerate, is actually triply degenerate.

Fortunately, this does not mean that finite size calculations are completely wrong. Both facts can be attributed to the centre-of-mass part of the wavefunction (CMWF) which is *not* present in Ψ_L but *is* present in numerical calculations, Subsec. 1.5.2. As far as isotropic states are considered, this seems to be the most serious effect coming from the finite-sizedness of the system and in the following we will discuss its origin and how it can be eliminated.

Centre-of-mass part of the wavefunction

The complete WF of the Laughlin state at $\nu = 1/3$ (for n particles) in the disc geometry (Subsec. 1.2, 1.5.1) might be

$$\Psi_{1/3}(z_1,\ldots,z_n) = \underbrace{F(Z)\exp(-|Z|^2/2\ell_0^2)}_{\Psi_{CM}(Z)} \times \underbrace{\exp\big(-(|z_1|^2+\ldots+|z_n|^2)/4\ell_0^2\big)\prod_{i<j}(z_i-z_j)^3}_{\Psi_L(z_1,\ldots,z_n)} \quad (52)$$

with $Z = z_1 + \ldots + z_n$ and for example $F(Z) = Z^3$ or any other analytic function with three zeroes Z_1, Z_2, Z_3. The CMWF Ψ_{CM} has the form (Sec. 1.5.1) of a WF for one particle somewhere in the lowest Landau level to which a single variable Z is attributed. In torus geometry, the WF must be changed in order to comply with periodic boundary conditions (PBC) which amounts to replacing $(Z - Z_i)$ terms by theta functions of the same argument, Subsec. 1.5.2. Example of Ψ_{CM} obtained from the numerically calculated ground state Ψ_{GS} in a system with four particles is shown in Fig. 22a. The CM part was extracted from the complete WF by the scheme $\Psi_{CM}(4\Delta) = \Psi(z_1+\Delta,\ldots,z_4+\Delta)/\Psi(z_1,\ldots,z_4)\Psi_{CM}(0)$. Note that this result fully matches what we expect from analytic considerations, α in Fig. 5a.

If we calculate quantities like the density or correlation function in the state $\Psi = \Psi_r\Psi_{CM}$, we evaluate integrals of the type

$$n_{\Psi_r\Psi_{CM}}(z) = \int \mathrm{d}z_1\ldots\mathrm{d}z_n |\Psi_r(z_1,\ldots,z_n)|^2 |\Psi_{CM}(z_1+\ldots+z_n)|^2 \delta(z_1-z)\,. \quad (53)$$

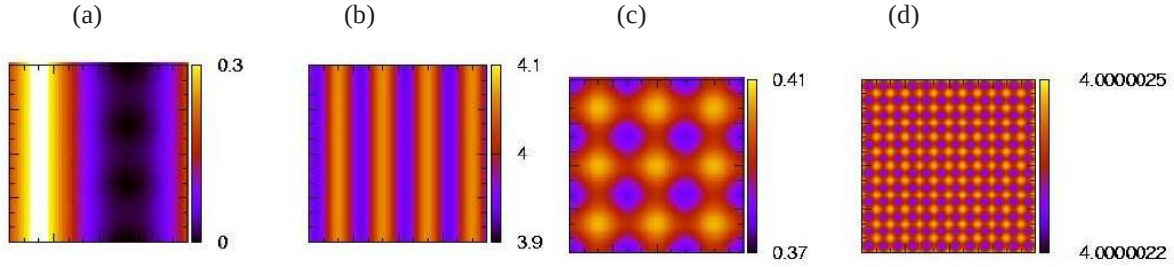

Fig. 22: *Left to right:* (1) $|\Psi_{CM}(Z)|^2$, $Z = z_1 + z_2 + z_3 + z_4$ for one of the three degenerate ground states in a 4 particle $\nu = 1/3$ system and (2) the density $n(r)$ of this state. (3) $|\Psi^1_{CM}(Z)|^2 + |\Psi^2_{CM}(Z)|^2 + |\Psi^3_{CM}(Z)|^2$ of those three states and (4) the sum of their densities (divided by three). Note that the last density is nearly constant (as it should be for the Laughlin state) and thus by adding up densities of the three states differing only in the CM part, we eliminated the effect of the CM part of WF.

Recast in CM and relative variables, this integral is a multidimensional convolution of Ψ_{CM} and Ψ_r. Assuming that Ψ_r is isotropic but non-constant which is true for the Laughlin WF, the function $n(z/4)$ can be thus shown to have the same periodicity as $\Psi_{CM}(z)$. Less exactly but in more illustrative terms: $n(z)$ is basically a smeared $|\Psi_{CM}(4z)|^2$. Note that this explains why $n(z)$ varies much stronger along x than along y.

These considerations can be summarized in the following way. Even though e.g. the Laughlin state is translationally invariant, the CM part of the wavefunction which is always present in the exact diagonalization studies, will cause the density to be inhomogeneous. Consider eigenstates of J. This determines the form of Ψ_{CM} to be as in Fig. 22a, cf (30) the density $n(z)$ of an N_e-electron state (a) will be $1/N_e$ periodic along x, Fig. 21 or Fig. 22b, (b) will be $1/3N_e$ periodic along y, Fig. 22d, (c) will be modulated much stronger along x than along y (compare scales in Fig. 22b and 22d) and (d) will rapidly converge to a constant for $N_e \to \infty$.

Similar ideas have first been presented by Haldane and Rezayi [32].

How to suppress the effect of the CM part of the WF

To suppress the effect of the CMWF it would be ideal to calculate the density as

$$n_{\Psi_r}(z) = \int \mathrm{d}z_1 \ldots \mathrm{d}z_n |\Psi_r(z_1, \ldots, z_n)|^2 \delta(z_1 - z)$$

rather than by (53). In other words, it would be nice if we could replace $\Psi_{CM}(z_1 + \ldots + z_n)$ by a constant in the numerically calculated wavefunction $\Psi_r \Psi_{CM}$.

Even though we could numerically calculate Ψ_{CM} and then calculate the density in the state Ψ/Ψ_{CM}, this is technically quite labourious and requires numerical evaluation of $(n-1)$-fold integrals. Instead we can make a trick. Consider again the example of the $\nu = 1/3$ GS. The state is triply degenerated in the CM part and the three different $\Psi^{1,2,3}_{CM}$ (as they come from ED in subspaces with sharp J) have the pleasant property that the sum of their squared moduli is nearly constant, or in a more restrained (and honest) terminology, its variations are much weaker than those of individual $|\Psi^i_{CM}|^2$, Fig. 22.

With this in mind we expect that the sum $n_{\Psi^1_{CM}\Psi_r}(z) + n_{\Psi^2_{CM}\Psi_r}(z) + n_{\Psi^3_{CM}\Psi_r}(z)$ will be a good approximation to $n_{\Psi_r}(z)$. The reader may check with Fig. 22 how well this is fulfilled.

Other finite size effects

Here, we will try to abstract from the effects due to the CM part of the calculated wavefunctions. Since the operator for density-density correlation depends only on relative coordinates we expect that $g(r)$ will be

free of the finite size effects described in previous paragraphs. Since the curves for $g(r)$ obtained from the $\nu = 1/3$ ground state in systems of different sizes (Fig. 12b) match very well for $|r|$ going at least to one third of the elementary cell we may have good confidence in these results even within the scope of infinite systems. In clear terms, we may believe that $g(r)$ of the infinite system is nearly the same as $g(r)$ obtained in a finite system (with $a : b = 1$) as far as up to $r \approx 0.35a$.

Another type of finite size effects which are 'finer' than those originating from the CM part of the WF is shown in Fig. 22, the rightmost plot. The density plotted should be constant after averaging over the three states degenerated in the CM part in the infinite system. The weak $(1/N_m)$-periodic structure ($N_m = 12$ in Fig. 22) which we still observe reflects the quantization of one particle momenta by the PBC. One particle can be localized only around one of N_m discrete set of points in the x-direction. This effect is the same along x and y, since we have lost the quantum number J (30), by averaging over the three states, belonging to $J = 2, 6, 10$ in the present case. Note, how extremely small this finite size effect is.

2.1.5 Conclusion: yet another comparison to composite fermion models

For a large part we were concerned with the $\nu = 1/3$, $2/3$ and $2/5$ incompressible ground states in this section. All these states, including their possible spin polarizations, can be described in terms of Landau levels (LL) filled with composite fermions (CF), Fig. 9a and Sec. 1.4. In particular, wavefunctions suggested by Jain, Subsec. 1.4.2, are very close to the many-electron ground states calculated by exact diagonalization, as it is demonstrated by comparing the wavefunctions calculated by the two approaches in terms of overlaps which approach unity [77] or of correlation functions shown in this Section, Figs. 11, 12 and 14a.

However, we have seen in this Section that this picture is not as intuitive as someone may believe. Correlation functions of states with p filled CF LLs are quite different from those of states with p filled electronic LLs. Changing orientation of the effective magnetic field following from the CF LL 'quantization' alters the correlation functions drastically. It is hard to establish a relation between the ground states at $\nu = 2/3$ and $2/5$ on the level of comparing the *electronic* correlation functions. We should also mention a discrepancy in the CF model for the $\nu = 2/3$ polarized state. It is both a particle-hole conjugate to the $\nu = 1/3$ Laughlin state and a state with two filled CF Landau levels and effective magnetic field antiparallel to the real magnetic field or attached flux quanta. As Wu, Dev and Jain [77] noted already in their original work about antiparallel flux attachment, these two approaches give two non-equivalent microscopic wavefunctions. Surprisingly enough, both wavefunctions have high overlaps (≈ 0.99) with the polarized ground state obtained by exact diagonalization [77]. Thus, either both models are in fact indeed equivalent or this result shows that even such high overlaps may be not enough to prove the correctness of a trial many-body wavefunction.

Another point worth of notice is that the 'CF cyclotron energies' (sometimes denoted by $\hbar\omega_{CF}$) extracted from exact diagonalization with electrons are not quite the same in $2/3$ and $2/5$ systems, Fig. 23, the scaling factor $5 : 3$ makes B_{eff} equal in both systems. In the picture of non-interacting CFs, only the direction of the effective field B_{eff} is reversed. Thus, if B_{eff} has the same modulus in both cases and Zeeman energy vanishes then $E_p(N_e = 8) - E_u(N_e = 8)$, i.e. the difference of energies of the polarized and singlet GSs for 8-electron systems, should be equal to four times the CF cyclotron energy in the both systems (cf. Fig. 9b). In the exact diagonalization spectra of $N_e = 8$ systems are regarded, the difference of $\hbar\omega_{CF}$ for $\nu = 2/3$ and $2/5$ is small, about 5%, Fig. 23. However, the quantitative agreement becomes worse when we attempt to extrapolate the energies to larger systems.

Also comparing $2/5$ to $2/3$, differences in the lowest excitations from the polarized and singlet ground states (energies, quantum numbers) are quite apparent, Fig. 23.

All these facts demonstrate that it can be misleading to think of the $2/3$ and $2/5$ states as of an exact copy of Landau levels completely filled with electrons. Composite fermion models must be taken seriously since they provide us with many very good predictions (explicite forms of wavefunctions, e.g.) but apart of that

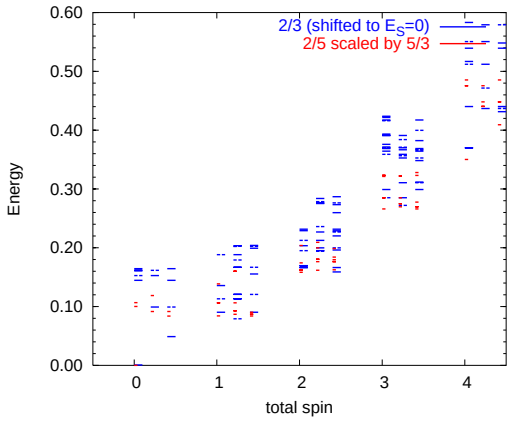

Fig. 23: Spectra of the $\nu = 2/3$ and $2/5$ systems with eight electrons, zero Zeeman energy (SRI). Energies have been shifted to set the singlet GS in both systems to zero energy. In the picture of non-interacting composite fermions, the energies of the polarized ($S = 4$) ground states (the $2/3$ and $2/5$ ones) should then be the same when B_{eff} is correctly rescaled (the indicated scaling of $5/3$). For each spin, the levels are sorted according to the orbital quantum number J (30), which can take on three non-equivalent values (left to right): $0, 1, 2$.

they are not exact, they fail to describe some phenomena like e.g. position of zeroes in Coulomb interacting states, Subsect. 2.1.2, the analogy between electronic and CF Landau levels is sometimes weak. One of the inherent problems not mentioned so far is the question of mixing between CF Landau levels: whereas LL mixing can be neglected for electrons in the limit $B \to \infty$, there is no such case for CFs.

The nature of many incompressible FQH states is therefore still not completely clear, for example the ground states at $\nu = 2/3$ and $2/5$. Results in this Section indicate that the singlet states at these filling factors comprise of pairs of spin up and spin down electrons which we would not expect from the CF analogy – at least not at first glance. Furthermore, in the $\nu = 2/3$ singlet with electron density n, the $\uparrow - \downarrow$ pairs seem to form a state which could be constructed by taking a system with the lowest LL completely filled with electrons of density $n/2$ and then replacing each electron by an $\uparrow - \downarrow$ pair. This behaviour is not observed in the $\nu = 2/5$ singlet. We may again conclude, that even though the $2/5$ and $2/3$ ground states are very closely related on the level of composite-fermion theories, their electronic properties are different. It can thus be misleading to extend our intuition concerning the (completely filled) electronic Landau levels to states interpreted as (completely filled) composite fermion Landau levels.

2.2 The half–polarized states at filling factors $2/3$ and $2/5$

In the previous section we dealt with the spin singlet and polarized ground states at filling factors $2/3$ and $2/5$ and it was mentioned that it is the Zeeman splitting (or better, $E_Z/E_C \propto \sqrt{B}$) which determines which of them is the actual ground state. It is the singlet state for vanishing Zeeman splitting (low magnetic fields) or the polarized state if the Zeeman term dominates (limit $B \to \infty$). All this can be understood within the composite fermion concept, Fig. 9a, where we even obtain the prediction that there is a *direct* transition (crossing) between these two ground states at some critical value of E_Z/E_C or equivalently, at some critical magnetic field B_C, if we sweep magnetic field and keep the filling factor constant, cf. also Sect. 3.

However, experiments by Kukushkin et al. [46] indicate that this picture may be incomplete. They suggest that some exactly half-polarized state becomes a stable ground state in the vicinity of B_C. In this Section we will describe one candidate for such a half-polarized state ground state and discuss its properties.

2.2.1 Ground state energies by exact diagonalization

At first glance, spectra of homogeneous small finite systems with Coulomb interaction (Sect. 3, Fig. 48) do not suggest any intermediate state at the transition. The picture is quite different when short-range interaction is considered. In an interval of magnetic fields around B_C the GS is a state with total spin equal

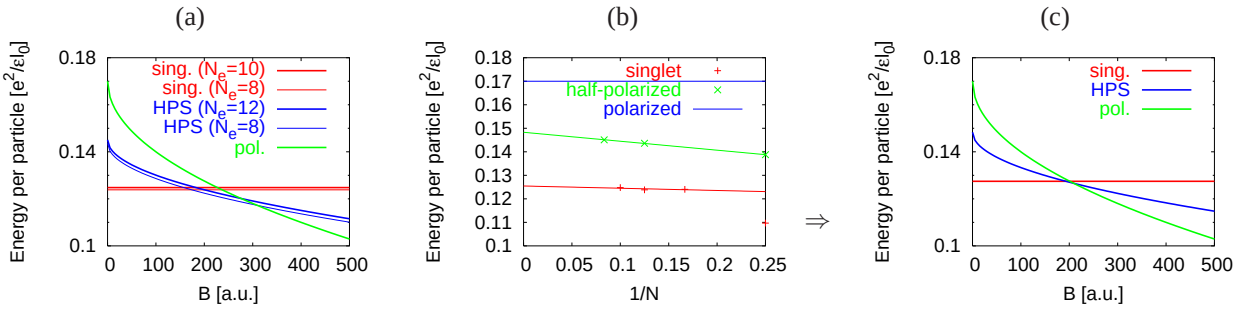

Fig. 24: Ground state energies at $\nu = 2/3$: the half-polarized state may become the absolute ground state in a narrow interval of magnetic fields. *Left:* Energies of SRI ground states in the subspaces $S = 0$ (singlet), $S = N_e/4$ (half-polarized) and $S = N_e/2$ (fully polarized) as a function of Zeeman splitting (or magnetic field; note the energy units $e^2/\varepsilon\ell_0 \propto \sqrt{B}$). In all cases, energies of the two largest systems available to calculations are shown. *Middle:* extrapolation of the GS energies to infinite systems ($1/N \to 0$). *Right:* The energy-versus-magnetic field diagram for extrapolated ground state energies. This indicates that even then the HPS will be a ground state close to the transition.

to $N_e/4$, Fig. 24a, i.e. a half-polarized state (HPS). This holds for all system sizes accessible to numerical calculation and, by extrapolating energies to $1/N \to 0$, Fig. 24b, it seems to hold also for infinite systems.

It is probably only through the finiteness of the system that a half polarized ground state did not appear in Coulomb interacting systems (Fig. 48). The SRI systems may be less sensitive to this generical drawback of exact diagonalization models. On the other hand, SRI models predict wrong values of B_C (see Subsec. 3.2.1) and thus the scheme presented in Fig. 24a must be checked in systems with Coulomb interaction.

Considering Coulomb-interacting systems, the scheme suggested in Fig. 24a is supported by extrapolations of GS energies performed by Niemelä, Pietiläinen and Chakraborty [57] in spherical geometry, Fig. 25a, and it is not supported by analogous calculations on a torus presented here, Fig. 25b. We would like to stress that the extrapolation of the energy of the HPS is based only on two points, the third point ($N_e = 4$) in Fig. 25b, is not very reliable, Subsec. 2.2.3. Therefore the question of whether the HPS becomes the absolute GS or not remains basically open until exact diagonalizations of larger systems become possible.

Nonetheless let us assume in this Section that a half-polarized state can indeed lower its energy sufficiently so as to become the absolute ground state. We will therefore focus on the $S = N_e/4$ sector of systems at filling factor $2/3$, and also at $2/5$ in Subsec. 2.2.5. Studies were mostly focused on the SRI states where it is easier to identify the best candidate for the half-polarized ground state. Its Coulomb-interacting counterpart is discussed later, in Subsec. 2.2.6.

By convention a half-polarized state with 12 (8) electrons will consist of 9 (6) electrons with spin up (majority spin) and 3 (2) electrons with spin down (minority spin).

2.2.2 Identifying the HPS in systems of different sizes

Provided some particular physical half-polarized state GS_∞ is the ground state in an infinite system, we may ask what its realizations in finite systems of different sizes are. Vice versa: given the half-polarized states calculated in a system of $N_e = 12$ (4, 8...) electrons, which state corresponds to GS_∞? In this way we can think of states which 'correspond to each other' in systems of different sizes. The trouble is, of course, that we do not know GS_∞.

Regarding the computational capacity available, we could study $\nu = 2/3$ systems with 4, 8 and 12 particles, the next larger system, $N_e = 16$, would require diagonalization in spaces of dimension many hundred million. It seems likely that the analogues to GS_∞ are the GSs in $N_e = 12$ and $N_e = 8$ systems (GS_{12},

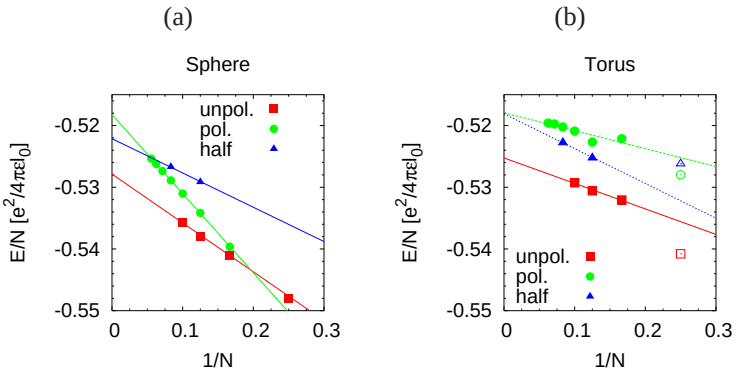

Fig. 25: Extrapolation $1/N \to 0$ of the GS energies for Coulomb interacting systems on a sphere and on a torus at $\nu = 2/3$.

GS_8) and that it is a low lying excited state (`st03`) in the smallest system, $N_e = 4$. In the following, reasons for this are proposed.

(i) GS_{12} and GS_8 belong to the same symmetry class defined by the 'crystallographic k^r' (27). They have both $\widetilde{k}^r = (\pi, \pi)$, i.e. they lie in the 'corner of the Brillouin zone' (Fig. 6, Subsec. 1.5.2). This is also closely related to the fact that both GS_{12} and GS_8 are non-degenerate.

(ii) The states GS_{12} and GS_8 are well separated from excitations within the $S = N_e/4$ sector and the energy of the lowest excitation is similar, $0.01\ (e^2/\varepsilon\ell_0)$, in systems of different size, Fig. 26.

(iii) Though not completely identical, the inner structure of GS_{12} and GS_8 is very similar as seen by the correlation functions, Fig. 27.

(iv) The GS of the $N_e = 4$ system has a lower symmetry than the formerly described states. Looking for a state of inner structure (correlation functions) similar to the one of GS_{12} and GS_8 within the sector $\widetilde{k}^r = (\pi, \pi)$, we find remarkable similarities with the second excited state ('`st03`', marked in Fig. 26), Subsec. 2.2.3. However, we should bear in mind that for $N_e = 4$ there is only a single electron with reversed spin in other words the system is indeed extremely small. A consequence is for example that $g_{\downarrow\downarrow}(r) \equiv 0$. Relevance of such states with respect to infinite systems is thus doubtful.

2.2.3 Inner structure of the half-polarized states

Focus of this part will be the correlation functions of the states GS_{12} and GS_8 and a brief comment will be made on $N_e = 4$ states. As mentioned above and as the kind reader may verify in Fig. 27, GS_{12} and GS_8 look indeed similar.

GS_{12} and GS_8 match in all three spin-resolved correlation functions, $g_{\uparrow\uparrow}(r)$, $g_{\uparrow\downarrow}(r)$, $g_{\downarrow\downarrow}(r)$, Fig. 27. The match is especially good (quantitative) on short distances, $r \lesssim 3\ell_0$. This suggests that states GS_{12} and GS_8 are not bound to some particular system size and we can thus hope that if we could make the system larger, they would eventually develop into the GS_∞.

Differences between correlation functions of GS_{12} and GS_8 at longer distances r are understandable, given the normalization (44). The $N_e = 12$ system is 'larger' than the $N_e = 8$ one, yet the integral $\int \mathrm{d}r g(r)$ must be the same. Perhaps the most apparent difference between various correlation functions is whether they have a maximum or a minimum 'in the middle' ($6\ell_0$ or $8\ell_0$ in Fig. 27). In ideal case, a strong maximum occurs when $g(r)$ is monotoneous in an infinite system while a minimum, or a weak maximum following a foregoing minimum, means that $g(r)$ has some structure, one or more maxima for finite r_i. In reality, however, the former behaviour occurs also when r_i is larger than the finite system size. A manifestation of

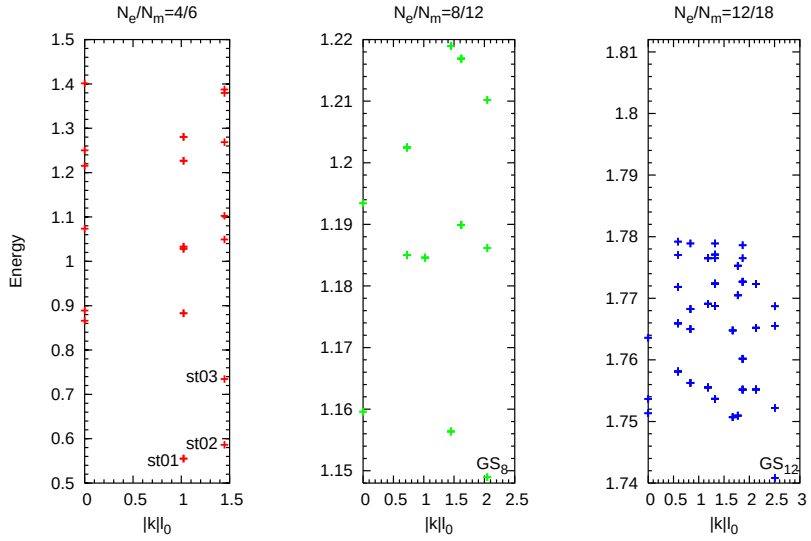

Fig. 26: Low lying energy levels in the $S = N_e/4$ (half-polarized) sector of $2/3$ systems with (*left to right*) $N_e = 4$, 8 and 12 particles. The states are sorted according to $|k^r|$ (Subsec. 1.5.2). The GS of an infinite system is likely to have $\widetilde{k}^r = (\pi, \pi)$ which is a point of very high symmetry in the k^r-space. This symmetry class is however distinct from the one of the singlet and polarized incompressible ground states.

this is seen in $g_{\uparrow\uparrow}(r)$, Fig. 27. The flat maximum at $r_i \approx 5\ell_0$, followed by a minimum, observed for the $N_m = 18$ torus does not occur for the smaller system ($N_m = 12$). Looking only at the smaller system we could have wrongly concluded that the correlation function is almost structureless.

Some further points are worth of notice.

(i) $g_{\uparrow\downarrow}(r)$ is suppressed nearly to zero at $r = 0$ in spite of the missing Pauli principle, only on account of the repulsive interaction. It displays strong maxima around $r \approx 3.4\ell_0$.

(ii) Even though by far not identical, $g_{\uparrow\uparrow}(r)$ and $g_{\downarrow\downarrow}(r)$ are similar to each other. The clear shoulder around $r \approx 2\ell_0$ seems to stem from the 'exchange hole' (of the LLL) $g_{\nu=1}(r) = 1 - \exp(-r^2/2\ell_0^2)$, see (45). After subtracting a suitably scaled function $g_{\nu=1}(r)$ the shoulder completely disappears and the remaining parts of both $g_{\uparrow\uparrow}(r)$ and $g_{\downarrow\downarrow}(r)$ are $\propto r^6$ close to $r = 0$, Fig. 28 and discussion below.

(iii) Up to a high precision the sum of $g_{\uparrow\uparrow}(r)$, $g_{\downarrow\downarrow}(r)$ and $g_{\uparrow\downarrow}(r)$ (with appropriate scaling, see Fig. 15 for explanation) is identical with $g_{\nu=1}(r)$, however with ℓ_0 replaced by $\sqrt{2}\ell_0$. Not shown here.

Let us now turn to the smallest system where $S = N_e/4$ states may occur (at $\nu = 2/3$), i.e. $N_e = 4$. Figure 27 shows correlation functions of the lowest two states in the sector of $\widetilde{k}^r = (\pi, \pi)$. Out of these, the second state (i.e. `st03`) seems to be analogous to $S = N_e/4$ GS's in the two larger systems ($N_e = 8$, 12): $g_{\uparrow\uparrow}(r)$ is again a sum of the 'correlation hole' and a function $\propto r^6$, $g_{\uparrow\downarrow}(r)$ shows a peaked structure with maximum around $2.8\ell_0$ (both of these features are missing for the lower state `st02`). However, as mentioned above, the $N_e = 4$ system is too small for a reliable study of $S = N_e/4$ states ($g_{\downarrow\downarrow}(r) \equiv 0$).

Back to the GS_{12} (called HPS here), it is very interesting to study the '$\propto r^6$ part' (P6P) of the like-spins correlation functions, $g_{\uparrow\uparrow}(r)$, $g_{\downarrow\downarrow}(r)$. What we mean by 'P6P' is the rest after we subtract the 'lowest LL correlation hole', i.e. the $g_{\nu=1}(r)$ part causing the shoulder in $g_{\sigma\sigma}(r)$ around $r \approx 2\ell_0$, curve A in Fig. 28a,b.

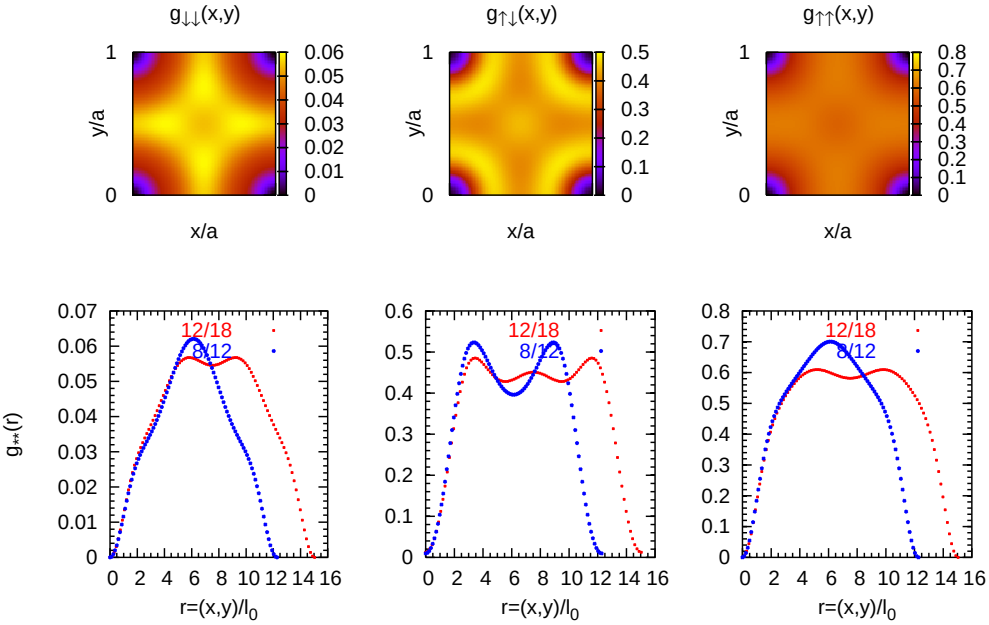

Fig. 27: The likely analogues of the half-polarized ($S = N_e/4$) GS$_\infty$(ground state in an infinite system) on a torus with $N_e = 8$ and $N_e = 12$ particles and filling factor $2/3$. *Left to right:* density-density correlation for $\uparrow\uparrow$ (majority spins), $\uparrow\downarrow$ and $\downarrow\downarrow$ (reversed spins), *upper row:* in the whole primitive cell; *lower row:* sections along the diagonal. Note the isotropy of the state, i.e. visual manifestation of its high symmetry.

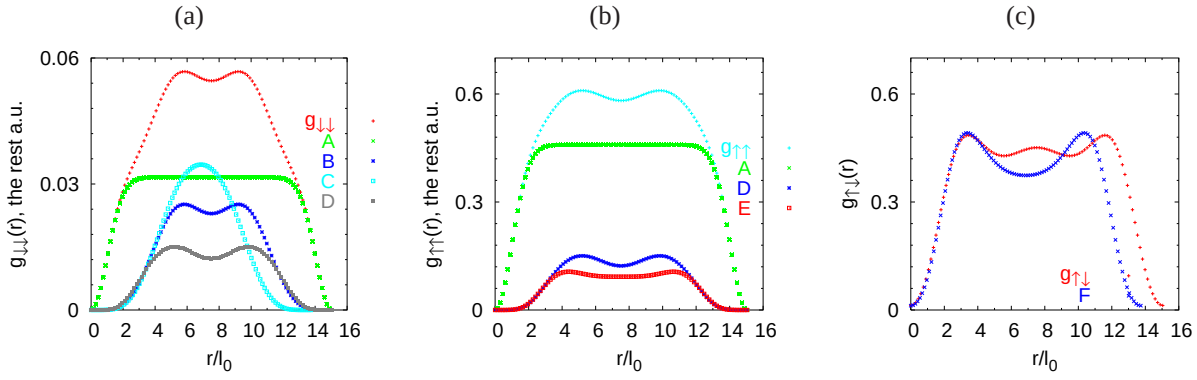

Fig. 28: The half-polarized state (GS in the $S = N_e/4$ sector) for $N_e = 12$ particles, analysis of the correlation functions (details in text). *Left to right*: (a) $g_{\downarrow\downarrow}$ (minority spin), (b) $g_{\uparrow\uparrow}$ (majority spin) and (c) $g_{\uparrow\downarrow}$. Legend for particular curves (in all plots). A: lowest LL correlation hole, $g_{\nu=1}(r)$ scaled to fit the shoulder. B and D: $g_{\downarrow\downarrow}(r)$ and $g_{\uparrow\uparrow}(r)$ without shoulder. C and F: $g_{\downarrow\downarrow}(r)$ and $g_{\uparrow\downarrow}(r)$ of the singlet state ($N_e = 10$, $\nu = 2/3$), $g_{\downarrow\downarrow}(r)$ without shoulder. E: $g(r)$ of the $\nu = 1/3$ Laughlin state. 'Without shoulder' means, that the curve A was multiplied by a suitable constant to fit the shoulder and subtracted.

One of many facts we can extract from Fig. 28 is that P6P/ $\uparrow\uparrow$ [refering to $g_{\uparrow\uparrow}(r)$] and P6P/ $\downarrow\downarrow$ are similar but not identical. For example, they both exhibit a peaked structure but the first maxima do not coincide, they occur at $5.0\ell_0$ and $5.8\ell_0$ for P6P/ $\uparrow\uparrow$ and P6P/ $\downarrow\downarrow$, respectively (curves B and D in Fig. 28a).

Let us compare the P6P/ $\downarrow\downarrow$ of the HPS with P6P/$\downarrow\downarrow$ of the singlet incompressible $2/3$ GS, curves B and C in Fig. 28a). Match of these two is very good up to $r \approx 4\ell_0$, the absence of the peak at $5.8\ell_0$ in the singlet state could be due to smallness of the system where the singlet state was determined ($N_e = 10$). It might appear in the next larger system, $N_e = 12$, cf. similar situation in Fig. 27.

On the other hand, P6P/$\uparrow\uparrow$ of the HPS seems to resemble the singlet state less than P6P/$\downarrow\downarrow$ of the HPS. The form of P6P/$\uparrow\uparrow$ seems to be not very different from the one of the correlation function of the Laughlin $1/3$ state, Fig. 12b, whose first maximum occurs however already at $r = 4.4\ell_0$ (curves D and E in Fig. 28b). In any case, P6P/$\uparrow\uparrow$ of the HPS matches better $g_{\nu=1/3}(r)$, i.e. the Laughlin state, than P6P of the $\nu = 2/3$ singlet state. Here we mean especially behaviour on ranges $\lesssim 3\ell_0$.

Last but not least, the correlations between unlike spins are also very similar in the singlet state and in the HPS, Fig. 28c, in particular positions of the maxima differ by as little as $0.1\ell_0$ (both are around $r \approx 3.4\ell_0$).

2.2.4 Discussion

Findings presented above suggest that the $\nu = 2/3$ half-polarized ground state in short-range interacting systems is a gapped state in which the singlet and polarized incompressible states coexist. Below, some key points regarding the HPS are summarized.

Symmetry and energy

Both in eight- and twelve-electron systems, the ground state has $\widetilde{k}^r = (\pi, \pi)$. This is one of two points of the highest symmetry in the k^r-space, another one is $k^r = (0, 0)$, Fig. 6. In particular, the 'highest symmetry' means that this k^r-point is not related to any other point by a symmetry operation in the k^r-space corresponding to relative translations, Sec. 1.5.2. This in turn implies that states with $\widetilde{k}^r = (\pi, \pi)$ or $(0, 0)$ – and only such states – are non-degenerate, except for center-of-mass and incidental degeneracies. Together with the relatively large lowest excitation energy $\Delta(N_e = 8, 12)$ from both GS_{12} and GS_8 (10% of the gap of the Laughlin state, Fig. 26) , this suggests that the ground state is gapped. Also the relation $\Delta(N_e = 8) < \Delta(N_e = 12)$ speaks in favour of this hypothesis. If the gap were to vanish in an infinite system, we would expect the lowest excitation energy to decrease with system size. Naturally, we must be careful, since we can compare systems of only two different sizes and the function $\Delta(N_e)$ may be non-monotonous. On the other hand, $\Delta(N_e = 12) \approx 0.01\ (e^2/\varepsilon\ell_0)$ is much larger than a typical level separation between excited states, Fig. 26 and for a mere finite size effect, this gap seems too large.

In spite of the similarities to the singlet and polarized incompressible ground states, $\widetilde{k}^r$ clearly distinguishes HPS from these two states, since they have both $\widetilde{k}^r = (0, 0)$. Also in spherical geometry, where $|\widetilde{k}^r| \propto L$ (end of Subsec. 1.5.2), these incompressible states have $L = 0$ while the HPS has $L = S$, where S is the total spin [57]. Thus, even though we showed that the HPS could be gapped, it is of different nature than the singlet and polarized ground states. Meaning of this different symmetry is however not clear.

It would be interesting to study this state in a system with hexagonal elementary cell [31] which was unfortunatelly out of the scope of this work. This geometry is nearer to an isotropic 2D system than a torus (it has a six-fold rather than a four-fold rotational symmetry) while it is still compatible with plane waves (in CDWs). Most importantly, there is only one point of the highest symmetry in this geometry and a straightforward question is whether or not the HPS will maintain its high symmetry.

Inner structure again

Features of the HPS described by points (i-iii) in Subsec. 2.2.3 are actually strikingly similar to those of the incompressible singlet state at $\nu = 2/3$. Investigation of the $g_{\uparrow\uparrow}(r)$ after the 'shoulder' was subtracted

(P6P/↑↑) suggests again some relation to the Laughlin state which is the particle-hole conjugate to the polarized incompressible state at $\nu = 2/3$.

Especially manifest is the hint at pairing between unlike spins, the maximum around $3.4\ell_0$ in $g_{\uparrow\downarrow}(r)$. On the other hand, the shoulder in correlation functions of like spins seems to be rather a manifestation of filling factor $> \frac{1}{2}$, since it occurs also for other states at filling $\nu = 2/3$ (than just for the singlet, polarized and half-polarized GS) and it does not occur at filling $\nu = 2/5 < \frac{1}{2}$, Subsec. 2.2.5. It suggests that some $\nu = 2/3$ states with less than full polarization can be interpreted in terms of holes rather than electrons even though particle-hole symmetry applies only for fully polarized states, Subsec. 2.1.1.

In the following Sections we will continue investigating the half-polarized states at filling factor $2/3$ by other methods and continue discussing the hypothesis of coexisting singlet and polarized states. First, however, we look at two different minor issues.

2.2.5 Half-polarized states at filling $\nu = 2/5$

At filling $2/5$, the situation is much less transparent than at filling $2/3$. First, only systems with four and eight particles are accessible to exact diagonalization, the twelve particle system implies matrix dimensions in the order of hundreds of millions. Second, the spectrum of the eight particle system in the $S = N_e/4$ sector is quite different from that of a $2/3$ system, Fig. 29:

(i) the ground state lies at a different point in the k^r-space, $(0, 0)$, than the $2/3$-HPS having $\widetilde{k}^r = (\pi, \pi)$.

(ii) The excitation energy from this GS is very small, less than a third of that one of the $2/3$ HPS.

(iii) The symmetry of the low excited states is lower than for $N_e = 8$, $2/3$ system.

Regarding the possibility that within the 8 electron calculations it is not the *lowest* energy half-polarized state at $\nu = 2/5$ to be the counterpart of the HPS at $\nu = 2/3$, there are two $2/5$ states displayed in Fig. 30: (a) the one with the lowest energy in $S = N_e/4$ sector and (b) the lowest state with the same symmetry as the $2/3$ HPS, i.e. $\widetilde{k} = (\pi, \pi)$.

Similarly, as for the $\nu = 2/3$ states, the $2/5$ HPS bear features of the polarized and singlet ground states. Let us regard the state in Fig. 30a:

(i) Near $r = 0$ the functions $g_{\downarrow\downarrow}$ (minority spin), $g_{\uparrow\downarrow}$ and $g_{\uparrow\uparrow}$ (majority spin) are $\propto r^6$, r^4 and r^2, respectively. In this respect, $g_{\downarrow\downarrow}$ and $g_{\uparrow\downarrow}$ resemble the singlet state and $g_{\uparrow\uparrow}$ resembles the polarized state.

(ii) Up to the first maximum, $g_{\uparrow\uparrow}$ of the HPS is the same as in the polarized state, but shifted by about $0.2\ell_0$ outwards. Positions of the first maxima mismatch slightly more (by $0.4\ell_0$). The strong maximum in the centre of the cell is not present in the HPS.

(iii) $g_{\uparrow\downarrow}$ of the HPS and the singlet GS match very well even beyond the first maximum. Positions of the maxima are identical, $r \approx 3.5\ell_0$. On contrary to the previous point, there is another maximum in the centre of the cell in the HPS state and nothing in the singlet state, indicating that the similarity between the singlet and the HPS has certain limits.

(iv) $g_{\downarrow\downarrow}$ of the HPS and the singlet GS also match very well up to $r \approx 4\ell_0$. Then there is a deep minimum in the HPS which is absent in the singlet GS.

Turning to the state (b), we might say that it is less alike to the singlet state. The minimum in $g_{\downarrow\downarrow}$ is much deeper than for state (a), the first maximum in $g_{\uparrow\downarrow}$ does not match the maximum seen in the singlet state. On the other hand, $g_{\uparrow\uparrow}$ seems to be more similar to the polarized state.

Lowest excitations in the high symmetry sectors show even less similarities to the singlet and polarized GSs, especially $g_{\downarrow\downarrow}$ is quite dissimilar beyond the $r \approx 0$ range and maxima in $g_{\uparrow\downarrow}$ match less well.

In conclusion, if there is a counterpart to the $2/3$ HPS at filling $2/5$ at all, we may expect it to be the state (a) (the absolute GS), even though hints for this are not very convincing. Again, this suggests that differences between filling factors $2/3$ and $2/5$ are not only of quantitative nature (gap energies, for instance) but

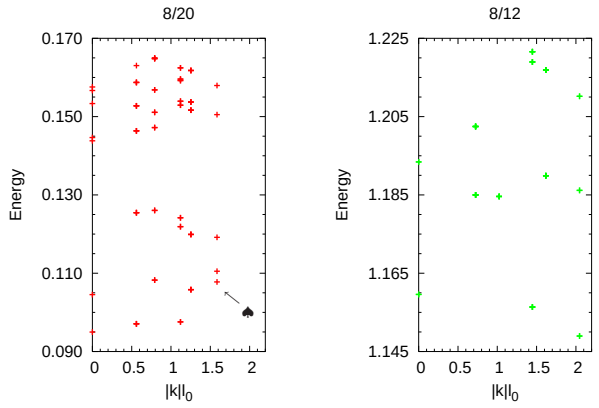

Fig. 29: Low lying half-polarized (i.e. $S = N_e/4$) states of a $2/5$ system, $N_e = 8$. The lowest state with the same symmetry as the HPS of $\nu = 2/3$ is marked by ♠.

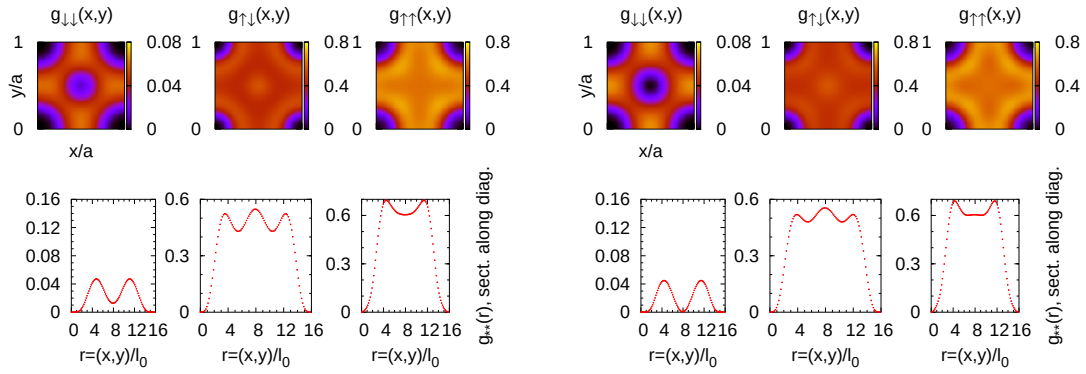

Fig. 30: Half-polarized states at filling $2/5$ and their inner structure (density-density correlation functions); eight electron system. (a) the GS in the $S = N_e/4$ sector is non-degenerate but it has a different symmetry, i.e. $(0, 0)$, than the HPS of $\nu = 2/3$. (b) the lowest half-polarized state (at $2/5$) with the same symmetry, i.e. $(\frac{\pi}{2}, \frac{\pi}{2})$ as the HPS of $\nu = 2/3$ (marked by ♠ in Fig. 29).

may be as substential as existence or non-existence of some particular ground state, which is *nota bene* completely unexpected on the level of non-interacting CF picture.

2.2.6 Short-range versus Coulomb interaction

Let us conclude with observations regarding the Coulomb- and short-range-interacting (SRI) systems in the sector of half-polarized states.

The spectra do not look very similar, Fig. 2.2.6a. However, the absolute ground states have in both cases the same symmetry, they lie in the same point of the k space.

The Coulomb and SRI ground states in the largest system available, $N_e = 12$, have very similar structure. The correlation functions $g_{\uparrow\uparrow}$ and $g_{\uparrow\downarrow}$ match nicely while $g_{\downarrow\downarrow}$ show some differences between the CI and SRI states. In spite of this, the overlap between the two states is as large as 95%. This allows for the following conclusions

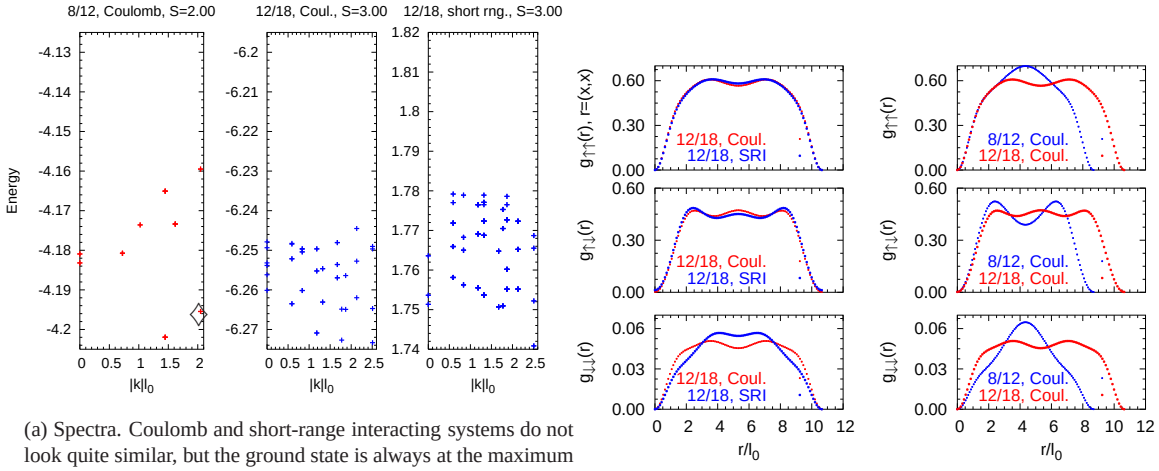

(a) Spectra. Coulomb and short-range interacting systems do not look quite similar, but the ground state is always at the maximum $|k|$.

(b) The ground state

Fig. 31: Half-polarized states in Coulomb interacting systems.

(a) The two states 'correspond to each other'. (b) The short-range part of the interaction seems to be essential for this state (very similar as for the Laughlin state). (c) Deviations in $g_{\downarrow\downarrow}$ (minority spin) might come from the fact that spin-down electrons are very far separated from each other (they have an effective filling of only $\nu = \frac{1}{6}$). Thus the long-range part of the interaction substantially influences their motion.

In $N_e = 8$ systems, the most likely analogue to the $N_e = 12$ ground state is the state $\diamondsuit$, Fig. 2.2.6a. This is the lowest 8-electron state with the same symmetry (value of $\widetilde{k}^r$) as the $N_e = 12$ ground state. Correlation functions of the two states (8- and 12-electron ones) match reasonably, Fig. 31(b). Compare also with differences between $N_e = 8$ and $N_e = 12$ short-range ground states, Fig. 27.

Among the excited states the level order is often modified, comparing the $N_e = 12$ Coulomb and short-range systems. When trying to assign CI to corresponding SRI states, calculating overlap between two states seems to be a more reliable tool than comparing correlation functions.

In summary, in spite of differences in the excitation spectrum, the half-polarized ground states of Coulomb and short-range systems seem to correspond to each other. Differences in the excited states and in the correlations between the minority spin electrons indicate that the definition of the short-range interaction should be improved when we study the half-polarized states. Since the minority spin electrons are relatively far from each other, non-zero values of higher pseudopotentials (V_m, $m > 1$, Subsect. 1.3.5) should probably be considered.

2.3 In search of the inner structure of states: response to delta impurities

Now that some candidates for the half-polarized ground state at filling $2/3$ have been introduced we wish to look at them more closely and learn more about their inner structure. The ultimate goal of such efforts can be to propose trial wavefunctions just as the Laughlin wavefunction at filling $\nu = 1/3$. Even though this has not been accomplished, the results presented below shed some light on relations between the half-polarized state and the singlet and polarized incompressible states.

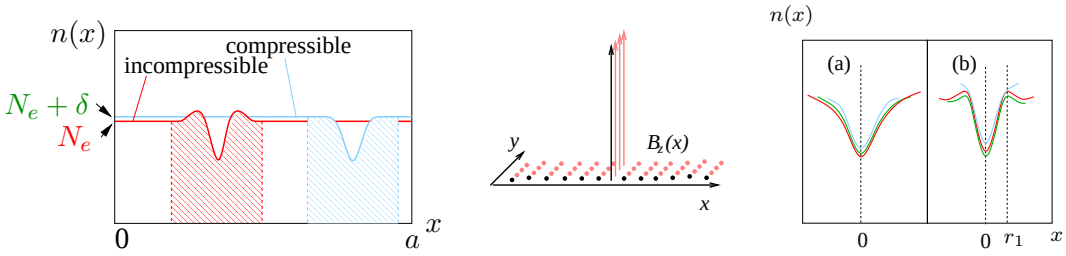

(a) Density response: incompressible- or compressible-like. Note that density integrated over the hatched area remains unchanged for the incompressible system when the inhomogeneity is switched off.

(b) δ-line impurity of the type $\delta_{\sigma\uparrow} - \delta_{\sigma\downarrow}$.

(c) Two possible ways of how a response to an inhomogeneity can change with system size; different lines in one sketch refer to the same state in systems of different sizes.

Fig. 32: δ-line inhomogeneity and sketches of possible resulting effects.

As a probing tool, the homogeneous states are subjected to a δ-line impurity and response in density and polarization is observed. In first quantization,

$$H_{impurity} = \sum_{i=1}^{N_e} W(r_i)\,, \qquad W(x,y) = \delta(x - x_0) \tag{54}$$

This inhomogeneity profile (Fig. 32) was chosen since it is compatible with the torus symmetry. For studies of point-like impurities, spherical geometry is more suitable since it preserves the rotational symmetry, cf. references in Subsec. 2.3.1. The δ-line form is particularly apt to unveil a tendency of the state to build plane charge or spin density waves. We should keep in mind, that due to the restriction to the lowest Landau level, even a δ-like potential has an effective cross section of ℓ_0 [61].

As we are dealing with spinful electrons, inhomogeneities can be principially of four distinct types:

$$\begin{aligned} H_{EI} &= W(r)\cdot(\delta_{\sigma\uparrow} + \delta_{\sigma\downarrow})\,, \qquad & H_{MI,\uparrow} &= W(r)\cdot\delta_{\sigma\uparrow}\,, \\ H_{MI} &= W(r)\cdot(\delta_{\sigma\uparrow} - \delta_{\sigma\downarrow})\,, \qquad & H_{MI,\downarrow} &= W(r)\cdot\delta_{\sigma\downarrow}\,, \end{aligned} \tag{55}$$

where the function $W(r)$ describes the spatial form of the impurity, Fig. 32 shows the form of $W(r)$ chosen in the present study. It is important to note that these impurities fail to conserve S^2 but they do conserve S_z. Also, owing to the form of $W(r) = W(x)$, they conserve k_y^r and thus also J (30) and they spoil only the k_x^r-symmetry. This is very convenient from the computational point of view as matrix sizes remain tractable. From the physical point of view, this inhomogeneity is a soft tool which does not completely destroy the high symmetry of the studied states. For example, it allows us to stay in the $S_z = N_e/4$ sector when we study the half-polarized states.

The first type (H_{EI}, electric impurity) is an ordinary non-magnetic impurity or external electric potential. The magnetic impurity (H_{MI}) favours particles with correct spin ($\downarrow$, if $W(r) > 0$) and costs energy for particles with wrong spin ($\uparrow$ in this case). The last two types describe an impurity which is seen only by one group of spins. In case that a system consists of two separated subsystems, one of spin up particles and another of spin down particles, these impurities allow to test only one of them without directly disturbing the other one.

Note that some inhomogeneity types in (55) may be redundant, depending on the state we apply them to. For instance, the effect of $H_{MI,\uparrow}$ and $H_{MI,\downarrow}$ must be the same up to a sign for all states in the $S_z = 0$ sector.

Before we turn to the exact diagonalization results, let us briefly think about what types of responses can be expected. Most importantly, consider the difference between compressible and incompressible states. As

a classical *compressible* system imagine a playground of fixed size filled with a gas of negatively charged footballs of density $n(r)$, $\langle n(r)\rangle = N$. A negative impurity at $r = 0$ will repel the gas causing $n(0) < N$, Fig. 32a right. Beyond some distance r_h, the density will reach a constant level again and this level will be slightly higher than the original density, $N + \delta = n(r) > N$, $|r| > r_h$, so that the constraint $\langle n(r)\rangle = N$ remains preserved. Some charge has been depleted away from the impurity, thereby compressing slightly the gas in the rest of the system. If the depleted charge equals the charge of the impurity, the charge distribution (charge of the footballs plus charge of the impurity) in the system will remain constant in spite of non-constant $n(r)$ and the gas particles far away from $r = 0$ will not 'see' the impurity anymore. This is the case of ideal *screening*.

A classical *incompressible* liquid, for example again charged footballs, will not react at all, because it cannot change its density. Even though particles of the liquid feel repulsion from $r = 0$, the density will remain constant $n(r) = N$. We can also encounter a different behaviour, Fig. 32a (left). Though the density decreases directly at $r = 0$, an oscillatory structure develops in $n(r)$, so that the integral density in the region $|r| < r_h$ remains as it was without the impurity. The density then also remains at its original value N beyond r_h. This is a non-ideal incompressible behaviour: at very short distances, the density can vary slightly, but averaged over distances of r_h (or larger), the density remains constant. Also, since no net charge was depleted from the region $|r| < r_h$, the impurity is *completely unscreened* on distances larger than r_h.

Compressible-like response as shown in Fig. 32a can be combined with quantum interferences (Friedel oscillations) and it is also possible to think of some overscreening effect which would lead to an oscillatory $n(r)$. This means the sole fact that $n(r)$ exhibits oscillations does not necessarily have to imply incompressibility. A more reliable criterion is that the integral density over $|r| < r_h$ remains the same with and without impurity. This procedure is delicate in finite systems where r_h can be comparable to the system size.

The last Figure, 32c, shows two possible ways of how responses change with system size. The right panel suggests that the state is not fixed to a particular size of the finite system and especially we could expect oscillations with period r_1 also in an infinite system. On the contrary, the left panel shows a state with no intrinsic length scale and e.g. the width of the peak is related to the (finite) size of the particular system.

Now, let us proceed to fractional quantum Hall states.

2.3.1 Electric (nonmagnetic) impurity

The effect of electric impurities on incompressible ground states has been under investigation since the early times of the fractional quantum Hall effect. The main reason is that some disorder is needed for the integer quantum Hall effect to be observable, but on the other hand, too strong disorder will destroy the effect [79]. For the fractional quantum Hall effect, two of the basic questions were, (i) how strong impurity potentials may be so that they do not destroy the gap and (ii) how does it change the ground state. Basic studies with the Laughlin state were performed as early as in 1985 [61, 86, 27].

Since the exact diagonalization is limited to finite, and in fact quite small, systems, it is very delicate to put forward statements about the infinite 2D electron gas. Therefore, when we use the word 'incompressible' we mean rather 'incompressible-like' in terms of Fig. 32. In fact, the main purpose of the following Subsections is to see how the polarized and singlet state respond to impurities in a *finite system* and later to compare them to the half-polarized state again in a *finite system*. We will focus on *short-range interacting* systems here.

The Laughlin state or the fully polarized $2/3$ state

The fully polarized $\nu = 2/3$ state is a particle-hole conjugate to the $\nu = 1/3$ Laughlin state in a homogeneous system, Subsect. 1.5.4. In this part we will study the latter state. Strictly taken, the particle-hole

symmetry is lost when an arbitrary impurity is considered since the Hamiltonian is no longer translationally invariant. Differences between the $\nu = 1/3$ and $2/3$ polarized states are however small if the impurity is weak. In particular, for inhomogeneities considered in this paragraph, it has been checked numerically that $n(x) - N_e$ are almost the same for the two states. Moreover, the larger N_e, the smaller are the differences.

The response of a $\nu = 1/3$ system to an impurity of the form (54), a δ-line along y, is shown in Fig. 33. Different curves show the ground state density $n(x)$ in systems of different sizes ($N_e = 4$ to 10 particles). The repulsive impurity is always located at $x = 0$ and it is weak, its strength is $\sim 10\%$ of the gap. These results agree very well with the densities presented by Zhang *et al.* [86], who considered a δ rather than a δ-line impurity, though for $N_e = 4$ systems only. Comparison between rectangular, spherical and disc geometry showed, in all cases, very similar behaviour [86]. Note also that findings in Fig. 33 assume short-range interaction whereas [86, 61] considered Coulomb interaction.

Results in Fig. 33a support the conclusions of Zhang and Rezayi. The oscillatory response of $n(x)$ is size-independent and it has a period $r_1 \approx 2.5\ell_0$. The response, measured by $n(0)$, does *not* vanish with increasing system size but it decays with distance from the impurity. Comparing $n(x)$ in Fig. 33a to the model cases in Fig. 32a, we may tend to classify the Laughlin state as an incompressible one. Incompressibility of the Laughlin state is locally not perfect, otherwise $n(x)$ would remain constant, at least in infinite systems. However, if some net charge were accumulated even in a larger region (of the order r_h) around $x = 0$, we would expect $n(x)$ at large distances to be consistently higher than the no-inhomogeneity value $n(x) \equiv N_e$. Recall the difference N to $N + \delta$ in Fig. 32a. If just a unit charge is depleted from the impurity, then $\delta = 1/N$. In infinite systems, the difference δ will vanish, but data in Fig. 33a come from rather small systems $N \leq 10$ where δ is not negligible. This is not seen in Fig. 33a.

Zhang *et al.* suggest that the observed response is a local charge density wave (28), a strong argument supporting this idea is given in point (iv) below. Under this view, it is not surprising that the response to a δ-line shown in Fig. 33(a) is very similar to the response to a δ-peak studied by Zhang. Only the envelope function, not the wavelength depends on the particular form of the exciting impurity.

We should again add several comments:

(i) oscillations observed in $n(x)$, Fig. 33a, are not related to Friedel oscillations which appear in the Fermi gas. This is where a sharp Fermi surface exists giving rise to interferences, just as in correlation functions of a free Fermi gas, Subsec. 2.1.1.

(ii) small wiggles on the $N_e = 4$ density in Fig. 33a are due to the center-of-mass (CM) part of the wavefunction. Being a finite size effect, they fall off rapidly with system size as we indeed see in Fig. 33a, Subsec. 2.1.4.

(iii) the ground state of the homogeneous system is triply degenerate in the CM part, Subsec. 2.1.4. This degeneracy is lifted by the inhomogeneity, but energy differences between these three states remain much smaller than their separation from the lowest excited states for the inhomogeneity strength considered [86].

The response $n(x)$ of any of the three states depends slightly on the position of the impurity within the elementary cell, but this dependence and also differences among the three states in energy and in $n(x)$ quickly vanish with increasing system size. In Fig. 33a always the impurity giving the strongest response in $n(x)$ was chosen.

(iv) Period of oscillations: As Rezayi and Haldane [61] note, numerical calculations as in Fig. 33 agree with results of the single mode approximation proposed by Girvin *et al.* [27]. The linear response function $\chi(q)$ (in the $\nu = 1/3$ Laughlin state) is dominated by the magnetoroton collective mode around $q_0\ell_0 \approx 1.4$. Would it be $\chi(q) = \delta(q - q_0)$, the density response to a point impurity potential would be $n(r) \propto J_0(q_0 r)$. This density profile looks like damped oscillations with the first node at $r = 1.7\ell_0$.

Regarding a more realistic profile of $\chi(q)$, this estimate for $n(r)$ is a very good approximation to $n(x)$ in Fig. 33a.

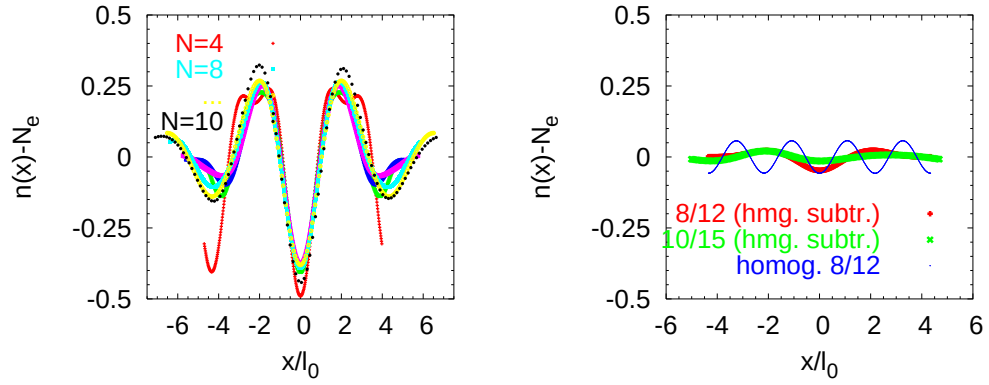

(a) The polarized state ($\nu = 1/3$ considered, see text) in systems with $N_e = 4$-10 electrons. Note that the response does not decay with increasing the system size.

(b) The singlet state. The thin line shows the CM oscillations in a homogeneous system, thick lines show responses to an impurity with CM oscillations subtracted.

Fig. 33: Polarized and singlet $2/3$ state and (non-magnetic) impurity in the form of a δ-line (along y). Normalized density along x is plotted.

As the purpose of the present work was to study systems with spin, we will now continue to spin singlet states at $\nu = 2/3$. Some quite new results for the $\nu = 1/3$ Laughlin state have been achieved by Müller [53].

The singlet state

The $2/3$ singlet ground state shows basically the same signs of incompressibility as the polarized state. The period of the density oscillations incurred by a δ-line impurity is almost the same ($r_1 \approx 2\ell_0$), and also in terms of classification of Fig. 32a, the singlet state shows an incompressible-like behaviour, cf. discussion of the polarized state. The striking feature of the singlet state is, that the strength of the response is about an order of magnitude less than in the polarized state. Thus in an 8-electron system, the density response is 'hidden' under the center-of-mass oscillations, Fig. 33b.

This strong difference between the singlet and polarized ground states is unexpected since 'incompressibility' gaps of both states are similar.

This hints at unusual stability of the singlet state with respect to charged inhomogeneities. In terms of perturbation theory, this is not due to energetic reasons but rather owing to small matrix elements of H_{EI} between the ground state and excited states. Energy of the first excited state, however, decreases when impurities are present and thus, in spite of the quite stable density of the GS, the gap will eventually collapse.

Regarding the response in systems of different size, we find a considerable attenuation when going from eight to ten-electron systems, Fig. 33b. Nevertheless we assume that the response remains finite even in the thermodynamic limit. To support this hypothesis, a fact worth of emphasis is that the $N_e = 8$ (10) singlet state occurs in systems with $N_m = 12$ (15) flux quanta, i.e. with system area $A = 2\pi\ell_0^2 N_m$ (1). These are the two smallest systems considered in Fig. 33a. For the these two systems we also observe a considerable attenuation of the $n(x)$ response when going from the $N_e = 4$ to $N_e = 5$ state, Fig. 33a, and this reduction in response is definitely only a finite size effect. As close as this analogy is, observations presented in Fig.

33b are not conclusive and an investigation of the singlet state in a larger system ($N_e = 12$) would be needed.

Let us just briefly mention, that non-magnetic impurities have no effect on the polarization of the singlet ground state.

2.3.2 Magnetic impurity in incompressible $2/3$ states

As far as spin polarized states are considered, magnetic impurities (55) cannot have any other effect than the electric impurities do. Therefore only the $2/3$ singlet ground state will be discussed here as the half-polarized states deserve to be considered separately, Subsec. 2.3.4.

Considering the *density*, Fig. 34a, we find a yet weaker response than for non-magnetic impurities, Fig. 33b. The response reminds of an incompressible system, in terms of Fig. 32a, and may remain finite in the thermodynamic limit, cf. discussion of non-magnetic impurities.

Polarization $n_\downarrow(x)/n(x)$ behaves quite differently, Fig. 34b: the response is large and it looks compressible. Again in terms of Fig. 32a. In particular, note that the polarization $n_\downarrow(x)/n(x)$ in Fig. 34b approaches ≈ 0.51 as we go 'far away' from the impurity, i.e. a different value than the polarization in the homogeneous case, 0.5.. Electrons with 'correct spin' ($\uparrow$) accumulate around the impurity, $n_\downarrow(0)/n(0)$ drops from the homogeneous value (0.5) by as much as by 5%, whereas the average polarization off the impurity slightly increases so as to keep the overall average value 0.5 as required by $S_z = 0$. This behaviour differs strongly from the density response, Fig. 34b.

It should also be noted that both density and polarization are here much less system-size dependent than in the case of non-magnetic impurities.

These are quite remarkable findings. It seems that the singlet state is *locally* much more 'incompressible' than the polarized state. On the other hand, the singlet state is relatively easily polarizable which is particularly striking when compared to the weak response in the density. If we assume the density in Fig. 33b to be the response of two independent liquids, then the polarization in Fig. 34b should be (i) smaller by a factor of five for $N_e = 8$ than what is observed and (ii) considerably smaller for $N_e = 10$ compared to the $N_e = 8$ case. This again contradicts the picture of two uncorrelated $1/3$ Laughlin liquids, one spin up, another spin down, which we could wrongly infer from the view of filled composite fermion LLs. Remind, however, that it is in fact not the claim of CF theories, that particles of $n = 0, \uparrow$ and $n = 0, \downarrow$ CF LLs are uncorrelated.

2.3.3 Integer quantum Hall ferromagnets

A brief introduction to integer quantum Hall ferromagnets (QHF) was given in Subsec. 1.6. It is instructive to keep in mind the scheme of Landau levels, Fig. 8.

Here we will focus on the $S_z = 0$ sector in prototypes of Ising and Heisenberg QHFs with neglected LL mixing. These states ($S_z = 0$) are analogues of the half-polarized states at filling $2/3$, the explanation follows. Disciples of CF teachings deem the $\nu = 2/3$ ground states to have $\nu_{CF} = 2$ completely filled CF LLs, Fig. 9b. Transitions between the singlet and polarized GSs occur, when the $(n, \sigma) = (0, \downarrow)$ CF LL crosses the $(1, \uparrow)$ CF LL. It is then plausible to neglect the low lying $(0, \uparrow)$ CF LL and look only at the two crossing CF Landau levels. The two ferromagnetic Ising states – the singlet, and polarized electronic GS at $\nu = 2/3$ – correspond to *all* CFs placed in the $(0, \downarrow)$, and $(1, \uparrow)$ CF LL, respectively, compare to Fig. 7b. Hence the half-polarized state ($\nu = 2/3$) corresponds to half-filled $(0, \downarrow)$ and half-filled $(1, \uparrow)$. Disregarding the fully occupied $(0, \uparrow)$ CF LL, i.e. counting only particles in the two crossing CF LLs (in total N_e CFs), the ferromagnetic Ising states are $S_z = \pm N_e/2$ and the 'half-half' state is $S_z = 0$.

In this Subsection we study the same situation as the one occuring at the $\nu = 2/3$ ground state transition (within the picture of crossing CF LLs) but for *electronic* Landau levels, i.e. with electrons instead of

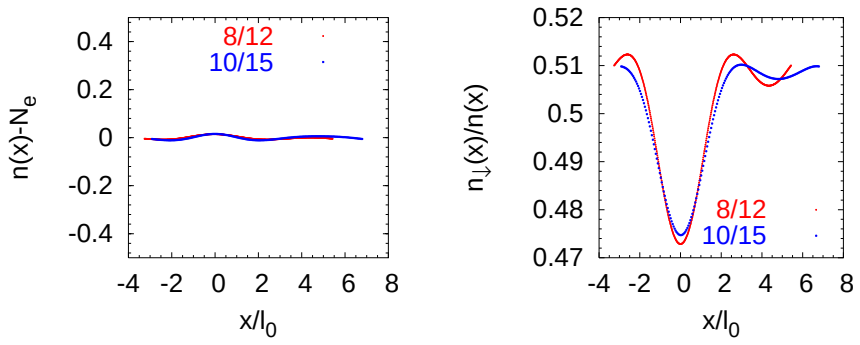

(a) Density. (b) Polarization.

Fig. 34: Singlet $2/3$ ground state for an attractive magnetic impurity $H_{MI,\uparrow}$ (55) in the form of a δ-line (along y). Normalized density and polarization along x are plotted.

composite fermions. We therefore study a $\nu = 1$ system with spin degree of freedom, where spin down (spin up) electrons lie in the $n = 0$ ($n = 1$) Landau level, respectively, and we disregard the fully occupied $(0, \uparrow)$ level. The physical system we model herewith has thus $\nu = 2$. Technically, this requires only implementing modified values of pseudopotentials, Fig. 2. Without electron-electron interaction, these two Landau levels are set to equal energy so as to model the LL crossing. Mixing to the fully occupied $(0, \uparrow)$ LL as well as to all higher LLs is neglected, since all these levels are well separated from the two crossing levels.

Heisenberg QHFs are not related to $\nu = 2/3$ and we investigate them just for the sake of comparison between Ising- and some other type of QHF. In the integer QHE regime, Heisenberg QHF occurs e.g. when $(0, \uparrow)$ and $(0, \downarrow)$ LLs cross (and $\nu = 1$) as it is the case for instance at vanishing Zeeman splitting. With CFs, this happens at $\nu = 1/3$, i.e. $\nu_{CF} = 1$, Fig. 9b.

We will first briefly discuss homogeneous states in these QHF systems and then we will turn to their response to magnetic inhomogeneities (δ-lines).

Ising quantum Hall ferromagnet

There are two degenerate ground states of an Ising ferromagnet: both with $S = N_e/2$, one $S_z = N_e/2$ and another $S_z = -N_e/2$. In general, excited states are no eigenstates to S^2 as a consequence of the omission of the fully occupied $(0, \uparrow)$ level and may only be classified according to S_z. They are all situated well above the ground states, Fig. 7b, and their energy grows with $N_e/2 - |S_z|$. In the following we will only speak about $S_z = 0$ states. The whole $S_z = 0$ sector is quite high in the complete spectrum. Unlike for a Heisenberg ferromagnet there is nothing like a $S = N_e/2, S_z = 0$ ground state for an Ising ferromagnet.

Low lying $S_z = 0$ states of the considered Ising QHF are apparently arranged into a flat dispersion branch, Fig. 35a. For a fully occupied Landau level, J 'coincides' with k_y^r. Precisely, $k_y^r = (N_e/2 - J)\sqrt{2\pi/N_m}$ for N_e even in the sense of (27). Centre-of-mass degeneracy is absent. The anomalous form of the branch in a $N_e = 8$ system, seems to be of finite-size origin, since $N_e = 10, 12$ and 14 spectra are all similar. States of the lowest branch have $\widetilde{k}^r$ of the form $(2\pi n/N_e, 0)$, $n = 0, \pm 1, \ldots, N_e/2$, or $(0, 2\pi n/N_e)$. This is in agreement with the symmetry between x and y (square elementary cell). It shows that rotational symmetry is absent in the low energy sector – otherwise we would observe also states with $\widetilde{k}^r = (k_x, k_y)$, $k_x, k_y \neq 0$. The lowest branch flattens and becomes well separated from excited states with increasing

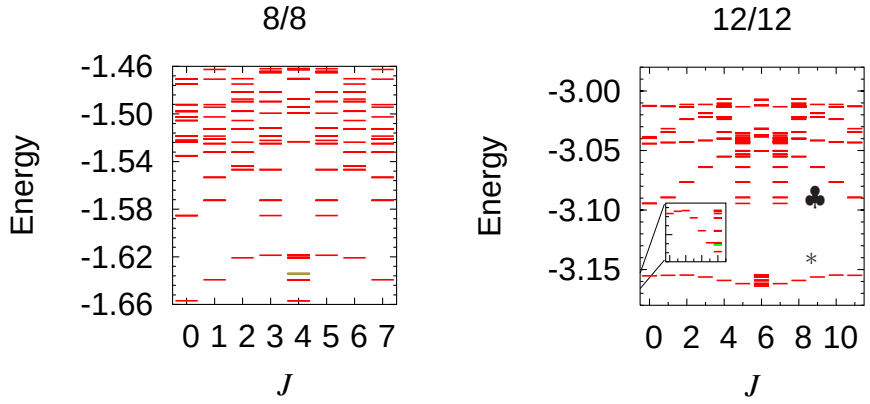

(a) Spectra. The lowest branch is marked by $*$, the second lowest by ♣. The state marked in different colour does not belong to the lowest branch.

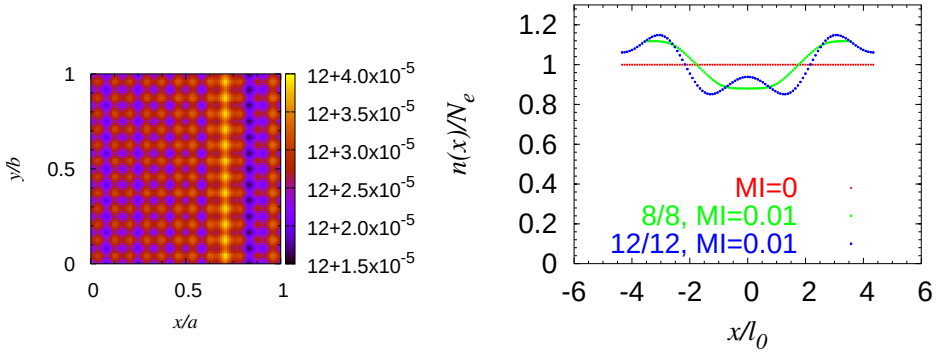

(b) *Left:* Density in the ground state, 12 particle system; *right:* change in density in response to a δ-line impurity, cf. Fig. 37b.

Fig. 35: Half-polarized states ($S_z = 0$) of an Ising quantum Hall ferromagnet. $\nu = 2$

system size, and the minimum energy remains at $\widetilde{k}^r = (0, 0)$. Also, other branches develop, the second lowest branch is described by $\widetilde{k}^r = (\pi n/N_e, \pm 2\pi/N_e)$ (plus the x-y symmetric partner) and minimum energy at points $(\pi, \pm 2\pi/N_e)$, see the $N_e = 12$ spectrum in Fig. 35a. Apart from these branches an isolated $\widetilde{k}^r = (0, 0)$ state is present (shown in gray in Fig. 35a) and it is hidden within the branch. We can hypothesise that this state becomes the absolute ground state i.e. gets separated from the lowest branch in sufficiently large systems.

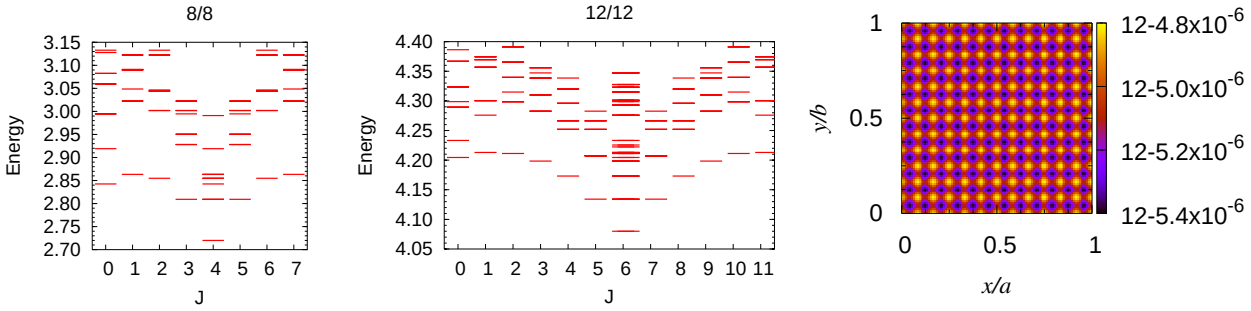

(a) Spectra. (b) Density, 12 particle system.

Fig. 36: Half-polarized states ($S_z = 0$) of a Heisenberg quantum Hall ferromagnet. $\nu = 1$

The flat branch is reminiscent of results of Rezayi[2] *et al.* [63] and could correspond to domain states, i.e. stripes along x or y with alternating spin polarization, in a system which does not prefer any particular domain size. The origin of the highly symmetric isolated (gray in Fig. 35a) state is unknown.

As it can be expected, low lying states have homogeneous density and it is true even for the whole lowest branch, as an example we show density in the ground state ($k^r = 0$), Fig. 35b. The anticipated domains would probably be visible first in correlation functions. States in the second lowest branch show unidirectional charge density waves.

In summary, in a homogeneous $\nu = 2$ Ising QHF we observe

(i) a flat branch of low lying states, which could become degenerate in infinite systems, Fig. 35a. This first branch probably consists of stripe domains – or spin density waves – of all possible wavelengths $\lambda = a/n$, $n = 0, 1, \ldots N_e/2$ just as in the system studied in [63]. Contrary to isotropic states (like Laughlin liquid), the wave must be parallel to one side of the square elementary cell.

(ii) second branch with pronounced dispersion, which could be a charge density wave

(iii) continuum of excited states above the two branches and

(iv) another state, with high symmetry, $k^r = (0, 0)$, which lies among the states of the lowest branch.

Heisenberg quantum Hall ferromagnet

The situation here is quite different from the Ising ferromagnets. The Hamiltonian (Coulomb interaction projected to the lowest Landau level) conserves the total spin S and it even commutes with S^+ and S^- which change S_z while keeping the length of the total spin. The ground state is fully polarized, $S = N_e/2$, but its z-component of spin is arbitrary, Fig. 7b.

Looking at the sector $S_z = 0$, Fig. 36b, the lowest state is thus the ferromagnetic $S = N_e/2$ state. Other low-energy states form again a branch, $\widetilde{k}^r = (\pm\pi n/N_e, 0)$ and $(0, \pm\pi n/N_e)$, $n = 0, \ldots, N_e/2$ (x-y symmetry present, rotational symmetry absent). Contrary to the Ising QHF, this branch does not seem to flatten. States in the branch fulfil $S = N_e/2 - n$: the ferromagnetic (ground) state is polarized and going up the branch, the polarization decreases. In this respect, the excitations of the lowest branch markedly

[2] The cited work concerns the situation when the lowest and the third Landau levels of different subbands cross. Rezayi *et al.* had first to show that this system is an Ising QHF. See subsection 1.6 for more details. In the $S_z = 0$ sector of his system Rezayi *et al.* found a multiply (almost) degenerate ground state with $\widetilde{k}^r$ just of the sequence $(2\pi n/N_e, 0)$, similar as we see in Fig. 35a for $N_e = 12$.

differ from spin density waves. What we observe in the Heisenberg QHF are most likely states with n weakly interacting spin waves which were observed under the same conditions on a sphere by Wójs and Quinn [76].

Half-polarized QHF states and magnetic impurity

If a homogeneous state cannot be established and domains formation is more favourable, then no particular domain size is preferred. This is the central message of the following paragraph and it applies to both Ising and Heisenberg QHFs described at the beginning of Subsection 2.3.3.

The two systems were subjected to a δ-line magnetic inhomogeneity, just as the incompressible singlet ground state in Subsec. 2.3.2. However, QHF systems and incompressible liquid states at $\nu = 1/3$ or $2/3$ behave quite differently. Looking at a QHF and comparing the response in systems of different sizes, we observe no intrinsic length scale, Fig. 37. Rather, the form of the response reflects the size of the system (cf. the left panel of Fig. 32c). This statement applies both to the Ising, Fig. 37b, and the Heisenberg QHF, Fig. 37a, where we show the polarization of the energetically lowest state in a system subject to the inhomogeneity.

It is also interesting to study the *density* of the disturbed QHF states. The density of the Heisenberg QHF remains almost unchanged (it is constant) unlike the density of the Ising QHF state, Fig. 35b right. This is understandable. Whereas in the Heisenberg QHF spin up and spin down one-particle states have exactly the same wavefunction, both spin up and spin down states are from the lowest Landau level, this is not the case for the Ising QHF. In that case, spin up and spin down states come from different Landau levels. Thus, even when the magnetic impurity shuffles the spin up and spin down particles somehow in the Heisenberg QHF, the density does not change.

Finally, we comment on densities in the inhomogeneous states in the Ising QHF. Results shown in Fig. 35b belong to quite small systems (12 particles at most). In the largest system studied, we observe a maximum in the density direct at the position of the impurity ($x = 0$) and the maximum approaches the value of density in a homogeneous system. With some imagination this allows for a hypothesis that – if domains are formed in an infinite system – the density will be inhomogeneous close to the domain boundary while remaining homogeneous inside a domain. However, we would have to study larger systems to confirm this speculation.

2.3.4 The half-polarized states

The inner structure of the half-polarized ($S = N_e/4$) ground state at filling $2/3$ is investigated in this Subsection. We will argue that this state (assuming short-range interaction) resembles rather the incompressible singlet and polarized ground states at $\nu = 2/3$ than the Ising quantum Hall ferromagnet in the $S_z = 0$ sector as described in Subsection 2.3.3.

In this Subsection, by half-polarized ground states we mean the 8- and 12-electron $S = N_e/4$ states GS_8 and GS_{12} as introduced in Sec. 2.2, cf. correlation functions in Fig. 28.

The ground state in a homogeneous system has a nearly constant density (oscillations due to the center-of-mass part wavefunction are less than 0.1% in the 12-electron system). This changes when a weak δ-line magnetic impurity along y is applied. Not only the polarization but also the *density* becomes inhomogeneous, Fig. 38. The first minima of $n(x)$ are at the same position $r_1 \approx 2.2\ell_0$ in the two system sizes considered and decaying oscillations are likely to follow at larger distances. Comparing the two system sizes in Fig. 38a, we find a much weaker response in the larger system, but this still does not have to imply a vanishing response in an infinite system, cf. discussion of the singlet state in Subsec. 2.3.1.

Unlike the Ising quantum Hall ferromagnet discussed in Subsect. 2.3.3, the half-polarized states seem to have an intrinsic length scale in $n(x)$ (of the order of r_1), Fig. 38a. It is remarkable that this r_1 matches

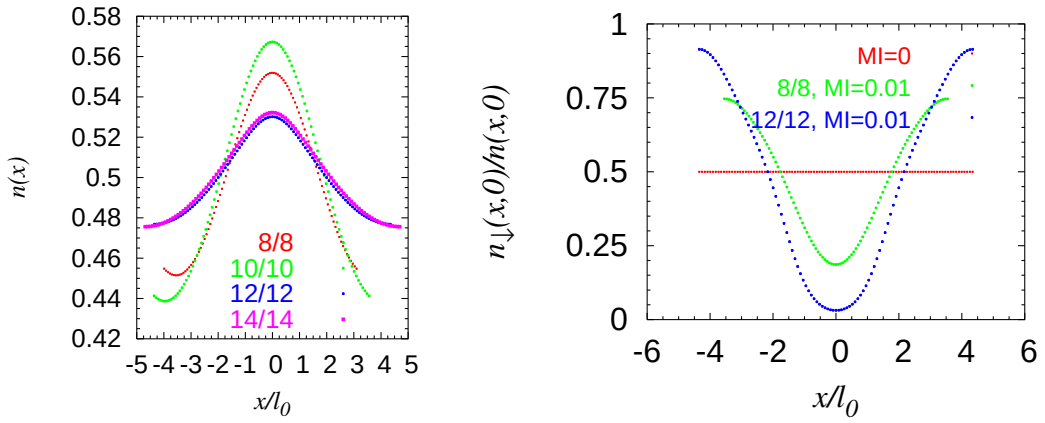

(a) Heisenberg QHF ($\nu = 1$). (b) Ising QHF ($\nu = 2$, crossing of $n = 0, \uparrow$ and $n = 1, \uparrow$ levels.

Fig. 37: Different quantum Hall ferromagnets (QHF), half-polarized states: polarization response to a magnetic δ-line impurity in systems of 8 and 12 particles.

quite well the position of the first maximum in the density of the Laughlin state ($1/3$) responding to an impurity, Fig. 33.

Contrary to the density, the *polarization* does not show an intrinsic length scale as positions of the first minima in $N_e = 8$ and $N_e = 12$ systems mismatch considerably, Fig. 38b. However, the polarization response here differs from the behaviour of the singlet state, Fig. 34b. Rather, Fig. 38b suggests that $n_\downarrow(x)/n(x) \to 0.75$ as we go away from the impurity for the half-polarized states. This behaviour was classified as 'incompressible' in Fig. 32a.

These observations suggest that the presence of an impurity will not lead to a splitting of the state into two domains (one with spin up, second with spin down), which we could expect for Ising QHF, Fig. 37. It seems that an impurity will rather change the polarization of the system only locally, in an 'incompressible manner', Fig. 32a. The density response has the same characteristic length scale as the singlet and polarized $\nu = 2/3$ ground states and such a length scale is absent in the polarization in agreement with behaviour of the singlet state, Fig. 34b.

A state with $S_z = N_e/4$ comprises of $\frac{1}{4}N_e$ electrons with spin down ('minority spins') and $\frac{3}{4}N_e$ electrons with spin up ('majority spins'). Since the two populations are not balanced, we may gain extra information by speaking to them separately. The simplest concept, assuming non-interacting electrons, would be that $H_{MI,\downarrow}$, $H_{MI,\uparrow}$ and H_{MI} (55) give rise to responses in ratio $\frac{1}{4} : \frac{3}{4} : 1$. *Very roughly*, this is indeed the case. Heights of the central peak ($x = 0$) for these three types of inhomogeneities are indeed approximately in this ratio, both for the density and for the polarization, Fig. 39. In the following we will discuss investigations with spin-dependent perturbations in more detail.

Let us separate the density of majority and minority spins, Fig. 40. We will argue that the half-polarized state with N_e electrons consists of two coexisting and weakly interacting liquids: $N_e/2$ electrons in a fully polarized liquid (with $S_z^p = N_e/4$) and $N_e/2$ electrons in a $S_z^u = 0$ state. Minority spins are thus present only in the $S_z^u = 0$ liquid whereas majority spins occur in both of them. Concentrate on Fig. 40c.

(i) Minority spins ($\downarrow$) react almost equally to $H_{MI,\uparrow}$ and $-H_{MI,\downarrow}$. They reflect only changes in the $S_z^u = 0$ liquid and there are as many up as down spins in it. In fact, the $H_{MI,\uparrow}$ impurity influences also the polarized liquid component, but we cannot see it in the density of minority spins provided the two liquids

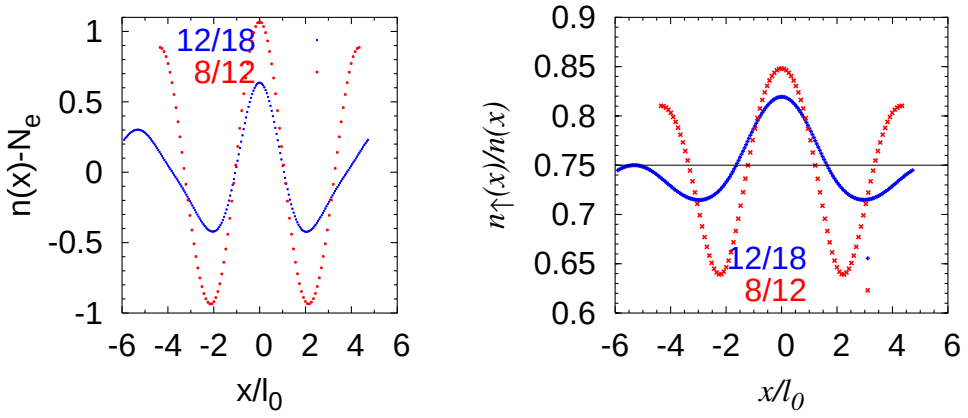

(a) Density. (b) Polarization.

Fig. 38: Half-polarized ground state ($S = N_e/4$) responding to a δ-line magnetic impurity, $H_{MI,\uparrow}$ (55).

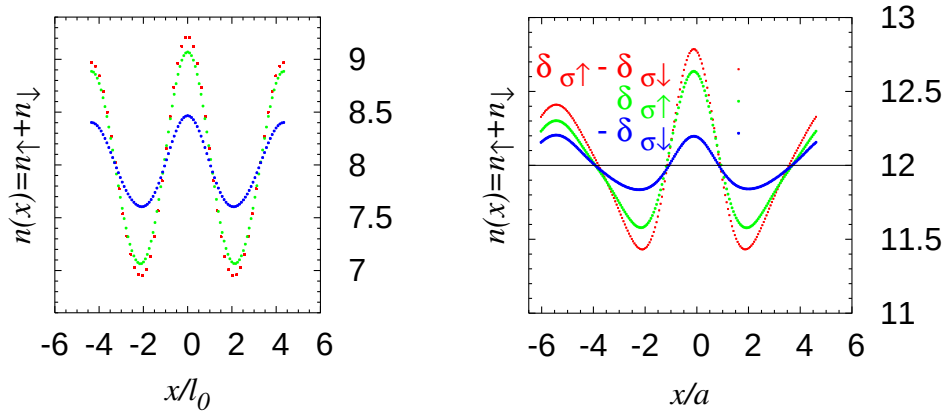

(a) 8 electrons, density. (b) 12 electrons, density.

Fig. 39: Half-polarized ground state ($S = N_e/4$) responding to a δ-line magnetic impurity. Different impurity types are considered: H_{MI}, $H_{MI,\uparrow}$ and $H_{MI,\downarrow}$ (55).

do not interact appreciably. The combined effect of $H_{MI,\uparrow} - H_{MI,\downarrow}$ causes a response of about the sum of these two.

(ii) Majority spins (↑) react differently to $H_{MI,\uparrow}$ and $-H_{MI,\downarrow}$. We should keep in mind that $n_\uparrow$ reflects changes in both (polarized and $S^u_z = 0$) liquids. The latter impurity inflicts changes only on the $S^u_z = 0$ part, whereas the former impurity acts on both liquids. If both liquids would have the same sensitivity to the considered impurities, we could expect responses in ratio $4 : 3 : 1$ (H_{MI} to $H_{MI,\uparrow}$ to $H_{MI,\downarrow}$). The fact that responses observed in Fig. 40c (measured by the height of the central maximum) are in ratio $3 : 2 : 1$ could be an indication that the polarized liquid is less sensitive than the $S^u_z = 0$ liquid.

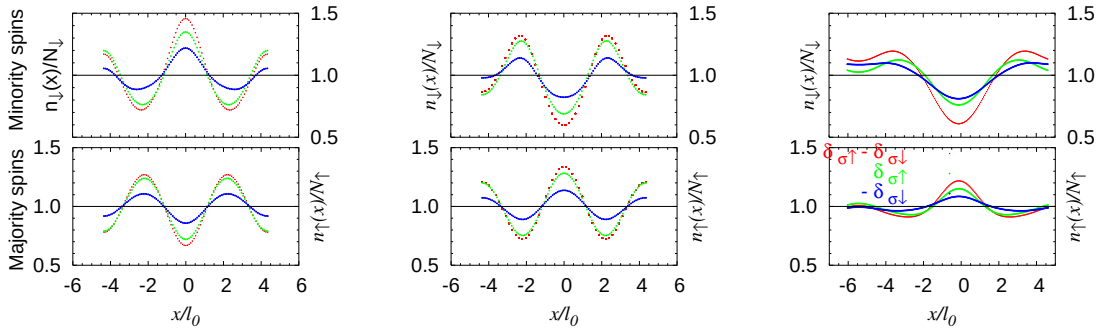

(a) 8 electrons, repulsive. (b) 8 electrons, attractive. (c) 12 electrons, attractive.

Fig. 40: The same as Fig. 39, but the density is decomposed into the density of majority spins ($n_\uparrow$) and minority spins ($n_\downarrow$). By attractive (repulsive) is meant that the δ-impurity at $x = 0$ is attractive (repulsive) for the majority spin.

(iii) Note also, that responses are the same (up to an inversion) for attractive and repulsive impurities, Fig. 40a and 40b, provided the impurities are weak.

Studies of the eight electron half-polarized state, Fig. 40b is not in conflict with this interpretation, responses in densities are quantitatively different though. However, we should be cautious in drawing strong conclusions as these systems with primitive cell of size 12 flux quanta correspond to the smallest system ($N_e = 4$) considered in Fig. 33 ($\nu = 1/3$ state plus an impurity) and in that case finite size effects are already very strongly pronounced. Thus, the twelve electron system can be considered as the smallest system with finite size effects *not* playing a major role.

Conclusion

The hypothesis of the coexistence of the spin singlet and polarized liquids in the half-polarized states (HPS) seems to be supported. We have pointed out some similarities between the HPS and the former two incompressible states. In contrast, response to magnetic impurities seems to be different for the HPS and the Ising quantum Hall ferromagnet (in the $S_z = 0$ sector) which would be the direct counterpart of the HPS if composite fermions are substituted by electrons.

In general, it is not very surprising that electronic systems ($\nu = 2$ Ising QHF) differ strongly from the CF-counterparts. We have already seen this in correlation functions in Subsec. 2.1.1. However, the observed differences seem to be too deep to allow us to establish a relation between QHF states and the half-polarized states introduced in Sec. 2.2.

2.4 Deforming the elementary cell

In this Section we discuss another way of how to investigate fractional quantum Hall states. We will exactly diagonalize $\nu = 1/3$ and $\nu = 2/3$ systems in elongated rectangular elementary cells. The dimensions are a by b, the aspect ratio is thus $a : b > 1$. The area of the rectangle is always kept constant, $ab = 2\pi\ell_0^2 N_m$ (1), and therefore

$$ab = 2\pi\ell_0^2 N_m\,, \qquad \Rightarrow a = \ell_0\sqrt{2\pi N_m \lambda}\,,\; b = \ell_0\sqrt{2\pi N_m/\lambda}\,,\; \lambda = a : b\,. \tag{56}$$

What can we expect? In the first approximation, we would say (i) nothing happens for an isotropic state such as the $\nu = 1/3$ Laughlin liquid and (ii) crystalline or wave-like states will change both in energy

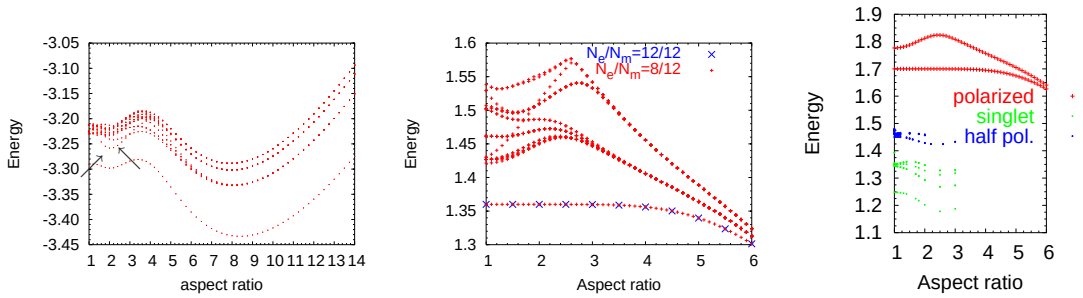

(a) Coulomb interaction $(1/3)$.

(b) Short-range interaction $(2/3)$. Blue crosses mark the energy of a full Landau level. See the comment [3] for details.

(c) Polarized, singlet and half-polarized states at $\nu = 2/3$. Overview.

Fig. 41: Spin polarized eight electrons at filling factor $1/3$ and $2/3$. Energy of the lowest states versus aspect ratio of the primitive cell. An overview of the polarized, singlet and half-polarized states in the same scale is presented in the last panel.

and in density. The reason is, that structures in homogeneous liquid states (as for example in correlation functions in Subsec. 2.1.1) are intrinsic and not incurred by the finite system size. Consequently, we expect the liquid state to change neither their energy nor their correlation functions, at least not on short distances, if $a : b$ is slightly varied. On the other hand, an integer multiple of the period of a wave-like or crystalline state must be necessarily equal to a and/or b, hence by varying the aspect ratio we force it to change its period. In a classical crystal this means compression, or better deformation, since total 'volume' ab remains constant, and we expect it to cost energy.

This investigation of $\nu = 2/3$ systems was partly motivated by the work of Rezayi *et al.* [63] who investigated one particular type integer quantum Hall ferromagnet. Their exact diagonalization on a torus showed an N_m-fold nearly degenerate ground state and the authors argued that these states comprised of stripes of alternating spin polarization (Subsec. 2.3.3) oriented parallel to one side of the rectangle, for example a. As they varied the aspect ratio, the states still remained degenerate, and their energy $E(\lambda)$ changed proportional to b. In fact, the degeneracy even improved: the small energy differences between the N_m states dropped. This was a strong argument for the stripe order, since then $\mathrm{d}E(\lambda)/\mathrm{d}b$ can be interpreted as energy per unit length of an interface between a spin up and spin down stripe.

2.4.1 Incompressible ground states

As usual, we will start with $\nu = 1/3$, being probably the best understood system. This will also be the only case where we will discuss Coulomb interacting systems, in the rest we will stay with short-range interacting systems.

Coulomb versus short-range interaction: $\nu = 1/3$

The spectrum of a Coulomb-interacting system has a quite rich structure, Fig. 41a. The ground state energy exhibits several minima as a function of the aspect ratio of the elementary cell. In fact even more structure seems to appear in larger systems, as far as it could be inferred from comparing 6, 8 and 10 electron systems. In the following, we will show that this structure occurs mainly due to the long-range part of the Coulomb potential, it should be possible to describe it mainly by the Hartree part of the total energy or simply that it is due to formation of charge density waves (CDW) resembling Wigner crystals. Differences between Wigner crystals and CDWs are discussed below. In fact, energy of the states in question, Fig.

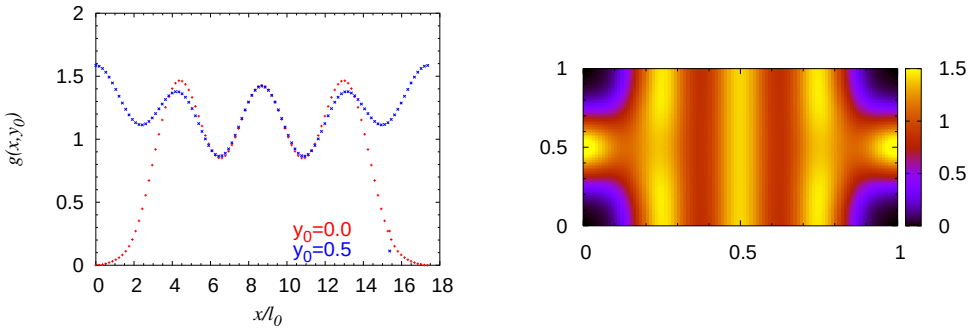

(a) The 'square' crystal state (aspect ratio 2).

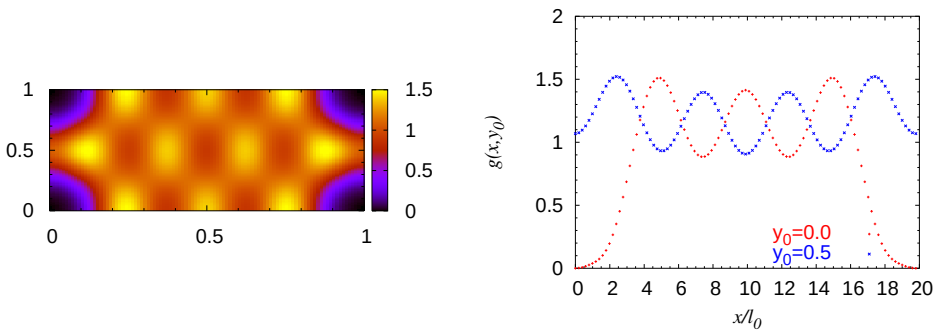

(b) The hexagonal crystal state, aspect ratio $4/\sqrt{3} \approx 2.31$.

Fig. 42: Charge density waves resembling Wigner crystal states are among the lowest excitations in a Coulomb interacting $1/3$ system. Their energy is minimized (as a function of aspect ratio) when the elementary cell matches the crystal geometry. Correlation functions in eight-electron systems are shown, length of x- and y-sides corresponds to the particular aspect ratio.

42, will contain strong exchange contributions. Nevertheless, these states are very similar to the *classical* states which minimize the Coulomb energy. In a second step, we will discuss how correlations (and energy due to correlations) depend on the aspect ratio, Fig. 41b.

In order to understand the the aspect-ratio dependence of energy of the Coulomb-interacting ground state, let us focus on two low excited states marked by arrows in Fig. 41a. These two states are just the CDWs mentioned above and they look almost like Wigner crystals: one hexagonal, another square, as density-density correlation shows, Fig. 42. It is then not surprising that the energy of such states is minimal, when the aspect ratio matches its geometry. For eight electrons considered here, this happens for[3] $4d : 2d = 2$ and $4d : (2\sqrt{3}/2d) = 4\sqrt{3}/3$ for the square and hexagonal crystal, respectively. Perhaps the most apparent difference between a CDW and an (unpinned) Wigner crystal is that for the latter state we expect the correlation function to drop almost to zero between the 'lattice sites' and this is not the case here, Fig. 42. The reason is that at filling factor $\nu = 1/3$, the system is too densely populated, or mean interparticle distance is too small, $r_{mean}/\ell_0 = \sqrt{2\pi/\nu} \approx 4.35$ (1) to allow the electron density (or correlation function) to vanish between two sites. Remember that an electron *within the lowest Landau level* cannot be localized

[3] d is the 'lattice constant'.

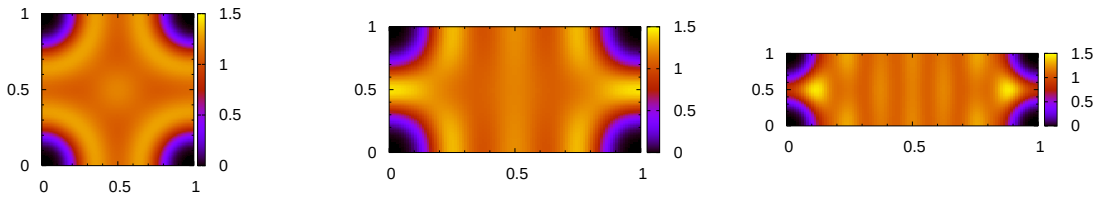

(a) Aspect ratio 1.00. (b) Aspect ratio 2.00. (c) Aspect ratio $2\sqrt{3} \approx 3.46$.

Fig. 43: Evolution of the Laughlin state with aspect ratio of the elementary cell (Coulomb interaction). Correlation functions are shown.

more strongly than on a length scale of the order of unity (magnetic length ℓ_0). Even if we assembled a hexagonal Wigner crystal at $\nu = 1/3$, the wavefunctions at neighbouring sites would strongly overlap and it is then more favourable for the electrons to retain some features of the Laughlin correlations. As a result we obtain a CDW (or a 'strongly correlated crystal' [47]) like the state in Fig. 42b. At lower filling factors, r_{mean}/ℓ_0 is larger and Wigner crystal states become possible. This can be interpreted as a quantum phase transition from liquid to solid as the filling factor is decreased and the extensive studies in this field suggest the critical value $\nu \approx \frac{1}{7}$, see Sec. 5.7 in Chakraborty [14] for a review.

The ground state (GS) energy reflects these geometrical conditions. This state also minimizes its energy when the square crystal can easily be formed, but at short distances it strictly preserves the liquid-like correlations, Fig. 43. It is isotropic at short distances, in Fig. 43b, the ring corresponding to the first maximum is circular and not deformed into an oval for instance, Fig. 42, and also $g(r) \propto r^6$ (not obvious in Fig. 43). It seems plausible that the increase of GS energy around $a : b \approx 3$, Fig. 41a, is due to the loss of isotropy at shorter distances. The ring of the first maximum in $g(r)$ disappears, Fig. 43c, the feature $g(r) \propto r^6$ however remains. It is important to know, that unlike the energy, the *structure* (correlation functions) of the ground state is quite insensitive to the type of interaction (Coulomb or short-range).

Let us now proceed to short-range interacting states. The crystalline states disappear from the realm of low-energy excitations. The ground state energy is completely independent on aspect ratio, it is zero, Fig. 41b. Energies of fully polarized $2/3$ states displayed therein are equal to those of $1/3$-systems up to a constant shift. This constant depends on aspect ratio, but the dependence is imperceptible up to $a : b \approx 4$ (for 4 electron system). In fact, the ground state is rigid in the following sense: a state can have zero energy only if there are three zeroes on the position of each electron in the wavefunction. The wavefunction is completely determined by this condition together with the confinement to the lowest Landau level. It is even surprising, that given how strictly determined the ground state is, it once resembles a liquid (for $a : b \approx 1$) and another time a CDW state (larger aspect ratios), Fig. 43c.

Assuming fully spin polarized electrons, $2/3$ and $1/3$ systems (e.g. $8/12$ and $4/12$) are particle-hole conjugated. Thus, spectra of these systems are identical up to a constant energy shift, which is just the Coulomb (or short-range interaction) energy of a completely filled lowest Landau level. Note that this energy *varies* with aspect ratio (both for Coulomb and for short-range interaction). The common statement that interaction energy of a full LL is a constant is valid in a broad range of aspect ratios, but not everywhere. In Fig. 41b, this holds up to $a : b < 4$, Subsect. 1.5.4. This is shown in Fig. 41b. The $\nu = 1/3$ Laughlin state has zero energy for any aspect ratio (not shown), the $2/3$ ground state energy is then just the Hartree-Fock energy of a completely filled Landau level. Beyond $a : b \approx 4$, this energy is no longer constant, indicating

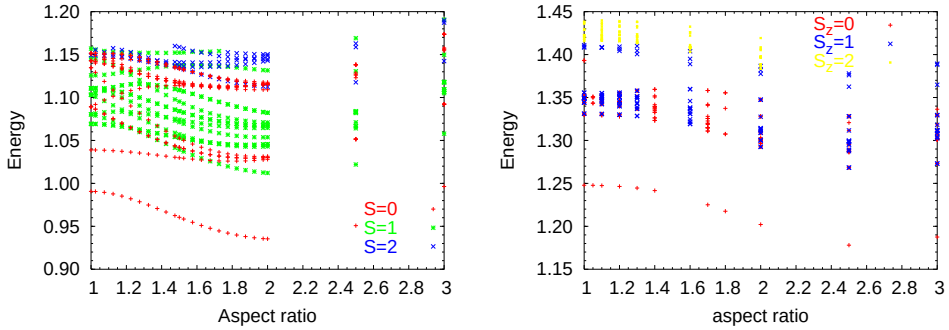

(a) Eight electrons.

(b) Ten electrons.

Fig. 44: Low lying states at filling $2/3$ under vanishing Zeeman splitting versus aspect ratio of the primitive cell. Note that energy of the singlet ground state remains about constant for aspect ratios $\lesssim 1.4$ in the larger system.

that the deformation of the elementary cell becomes pathologic and beyond this point (at latest), the model no longer describes a 2D system but rather an effective 1D system.

Consider $a/b \gg 1$. Then the N_e electrons are located on a very thin cylinder [62] of length $\propto \sqrt{a/b}$ (area of the cylinder is fixed by filling factor, $ab = 2\pi N_m$) and single electron states resemble 'rings on a pole'. The mean distance between electrons is then $\propto \sqrt{a/b}/N_e$ and Coulomb energy is then proportional to $(a/b)^{-1/2}$. The increase of the ground state energy for very large aspect ratios, Fig. 41a, is due to the repulsion between an electron and its own periodic image in the 'short-direction'.

Excited states are sensitive to deformation of the elementary cell even more. Energy levels group into branches beyond $a/b \approx 2$, Fig. 41b. Keeping in mind the transition towards an effective 1D model, these branches can be attributed to 0, 1, 2, etc. pairs of 'rings on a pole' sitting at neighbouring sites. In illustrative terms, there is no longer enough room for two electrons to be positioned in 'vertical' direction (along y axis, i.e. the shorter side of the elementary cell) except when they freeze into a crystal.

In conclusion, going beyond aspect ratio ~ 2 (in a $N_m = 12$ system) the system cannot be taken as a faithful model for an isotropic infinite system.

The singlet state

The singlet ground state is apparently more sensitive to varying the aspect ratio. Its energy changes at much smaller deformation than that of the polarized state, Fig. 41c. However, comparison between systems of different sizes shows that its energy is also constant, provided that the aspect ratio is not much larger than one and the system is large enough, Fig. 44. This is another hint at isotropy of the state. A crystalline state responds more strongly to a change of a/b, since this is in principle an attempt to compress the lattice in one direction while expanding it in the other direction. Recall just the CDW states in $\nu = 1/3$ systems marked by arrows in Fig. 41a.

This is in agreement with a direct observation of correlation functions, Fig. 45. In particular, the ring structure in $g_{\uparrow\downarrow}(r)$ (or maximum at $r_0 \approx 3.4\ell_0$) remains preserved even for aspect ratios $a : b \approx 3$, Fig. 45 right. This is similar to how the ring structure of the first maximum was preserved in the deformed $\nu = 1/3$ Laughlin state, Fig. 43b. Also, looking at $g_{\uparrow\uparrow}(x)$ and $g_{\uparrow\downarrow}(x)$ in the deformed singlet state, the *sum* of these two seems to remain constant beyond r_0 even in deformed systems, in spite of $g_{\uparrow\downarrow}(x)$ decreasing beyond $x = r_0$. This was just the conclusion in $a : b = 1$ systems, Fig. 15, and it suggests that the singlet state did not change much even in a quite strongly deformed system ($a : b \lesssim 3$). Moreover, this finding allows

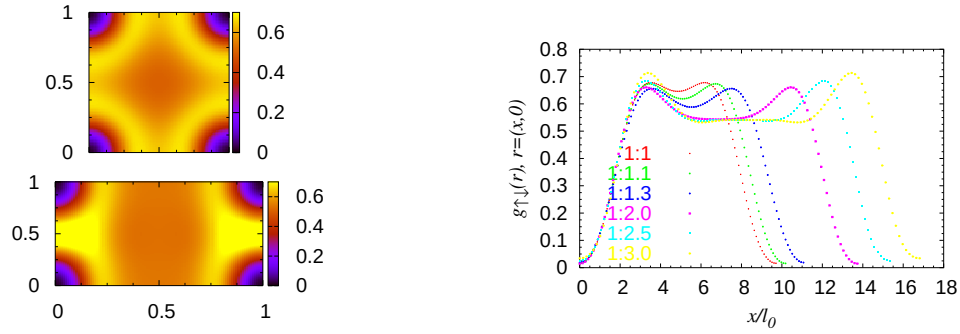

Fig. 45: The singlet $2/3$ state in elementary cells of different aspect ratios: density-density correlation between unlike spins (the two aspect ratios shown in 2D plots are $a : b = 1$ and 2).

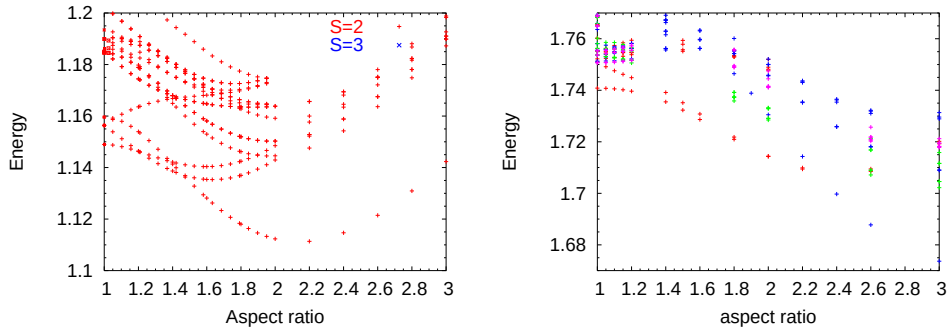

(a) 8 electrons.

(b) 12 electrons. Colours indicate different J's.

Fig. 46: Half-polarized states ($S = N_e/4$) at filling $2/3$ versus aspect ratio. States with next larger spin are well above (out of scale here).

us to use deformed systems to study what happens on slightly larger distances than distances accessible in a square cell of a fixed area because maximum distance between two electrons in a deformed elementary cell, $\frac{1}{2}\ell_0\sqrt{2\pi N_m}(\lambda + 1/\lambda)$, grows with increasing λ.

Regarding the energy, which seems to react more sensitively to deformations than the correlation functions, the following speculation seems plausible. If the singlet state is a liquid of $\uparrow - \downarrow$ pairs of characteristic size $r_0 \approx 3.4\ell_0$, Subsec. 2.1.1, it ought to be more sensitive to aspect ratio variations than the Laughlin state just because such a pair in the $\nu = 2/3$ singlet state is larger than a single electron in the $\nu = 1/3$ Laughlin state.

2.4.2 Half-polarized states

The half-polarized states can be expected to suffer severely under the finite size of the system. A system with eight electrons contains only two electrons with minority spin. Contrary to fully polarized systems (where eight particles is already fair enough), it is thus the smallest system with $S = N_e/4$ where many-body effects can be studied.

Let us compare how systems of two different sizes respond to varying aspect ratio. In an eight-electron system, Fig. 46a, there are four low lying states: the ground state at $a/b = 1$ with $\widetilde{k}^r = (\pi, \pi)$, a $(0, 0)$

state which becomes the ground state at $a/b > 1.5$ and a pair of degenerate states, $(0,\pi)$ and $(\pi,0)$ ($\widetilde{k}^r$ is defined in Subsec. 1.5.2). The former two states are isotropic (and lie in high symmetry points of the Brillouin zone), the other two are spin-density waves in x and y direction, judging by the correlation functions (not shown). Moving away from aspect ratio one, degeneracy of the latter two is lifted – just as the $90\,\mathrm{deg}$ rotational symmetry of the elementary cell is broken – and the wave along x (the longer side) becomes energetically more favourable. It is quite conspicious that this state evolves parallel to the (π,π) state for aspect ratios above ≈ 1.4. For these values of $a:b$, the inner structure of these two states seems to be very similar, too.

In the low-energy sector, a $(0,0)$ state is absent in a 12-electron system, Fig. 46b. In other respects, however, the situation is quite similar to the smaller system. There is a well-separated (π,π) ground state in a square cell and this state becomes nearly degenerate with a $(0,\pi)$ state for aspect ratios $\gtrsim 1.4$. Also, the energy of these two states decreases with increasing aspect ratio and eventually reaches its minimum. In contrast to the smaller system, the minimum occurs later, at $a:b \approx 2.4$ (Fig. 46b) compared to ≈ 1.6 in Fig. 46a, but this occurs also for the incompressible states, e.g. the singlet at $\nu = 2/3$ (Fig. 44a vs Fig. 44b). The correlation functions of these two states, $(0,\pi)$ and (π,π), are similar to those of the $(0,\pi)$ and (π,π) states in the eight-electron system (not shown).

Now turn to the correlation functions of the $(0,\pi)$ and (π,π) states in a 12-electron system, Fig. 47. Both states are quite isotropic, for a square elementary cell, first at a very close look, we find a slight x versus y anisotropy in the $(0,\pi)$ state. However, already under slight variation of the aspect ratio, stripe structures parallel to the shorter side evolve ($a:b = 1.2$, Fig. 47a). In this respect, both states look quite similar, Fig. 47 (or compare Figs. 47a and 47b), and we should stress that the differences in the correlation functions between the isotropic (at $a:b = 1$) and the wave-like state ($a:b = 1.8$) are very large, both in isotropy/anisotropy and in the short-range behaviour, Fig. 47c. This is in a strong contrast to the behaviour of the incompressible states, e.g. the Laughlin state which preserves lot of its original isotropy even at $a:b \approx 2$, Fig. 43.

These observations suggest the following interpretation. The half-polarized ground state at $\nu = 2/3$ is an isotropic state which however inclines to the formation of a spin-density wave. The wave has the shortest period allowed by the number of electrons, i.e. it resembles an antiferromagnetic ordering ($\uparrow\downarrow\uparrow\downarrow\ldots$ rather than $\uparrow\uparrow\downarrow\downarrow\ \ldots$, for instance) as the correlation functions in the rightmost column in Fig. 47a suggest. Since there are just three $\downarrow$-electrons in the system, we expect two stripes (the third $\downarrow$-electron is just at the origin) in $g_{\downarrow\downarrow}(x,0)$ in the case of $\uparrow\downarrow\uparrow\downarrow\ \ldots$ ordering. In more detail, see Fig. 47d: the minima/maxima in $g_{\uparrow\uparrow}(x,0)$ match well with the maximum/minima in $g_{\uparrow\downarrow}(x,0)$. In other words, spin up is followed by spin down. However, the amplitude of oscillations in $g_{\downarrow\downarrow}(x,0)$ is moderate, Fig. 47c, and hence we should rather classify the state as a 'spin density wave' than e.g. a state with stripe domains of alternating spin polarization.

On the basis of the present investigation, it is not clear whether in a large enough system, this spin wave state is the ground state, a low-energy excitation or it is degenerate with the isotropic ground state. Even though the GS at $a:b > 1$ (spin wave) has a lower energy than the isotropic state at $a:b = 1$, Fig. 46b, this does not say much about which state would be the ground state in a larger system. We saw a similar situation for the $\nu = 1/3$ Laughlin state, Fig. 41a, or the singlet $\nu = 2/3$ state, Fig. 44. The energy of the ground state was not at its minimum at $a:b = 1$, yet the isotropic ($a:b = 1$) state is probably the real ground state in the thermodynamic limit. The question how to decide which state – isotropic or anisotropic – will be preferred in infinite systems remains open, but comparison between systems of more different sizes could be very helpful.

2.4.3 Conclusions

It has been demonstrated that isotropic states like the fully polarized or singlet incompressible $\nu = 2/3$ ones tend to be insensitive to slight deformations. The response was observed in the energy of the state

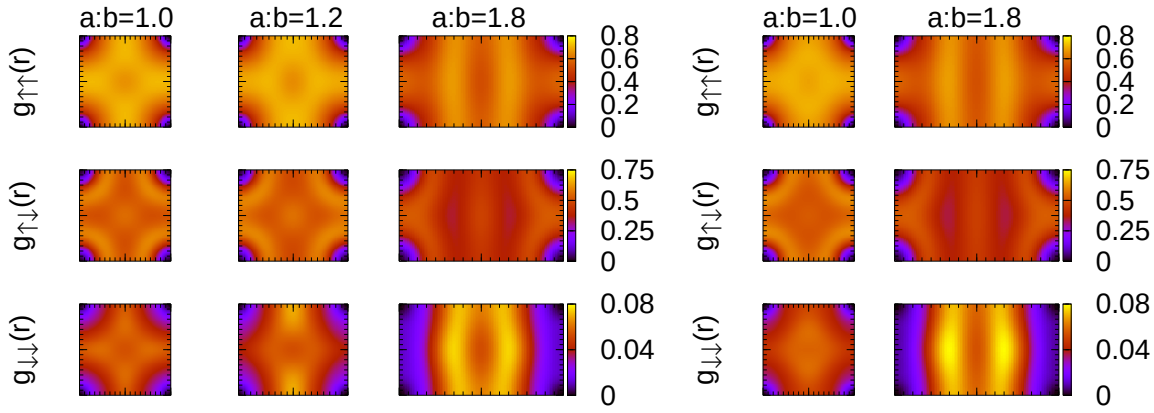

(a) The lowest state, $\widetilde{k}^r = (\pi, \pi)$.

(b) The first excited state, $\widetilde{k}^r = (0, \pi)$.

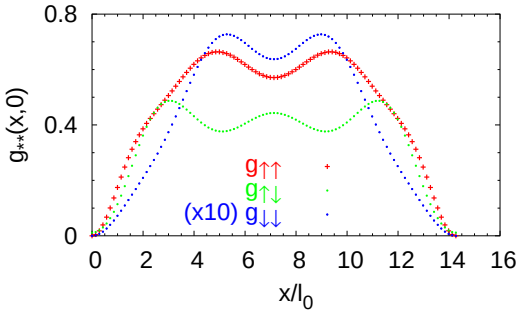

(c) $g_{\uparrow\uparrow}$, $g_{\uparrow\downarrow}$ and $g_{\downarrow\downarrow}$ of the lowest state in a deformed cell.

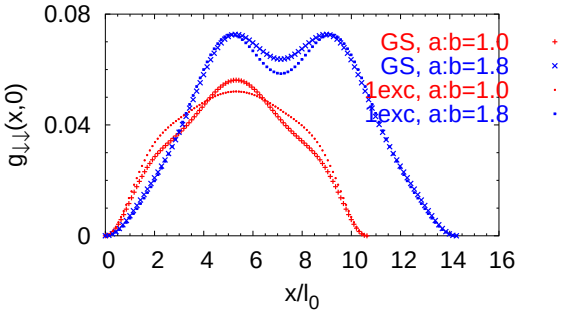

(d) $g_{\downarrow\downarrow}$, section along x for square and deformed elementary cell.

Fig. 47: Evolution of two half-polarized states lowest in energy with growing aspect ratio of the elementary cell (12 electrons, $\nu = 2/3$, short-range interaction). Correlation functions are shown.

and in its correlation functions, where we saw that especially the short-range behaviour remains basically unchanged. The insensitivity improves with increasing the system size (number of particles). We also registered some differences between the singlet and polarized state. In systems of equal size (area) the former state was disturbed by smaller deformations. This agrees with our previously mentioned hypothesis (Subsec. 2.1) that the singlet ground state consists of pairs of electrons with unlike spin. Since the typical size of such a pair was rather large ($3.4\ell_0$), the singlet state will suffer under the finite size of the system more than the polarized state where the 'relevant particles' are still electrons whose size is about ℓ_0. Imagine filling a container once with ten tennis balls ($\sim$ polarized state) or with five footballs ($\sim$ singlet state). Slightly deforming the container will probably affect the latter system stronger.

Investigation of the half-polarized state revealed that while the state is isotropic in a square cell, it tends to build a unidirectional spin density wave for aspect ratios not far from one. In this regime, it also becomes degenerate with *one* other state. Correlation functions of the both states (in deformed elementary cells) are quite similar to each other. We suggested that these states have an antiferromagnetic ordering in agreement

with both correlation functions and wavevectors of these two states, $\widetilde{k}^r = (0, \pi)$ and (π, π). The question which state (isotropic or spin wave) is the real ground state in an infinite system remained unanswered.

2.5 Summary and comparison to other studies

2.5.1 The incompressible states: the polarized and the singlet ones

We studied various properties of the fractional quantum Hall states with spin degree of freedom at filling factors $1/3$, $2/3$ and $2/5$: correlation functions, response to magnetic and non-magnetic δ-line impurities or to deformation of the elementary cell. Briefly summarized:

(i) The results are in agreement with the concept of incompressibility of these states and also (in the case of $\nu = 1/3$) with some earlier studies, e.g. [86].

(ii) Even though these states can be imagined as composite fermion systems with integer filling, the analogy to Landau levels completely filled with *electrons* can often be misleading. For instance electrons of unlike spin are strongly correlated in the $\nu = 2/3$ singlet state while they are completely uncorrelated in a $\nu = 2$ singlet state.

(iii) We inferred pairing of spin up and spin down electrons in the $\nu = 2/3$ singlet state. In the spin-unresolved density-density correlations, this state looks as if the two electrons in each pair were located exactly at the same position and the pairs then formed a $\nu = 1$ state. This conclusion was not possible for the $\nu = 2/5$ singlet state thereby highlighting differences between fillings $2/5$ and $2/3$ which are very closely related within composite fermion theories.

2.5.2 Half-polarized states

We identified a highly symmetric half-polarized state at filling factor $2/3$ which *could* become the absolute ground state in a narrow range of Zeeman energies (or magnetic fields). Such a state is completely unexpected in mean-field composite fermion theories. Extending earlier studies with exact diagonalization on a sphere we showed that extrapolating the energy of this state from finite size exact diagonalizations to the thermodynamic limit is problematic and the question whether the half-polarized state really becomes the absolute ground state remains open.

Investigations on this state both for short-range and Coulomb interacting systems showed strong similarities to the incompressible singlet and polarized states at $\nu = 2/3$. Consequently, we suggested that the singlet and the polarized state coexist within the half-polarized state. The state *might* be gapped for short-range interacting electrons but even if yes, it is probably not gapped for Coulomb interacting systems. These differences in spectra accentuate the fact that extrapolations to infinite systems should be taken with extreme caution. It also means, that the definition of the short-range interaction should be reconsidered. The model may be an oversimplified if we study the half-polarized states since the mean distance between two minority spin electrons is rather large, higher pseudopotentials should also be taken into account.

The half-polarized state forms a pronounced spin-density wave, or antiferromagnetic order, when anisotropy is introduced from outside (deformation of the elementary cell) but we could not conclude whether this spin-wave will be more energetically favourable than the isotropic form in much larger systems.

2.5.3 Half-polarized states: other studies

Let us first briefly recall other suggestions which appeared since Kukushkin *et al.* presented their experiment showing a plateau of the polarization at the value of one half. All works mentioned below can be applied both to filling factor $2/3$ and $2/5$ in principle. Unless necessary, we will not distinguish between these two cases.

Ganpathy Murthy [54] was attracted by the idea that correlations favour either the spin singlet or the fully polarized state. At the point where the two ground states cross (recall Figures 24 and 9a), electrons could prefer to form a translationally non-invariant state consisting of regularly alternating areas of (locally) singlet and (locally) polarized states arranged into a partially polarized density wave (PPDW). He argues that this structure ought to have square rather than a hexagonal symmetry. The energy of the PPDW state is evaluated within the Hamiltonian theory of composite fermions [56] and it is shown that the PPDW state is stable (against one-particle excitations) and lower in energy than the (homogeneous) singlet and polarized states. The period of the density wave should be $2\sqrt{\pi}\ell^*$ (19) which is $7.93\ell_0$ for filling $2/5$ and $6.14\ell_0$ for $2/3$. Charge modulation in the wave should be quite weak (in the order of 1%).

Apal'kov, Chakraborty, Niemelä and Pietiläinen [10] object that the energy of the PPDW is too high and claim that a homogeneous Halperin state in the two crossing CF Landau levels (see below) should have a lower energy. Without invalidating the following results, this estimation seems to be however incorrect [55]. As the mentioned Halperin state cannot account for the half-polarized states, Apal'kov *et al.* suggest another candidate for the half-polarized state, a non-symmetric excitonic liquid. They consider only the 'active levels' meaning the two CF Landau levels which cross. These (*two*) levels have total filling of *one*, i.e., there are only N_m electrons for N_m places in the $\uparrow$ level and N_m places in the $\downarrow$ level. By convention, they define a $\uparrow$-particle as an 'electron' and a missing $\downarrow$-particle as a 'hole'; an 'electron'-'hole' pair is an 'exciton' and a pair of a $\downarrow$-particle and a missing $\uparrow$-particle is 'vacuum'. Owing to the constraint $N_\uparrow + N_\downarrow = N_m$, one-particle states can be mapped onto a system consisting solely of 'vacua' and 'excitons'. The partial filling factor $N_\downarrow/N_m \in [0;1]$ then gives simultaneously the polarization and the number of 'excitons' (by N_m). Note, that 'excitons' are bosons by virtue of an integer spin.

From this viewpoint, the $\nu = 1$ quantum Hall ferromagnet (being described by the Halperin $(1,1,1)$ state) is a Bose condensate of excitons. In that case, all the excitons are non-interacting and have zero angular momentum L. This is most easily seen by the fact that $g_{\uparrow\downarrow}(0) = 0$. On an 'electron' ($\uparrow$ particle), there is no $\downarrow$ particle, i.e. there *is* a 'hole'. In an exciton (hydrogen atom), the only wavefunctions with $\psi(r=0) \neq 0$ are those with $L = 0$. On the other hand, $g_{\uparrow\downarrow}(0) = 0$ follows from the fact that the Halperin state has maximum polarization and thus the spatial part of the wavefunction must be totally antisymmetric. Apal'kov *et al.* suggest that the half-polarized state at $\nu = 2/3$ or $2/5$ could be a condensate of excitons with $L = 1$ for which they call it nonsymmetric.

To support this idea, they perform exact diagonalizations in a $\nu = 1$ system with several model interactions which are meant to describe the two – active – crossing CF Landau levels. These interactions are derived from the Coulomb potential with suppressed short-range component, probably (without justification) with the intention to describe interacting composite fermions. Stability of the half-polarized state is substantiated by showing that the energy versus polarization curve has a downward cusp at half-polarization. On the other hand, $g_{\uparrow\downarrow}(0) \neq 0$ in the half-polarized state indicates that the 'excitons' do not have $L = 0$. The particular value of $L = 1$ is demonstrated by other means.

Finally, the idea of Eros Mariani [51] should be presented. Parallel to the previous two works, the two 'active' crossing CF Landau levels are considered. An assumption is made that they both have a partial filling of $1/2$ rendering (after a *second* Chern-Simons transformation) two Fermi seas of 'free' composite fermions (of second generation). Mariani *et al.* show that interaction of these objects with fluctuations of the gauge field leads to an attractive effective interaction between particles with opposite spin and momentum. In analogy to superconductive pairing, this implies a gapped ground state. An estimation of the gap is given.

2.5.4 What are the half-polarized states then?

Presently, it is not clear which (if any) of the candidates proposed in the previous subsection describes the half-polarized reality. As Murthy correctly mentions, the final answer should be given by exact diagonalization of a large enough system. Unfortunatelly, we dispose of systems not larger than 12 particles. Nonetheless let us compare the candidates with what was presented earlier in this chapter.

The downward cusp in energy-versus-polarization dependence cannot be assured by the calculations presented here. However, if the lowest half-polarized state indeed becomes the absolute ground state at the transition between the singlet and polarized state (see extrapolations in Fig. 25), the cusp is likely to be present. In the other case, it will turn into an upward cusp, as the calculated spectra suggest.

Results presented here indicate, that the half-polarized ground state ($2/3$) has $(\widetilde{k}_x^r, \widetilde{k}_y^r) = (\pi, \pi)$ and that it shows similarities to the singlet and polarized ground states (Fig. 27). In particular $g_{\uparrow\downarrow}(0) \approx 0$, which is in contrast with the model of a nonsymmetric exciton liquid (cf. the correlation functions in [10]). Comparison between short-range interaction and Coulomb half-polarized states (Fig. 2.2.6) suggest that, similar to the Laughlin state, the short-range part of the interaction plays the major role. From this point, the model discussed by Apal'kov *et al.* [10] seems to be more appropriate rather for some other systems.

Positioning of the half-polarized state out of the centre of the Brillouin zone could be an indication that it is indeed a standing wave. This is also supported by spectral properties when the elementary cell is deformed, Fig. 46. The two lowest states becoming degenerate at aspect ratios larger than 1.4 could be a charge/spin-density wave (note also the correlation functions, Fig. 47). The fact, that the energy of the ground state lowers with increasing aspect ratio could indicate that this state is more stable than an isotropic one. However, caution is advised here, since the singlet incompressible ground state does the same, Fig. 44, while its isotropic form is the true ground state.

Theory of the 'superconductive' pairing was not addressed so far. Comparisons on the level of correlation functions, possibly in k^r-space, are in principle possible, but quite complicated because of the two Chern-Simons transformations involved.

3 Quantum Hall Ferromagnetism at $\nu = 2/3$?

Like the previous Chapter, this Chapter also starts from the fact that there are two distinct ground states at filling factor $2/3$: a spin-singlet and a fully polarized one. Their structure was studied in Chapter 2 and we also interpreted them in terms of composite fermions, Fig. 9a. Whichever of these two becomes the absolute ground state depends on the Zeeman splitting which favours spins aligned parallel to magnetic field. The singlet state is the lowest in energy for vanishing Zeeman splitting. However, increasing the Zeeman splitting, its energy remains unchanged while the energy of the fully spin polarized state decreases and eventually this other state becomes the absolute ground state. This simplest scenario, sweeping the Zeeman energy while magnetic field is kept constant, is not very usual, albeit it is experimentally possible [50]. However, even if we simply sweep the magnetic field (and keep constant filling $\nu = 2/3$ which requires a simultaneous change of the electron density), the Coulomb energy of the singlet state changes $\propto \sqrt{B}$ and that is slower than the Zeeman energy of the polarized state in the limit of large B. Therefore, the qualitative discussion above is still valid. The total energy bilance of the two ground states (in SI units) is thus

$$\text{polarized:} \qquad E_p(B) = \frac{e^2}{4\pi\varepsilon\ell_0} E_p^C - g\mu_B N_e B = -|C_p|\sqrt{B} - |D_p|B\,,$$

$$\text{singlet:} \qquad E_s(B) = \frac{e^2}{4\pi\varepsilon\ell_0} E_s^C = -|C_s|\sqrt{B}\,,$$

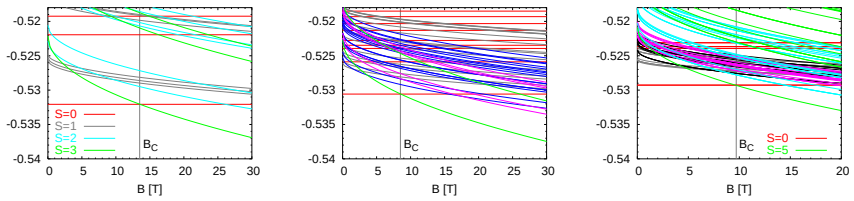

(a) $N_e = 6$ (b) $N_e = 8$ (c) $N_e = 10$

Fig. 48: Energies of low lying states at $\nu = 2/3$ in a homogeneous Coulomb-interacting system with Zeeman field: transition from an incompressible singlet ground state to a fully polarized incompressible ground state. Different numbers of particles in a square with periodic boundary conditions are considered, the scenario is however the same in all cases.

where N_e is the number of particles and $E_p^C > E_s^C$ are the total Coulomb energies in units $e^2/4\pi\varepsilon\ell_0$ (as calculated by exact diagonalization, for example; not per particle). Obviously, $E_p(B) < E_s(B)$ for B large enough. What the critical field B_c is, where both energies are equal, depends on $(E_p^C - E_s^C)/N_e$. This quantity is accessible only numerically and depends on N_e although we may hope that it stays nearly constant for large N_e.

Figure 48 demonstrates this singlet to polarized transition for $4, 6, 8$ and 10 Coulomb-interacting electrons on a torus. Note that the energy units in Fig. 48, $e^2/(4\pi\varepsilon\ell_0) \propto \sqrt{B}$, change with magnetic field. In these units, the potential (Coulomb) energy of all states stays constant (singlet state) and Zeeman energy scales as $\propto e^2/(4\pi\varepsilon\ell_0) \cdot \sqrt{B}$.

A close look at Fig. 48 shows that the magnetic field B_c, at which the ground state transition takes place, varies non-monotonically. However, an extrapolation of energies of the two ground states to $1/N \to 0$ allows for a rough estimate of $B_c \approx 7$ T in an infinite system, Subsect. 2.2. This is in quite good agreement with experiments [45], even though in some samples B_c as low as ≈ 2 T was observed [46, 70]. This could be due to deviations from an ideal 2D system, Subsect. 3.1.

In the following we want to show that the existence of the spin structures and the formation of domains are of central interest for the understanding of the ground state transitions.

The ground state is always either a singlet or fully polarized in a homogeneous system. The energies of these two states are equal at the transition. This is similar to an Ising ferromagnet, if we label the polarized state by pseudospin up and the singlet state by pseudospin down. In an infinite system at non-zero temperature, the Ising ferromagnet prefers a state with domains, some with (pseudo)spin up, others with spin down, to the two homogeneous states. First because entropy of the former is higher [41] and second because the total magnetization of a domain state is approximately zero while, locally, most spins are parallel to their neighbours thereby minimizing the energy of magnetic stray fields [11]. None of these two mechanisms was included in the studied model of a $\nu = 2/3$ system. Nevertheless, the question was addressed how the system responds if such a domain-inducing mechanism is modeled by a magnetic inhomogeneity. Will the ground state split into regions of different spin polarization? With this question in mind, the inhomogeneity should prefer the singlet ground state in one part and the polarized ground state in another part of the system.

From the experimental side, there are quite strong hints at ferromagnetism, mentioned in the introduction. Hysteresis, saturation (in time) of magnetoresistance, Barkhausen jumps etc. hint at ferromagnetic states with domain structure near the transition point. Intention of the present study is to support this interpretation.

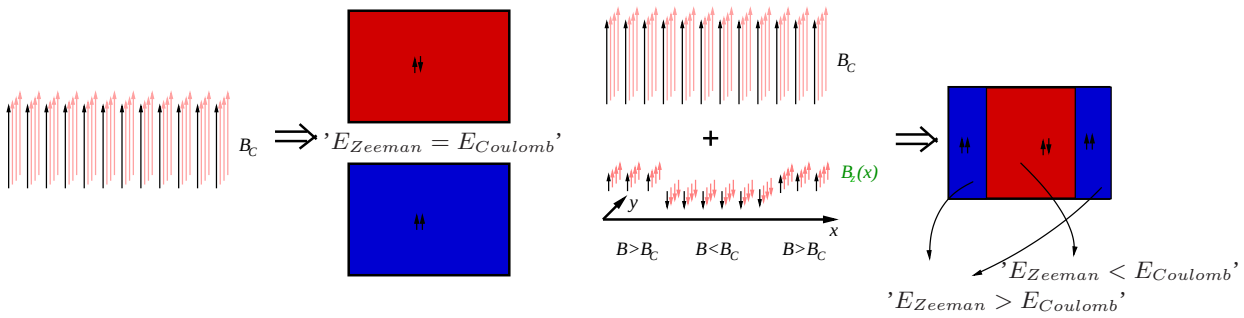

(a) Homogeneous system.

(b) System with 'domain-enforcing' inhomogeneity.

Fig. 49: An idea of how to enforce domains at the crossing of singlet and polarized ground states of $\nu = 2/3$. An average Zeeman field is chosen so that the both homogeneous states have the same energy. Modulation of the Zeeman field prefers the singlet state 'in the middle' and the polarized state 'at the edges' (note however the periodic boundary conditions).

3.1 Attempting to enforce domains by applying a suitable magnetic inhomogeneity

This and the following sections will be concerned with various attempts to induce the formation of domains close to the transition point. At the beginning we must discuss (i) how to enforce domains, what to add to the Hamiltonian, which form of inhomogeneity and (ii) how to detect them, which quantities should be observed.

3.1.1 First attempt: the simplest scenario

The simplest scenario is sketched in Fig. 49. In the homogeneous case, the Hamiltonian consists of two terms

$$H = H_{Coul} + H_{Zeeman} = \frac{e^2}{4\pi\varepsilon} \sum_{i<j} \frac{1}{|r_i - r_j|} + \sum_j g_0 \mu_B B \sigma_z^j \,, \tag{57}$$

the Coulomb interaction and the Zeeman term. If the Coulomb energy is fixed, the energies of the two incompressible ground states can be shifted with respect to each other by varying the Zeeman term. If B is fixed at $B = B_c$ (i.e. the two ground state have the same energy), the Zeeman energy can be still varied by means of the g factor. Decreasing g slightly, the singlet state will become the absolute ground state, increasing g the polarized state will prevail.

The idea of a 'domain-enforcing' inhomogeneity is to the turn the constant g into $g(x_j) = g_0 + g_1(x_j)$ in (57) and $g(x) > g_0$ in one part of the system whereas $g(x) < g_0$ in another.

Or, speaking in terms of Fig. 48: we slightly modulate the magnetic field B and in one part of the system we consider $B > B_c$ while in another $B < B_c$. By slightly we mean that only the spin degree of freedom is affected, not the orbital. This is an approximation.

The full Hamiltonian to consider is thus

$$\begin{aligned} H &= H_{Coul} + H_{Zeeman} + H_{MI} \,, \qquad (58) \\ H_{MI} &= \sum_j g_1(x_j) \mu_B B \sigma_z^j \,, \quad \langle \varphi_i | H_{MI} | \varphi_j \rangle = \delta_{ij} E_{MI} \begin{cases} i = 0, 1, \ldots, \frac{1}{4} N_m & : \quad 1 \\ i = \frac{1}{4} N_m + 1, \ldots, \frac{3}{4} N_m & : \quad -1 \\ i = \frac{3}{4} N_m + 1, \ldots, N_m & : \quad 1 \end{cases} \end{aligned}$$

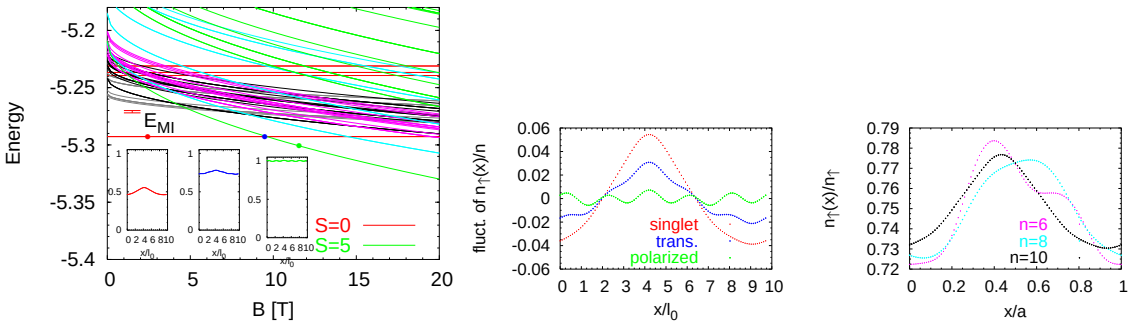

(a) An overview: spectrum and (inset) polarizations of the singlet, transition and polarized ground state (left to right).

(b) Polarization of the three states in detail ($n = 10$). Mean polarization subtracted.

(c) The transition in systems of different sizes.

Fig. 50: Response of a ten-electron system to a weak ($E_{MI} = 0.002$) magnetic inhomogeneity of the form given in (58). No sings of domain formation observed: the transition state does not respond stronger than the incompressible states.

where $|\varphi_j\rangle$ is a one-particle state localized around $x = (j/N_m)a$, cf. (21). This roughly corresponds to $g_1(x)$ having a 'rectangular wave' form ($g_1 = 1$ for $0 < x < \frac{1}{4}a$ and $\frac{3}{4}a < x < a$ and $g_1 = -1$ for $\frac{1}{4}a < x < \frac{3}{4}a$).

The basic results of this model are: the ground states slightly change in accord with the inhomogeneity and nothing peculiar happens near the transition. As we sweep the magnetic field through $B = B_c$, even in the presence of a weak inhomogeneity, the singlet state evolves 'smoothly and monotonously' into the polarized state, without any remarkable intermediate states.

Typical results are shown in Fig. 50. A magnetic inhomogeneity (58) was applied to a ten-electron Coulomb-interacting system and its strength E_{MI} was chosen to be $\sim 10\%$ of the incompressibility gap. Regarding the ground states and the gap, the spectrum remains virtually unchanged. Fig. 56a shows a comparison of the spectra between homogeneous and inhomogeneous systems. Looking now at the singlet and polarized ground states, we find a spatially varying spin polarization[1] $n_\uparrow(x)/n(x)$, Fig. 50a. However, the mean values of the polarization still remains at 0.5 (1) as it was in the homogeneous singlet (polarized) state, Fig. 50a, leftmost (rightmost) inset. The polarization of the 'transition state' has a mean value of 0.75, i.e. just in the middle between the polarized and the singlet state. This is not surprising, since the 'transition state' was taken to be a symmetric linear combination of the two crossing states (see Subsect. 3.1.2). What is more interesting, is the *variation* of the polarization around the mean value, Fig. 50b: in this point, the 'transition state' lies just between the singlet and polarized states. Contrary to what we observe in Fig. 50a (middle inset), formation of domains near the transition would mean that the polarization of the transition state should vary between 0.5 and 1.

It could be that the system is simply too small for domains to evolve near the transition. On the other hand, this does not seem to be the case, since the response to the inhomogeneity does not grow with increasing system size but rather stays about the same, Fig. 50c.

The particular parameters of the model presented in Fig. 50 could have been chosen unluckily so that domains could not evolve. Let us therefore discuss the inhomogeneous $\nu = 2/3$ systems more thoroughly.

[1] Throughout this Chapter, we will refer to $p(x) = n_\uparrow(x)/n(x)$ as to polarization. In the literature, another definition is more common, $P(x) = [n_\uparrow(x) - n_\downarrow(x)]/n(x)$, both quantities are, however, equivalent: $P(x) = 2p(x) - 1$.

3.1.2 Turning crossing into anticrossing: inhomogeneous inplane field

At $B = B_C$ there is actually a crossing between the singlet and polarized ground states, Fig. 50a, rendering the transition jump-like just as in a homogeneous system. For the transition state (the middle curve in Fig. 50b), we took a fifty-fifty linear combination of these two ground states. One could say, the transition occurs in an infinitesimally small interval of magnetic field around B_c.

In a realistic system, the transition is unlikely to happen all simultaneously in the whole system. Two mechanisms causing a more continuous transition in a finite interval of B are conceivable:

(i) weak inhomogeneities: The spectrum (as a function of B) looks basically the same as in Fig. 50a, *but* there is an anticrossing at $B \approx B_C$.

(ii) strong inhomogeneities: The energy gap between the pair of the crossing ground states and the excited states at $B = B_c$ (Fig. 50a) is reduced compared to the incompressibility gaps of the singlet and polarized ground states far away from B_C, i.e. for $B \to 0$ and $B \to \infty$. Under influence of stronger inhomogeneities, it could be that some originally excited state (or more states) become ground state around $B \approx B_C$ while singlet and polarized incompressible states remain lowest in energy only far away from B_C. If this turns out to be the case, it could be that more states (possibly of different S_z) can be mixed by the inhomogeneity, eventually rendering the ground state compressible.

In this Subsection we will discuss the former possibility, the latter will be the topic of Subsect. 3.1.3.

The ground state transition in Fig. 50a is a crossing even in the presence of the magnetic inhomogeneity H_{MI} (58) because the symmetry of H_{MI} is too high and it does not mix the two crossing ground states. In particular, $[H_{MI}, S^2] \neq 0$ but $[H_{MI}, S^z] = 0$ and the singlet state $|S\rangle$ has $S_z = 0$ whereas the polarized state $|P\rangle$ is $S_z = N_e/2$. Consequently $S_z|S\rangle = 0$ and $S_z|P\rangle = (N_e/2)|P\rangle$, therefore $\langle P|H_{MI}|S\rangle = (N_e/2)^{-1}\langle P|S_z H_{MI}|S\rangle = (N_e/2)^{-1}\langle P|H_{MI}S_z|S\rangle = 0$. The inhomogeneity H_{MI} mixes states with different S but only those with equal S_z. The fully polarized ground state ($S = N_e/2$, $S_z = N_e/2$) has also an $S_z = 0$ counterpart, since the homogeneous Hamiltonian commutes with spin lowering operator. This state, however, is a highly excited state at $B \approx B_C$, since its Zeeman energy is zero.

Which terms added to the Hamiltonian can break this symmetry and what will then be the response of the ground state?

Weak (inhomogeneous) inplane magnetic fields will have the desired effect. This scenario is not unlikely to occur in a realistic system. It merely means, that the extra fluctuating magnetic field which interacts only with the spins, is not pointing exactly in the direction of the (strong) external magnetic field causing the Landau level quantization. The existence of such symmetry-breaking inhomogeneities is very likely in realistic systems, although they might be very weak e.g. hyperfine interaction with nuclear spins.

Let us consider a Hamiltonian with inplane magnetic inhomogeneities (IMI) of the form

$$\begin{aligned} H &= H_{Coul} + H_{Zeeman} + H_{MI} + H_{IMI}\,, \qquad (59)\\ H_{IMI} &= \sum_j g_0\mu_B B_x(x_j)\sigma_x^j\,, \quad \langle\varphi_i|H_{IMI}|\varphi_j\rangle = \delta_{ij}E_{IMI}\begin{cases} i = \frac{1}{4}N_m: & 1\\ i = \frac{3}{4}N_m: & -1\\ \text{otherwise}: & 0\end{cases}\end{aligned}$$

The main claim of this Subsection is that weak H_{IMI} only opens an anticrossing at the ground state transition. In other words, the relevant states still basically form a two-level system comprising of the (slightly disturbed) singlet and polarized ground states. The width of the anticrossing grows with increasing strength of the inplane field inhomogeneity, E_{IMI}. As to the width we refer either by the level splitting, Fig. 51b, or by the range of magnetic field where $\langle S_z\rangle$ noticeably changes, Fig. 56.

This fact is best demonstrated in Fig. 51. Inhomogeneities are weak there (compared to both incompressibility gaps $E_g^P \approx E_g^S$), i.e. $E_{MI}, E_{IMI} \ll E_g$, and the spectrum remains almost unchanged, Fig. 51a. The energy levels of the inhomogeneous system (points) are almost equal to the energies in a system free

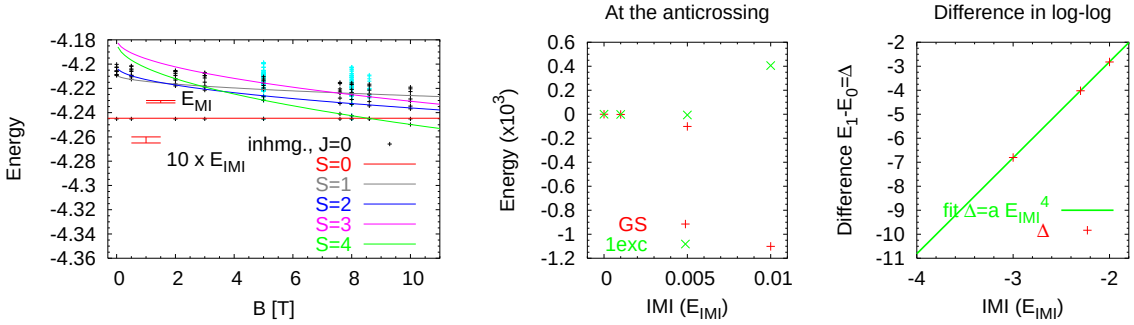

(a) Spectrum. Solid lines: homogeneous system; points: inhomogeneities switched on.

(b) Energy of the lowest two states at the anticrossing as IMI is being turned on. *Right:* level splitting

Fig. 51: Response (of an eight-electron system) to a weak inhomogeneity in perpendicular and inplane direction (59). Perpendicular component E_{MI} is the same as in Fig. 50. Exponent four comes from $N_e/2$, see explanations in the text.

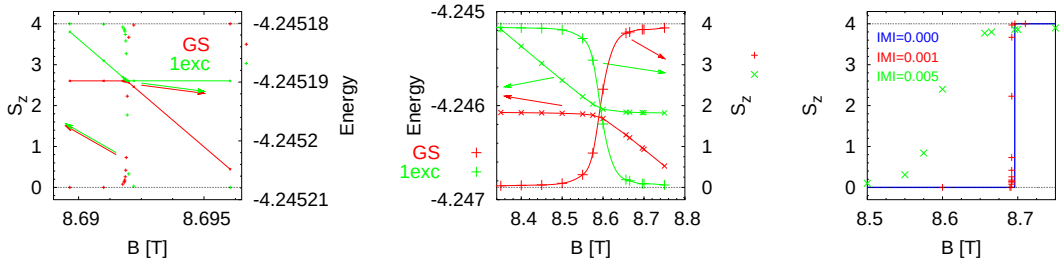

(a) Weak IMI. ($E_{IMI} = 0.001$)

(b) Intermediate IMI. ($E_{IMI} = 0.005$)

(c) Crossing at different values of IMI.

Fig. 52: Inplane magnetic inhomogeneity (IMI) turns the crossing between the singlet ground state and the polarized ground state, Fig. 51a, into an anticrossing. The cross-over between the two ground states can be observed either in the spectrum or in $\langle S_z \rangle$ of the ground state as B is swept through B_c.

of impurities (lines). Only directly at $B \approx B_C$ an anticrossing opens and the level separation ΔE grows with increasing E_{IMI} (E_{MI} is kept constant), Fig. 51b. Even for a quite strong inplane inhomogeneity (of the order of E_g), the level splitting remains small ($\ll E_g$). The reason for this is simple: H_{IMI} couples only states which differ by ± 1 in S_z, since it is a one-particle operator (allowing for only one spin flip at once). Thus, a coupling of the two ground states occurs for a $N_e = 8$ system first in the fourth order of perturbation theory ($N_e = 8$ implies $S_z = 4$ for fully polarized system). This interpretation fully agrees with the finding $\Delta E \propto (E_{IMI})^4$, Fig. 51b. We can therefore expect that, for an inhomogeneity of constant strength, the level splitting will vanish exponentially at $N \to \infty$ as long as E_{IMI} is much smaller than the gap at $B \approx B_C$.

Another view at the crossing for $E_{IMI} \neq 0$ is presented in Fig. 52. If we focus on the ground state and sweep B through B_C, we may observe how $\langle S_z \rangle$ (or $\langle S \rangle$) of the ground state smoothly passes from 0 to $N_e/2 = 4$. The transition observed in this way (i.e. $\langle S_z \rangle \approx 2 = N_e/4$) coincides with the transition

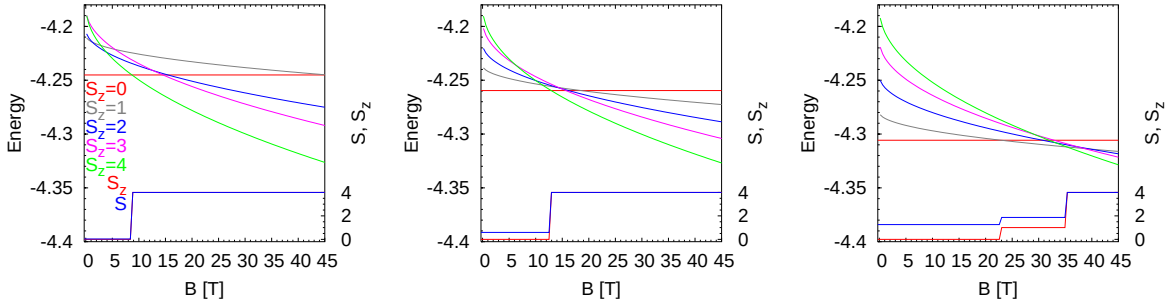

(a) Weak MI. ($E_{MI} = 0.002$) (b) Intermediate MI. ($E_{MI} = 0.01$) (c) Strong MI. ($E_{MI} = 0.02$)

Fig. 53: Stronger MI's bring another ground state into play ($S_z = 1$) and the transition from the singlet to the polarized ground state becomes more gradual.

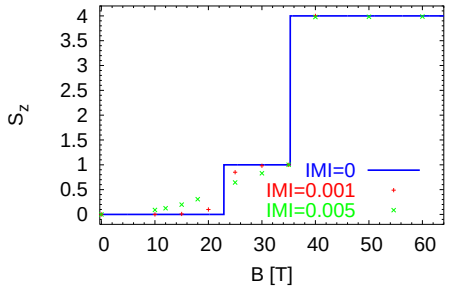

Fig. 54: Strong perpendicular magnetic inhomogeneity, just as in Fig. 53c, combined with inplane inhomogeneity (IMI). $\langle S_z \rangle$ of the ground state.

observed in the spectrum (the 'anticrossing region'), Fig. 52a,b. The larger E_{IMI}, the smoother the transition and the broader the range of B in which the transition occurs, Fig. 52c.

So as to conclude: most importantly, an inplane magnetic inhomogeneity (IMI) transforms the ground state transition into an anticrossing. This effect should fade away for larger systems ($N_e \gg 1$). We also remark, that the IMI shifts the transition point B_C to lower fields, Fig. 52c, but this effect seems to be rather small for inhomogeneity strength not exceeding the incompressibility gap.

3.1.3 Strong inhomogeneities

In the following we suppress the inplane inhomogeneities again and let us study stronger perpendicular inhomogeneities of the form (58).

If the strength of the 'rectangular wave' impurity becomes comparable to the gap at $B \approx B_C$, $E_{MI} \approx E_g$, the situation at the 'singlet-to-polarized' transition changes dramatically. The excitation gap closes and many states of different spin polarizations crowd around the ground state. Even at zero temperature and in spite of lack of anticrossings of states with different S_z (i.e. S_z is a good quantum number again), the transition becomes more gradual, when measured by S_z of the ground state, Fig. 53c.

Primarily, this is owing to the $S = 1$ state which profits best from the inhomogeneity. Keeping in mind its value of $k^r = (1.07, 0)\ell_0^{-1}$, this state seems to be a spin density wave in x-direction pinned by the inhomogeneity potential. It is also important that states with other spins are very near to it.

This $T = 0$ transition can be again smoothened by an inplane inhomogeneity, as shown in Fig. 54. Here, the transition $S_z = 0 \to 1$ becomes much more gradual than the transition $S_z = 1 \to 4$. Reason for this is

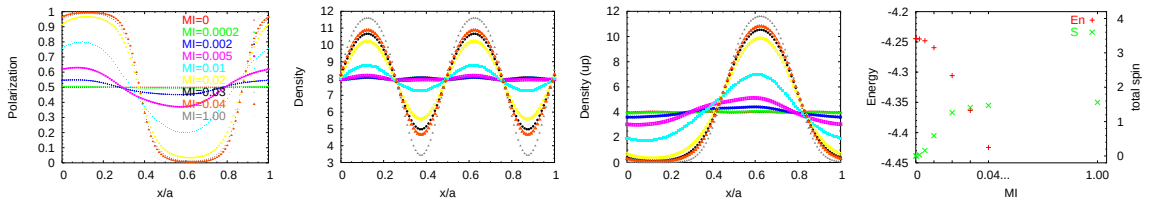

(a) Polarization $n_\uparrow(x)/n(x)$. (b) Density. (c) Density $n_\downarrow(x)$. (d) Energy and S.

Fig. 55: Destruction of the singlet state by very strong magnetic inhomogeneities: the system splits into two domains, one with spin up, another with spin down and the electrons avoid the 'interface region' (minima in the density).

again that the inplane inhomogeneity couples directly only states with $\Delta S_z = \pm 1$. Other quantities than just S_z (e.g. polarization) are shown in Fig. 56.

A strong magnetic inhomogeneity has also another quite pronounced feature: the singlet-polarized ground state transition B_C shifts to higher magnetic fields, Fig. 53. This effect is considerably stronger than the shift to lower fields in case of the inplane inhomogeneity (Fig. 52). Origin of this shift to higher B is the decreasing energy of the singlet ground state, Fig. 53 or Fig. 55d.

Let us look at this issue more closely. Increasing E_{MI}, there is no apparent transition (crossing) in the ground state of the $S_z = 0$ sector (not shown). The total spin of the ground state increases smoothly from zero and saturates around $S \approx 1.6$ for $E_{MI} \approx 0.02$, Fig. 55d. Beyond this point, the label 'singlet ground state' becomes inappropriate. At such values of E_{MI}, the polarization achieves the maximum variation between zero and one, Fig. 55a. The eight electrons, four with spin up, four with spin down, split into two nearly independent groups: the spin up (down) electrons gather in the region where $g_1(x)$ is positive (negative), see (58). Such a state where e.g. no spin up electrons occur in the 'wrong region' (Fig. 55c, $E_{MI} = 0.02$) is no longer even remotely related to the homogeneous incompressible state, even though it has $S_z = 0$. Rather, we could interpret it as two $\nu = 1/3$ systems living next to each other: one with spin up, another with spin down. The strong spatial variation of density in this system, Fig. 55b, indicates that electrons try to avoid the 'interface region'; an alternative point of view is to compare the 'spin-down domain region' (seen in the polarization, Fig. 55a) with the density of spin down electrons, Fig. 55c. However, we must always be aware that we investigate only a finite system which is too small to observe the 'inside' of a domain where we expect the density to be constant. In a sufficiently large system, the maximum in Fig. 55c should spread into a plateau. Therefore, also conclusions about the interface region must be interpreted with caution.

3.1.4 Quantities to observe

Polarization is the most natural quantity to study when looking for domains of polarized and singlet states. Nevertheless, it could be useful to search for other observables as they might bring some more information on what is happening in the states.

Here, we suggest to study the *local* expectation values (or densities) of otherwise 'global' operators such as S_z or S^2. These are defined by

$$S_{x,z}(r) = S_{x,z} \otimes n(r)\,, \qquad S^2(r) = S^2 \otimes n(r)\,, \text{ where } \qquad n(r) = \sum_{i=1}^{N_e} \delta(r - r_i)$$

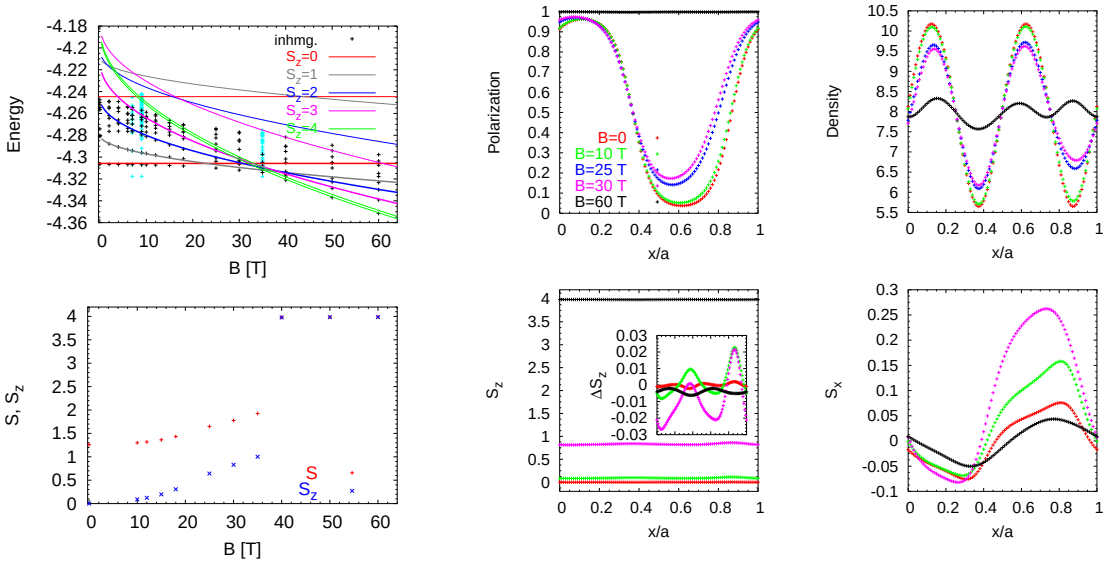

(a) Spectrum and $\langle S_z \rangle$, $\langle S \rangle$ of the ground state.

(b) The ground state in different quantities.

Fig. 56: Response to strong inhomogeneity of the form in (59). $E_{MI} = 0.02$, $E_{IMI} = 0.005$.

and they should be plotted in the form $S_z(r)/n(r)$. Their meaning is the following: Imagine an n-electron state which is an equal-weight superposition of two states: one localized in the region $0 < x < a/2$ which is fully spin polarized ($S_1 = n/2$) and another localized in $a/2 < x < a$ which is a spin singlet. This state is $S_z = n/4$, yet its $S_z(x)/n(x)$ is equal to $n/2$ or 0 in the two respective regions.

What these quantities reveal is demonstrated in the case of a strong magnetic inhomogeneity, both perpendicular and inplane, Fig. 56. The low-energy part of the spectrum does not change considerably, Fig. 56a, even though the singlet state is separated almost completely into a spin-up and a spin-down domain by the inhomogeneity, seen in the polarization, Fig. 56b. Note that again the states near the transition have smaller variations in the polarization than the 'inhomogeneous singlet-state'.

The lower two plots of Fig. 56b show $S_z(x)/n(x)$ and $S_x(x)/n(x)$. Obviously, S_z stays quite constant with x, at least on the scale ranging from $S_z = 0$ (singlet) to $S_z = 4$ (fully polarized). Albeit polarization (or relative density of spin down electrons) varies strongly, $S_z(x)$ remains nearly constant. This indicates that the state does not really separate into domains of locally different S_z. Observation of the quantity $S^2(x)$ (not shown) points in the same direction.

Local expectation values of S_x indicate that states near the transition are more susceptible to inplane inhomogeneities. At any B, this response is much stronger than for perpendicular inhomogeneities. The following picture explains this behaviour: if we imagine a 'classical' spin vector pointing in z-direction and accept that it fluctuates by a small angle $\Delta\varphi$, then $S_z \propto \cos\Delta\varphi \approx 1$ whereas $S_x \propto \sin\Delta\varphi \approx \Delta\varphi$.

3.1.5 Different geometries of the inhomogeneity

Disregarding entropy, it is unlikely that a domain state will be the ground state in a homogeneous system. If it is an excitation we can hope to encourage it energetically by including a suitable inhomogeneity like

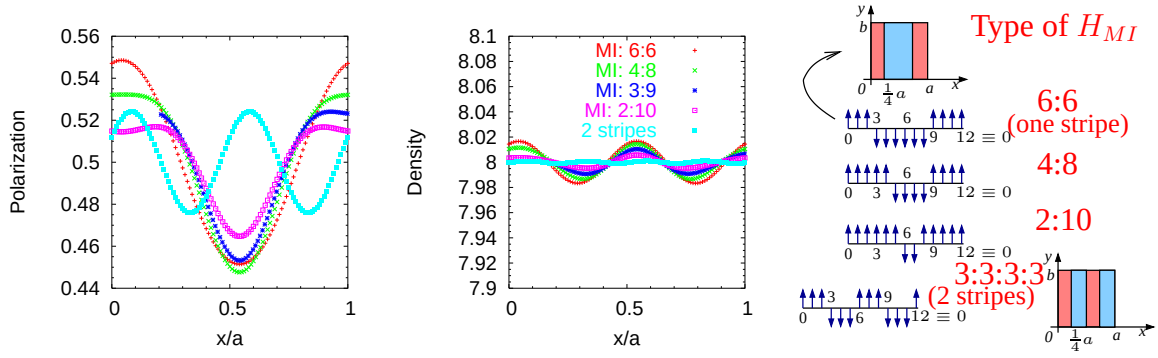

(a) Polarization.

(b) Density.

(c) Various inhomogeneities H_{MI} used.

Fig. 57: Response of the singlet to various weak magnetic inhomogeneities. The inhomogeneity is similar to the one in (58) but it divides the system into two areas (stripes) of various ratios ($6:6$ through $2:10$) or it consists of two stripes with size $3:3:3:3$.

H_{MI} in (58). However, we do not *a priori* know what 'suitable' means. So far, we divided the system into two *equal* parts by H_{MI}.

How the singlet state responds to inhomogeneities of different forms is shown in Fig. 57. Different lines correspond to the 'rectangular wave' inhomogeneities with different ratios of the 'plus' and 'minus' parts. All these inhomogeneities are thus a single stripe of various width (per elementary cell) parallel to y .

Also, response to H_{MI} consisting of two stripes is shown (i.e. 'rectangular wave' with half period).

Responses are basically very similar to each other and it seems by having focused on H_{MI} of the form of (58) we did not choose a particularly clumsy one. One particularly interesting information which can be extracted from Figure 57 is that the polarization response is always at least an order of magnitude larger than in the density, 10% against 0.3% in the present case. This confirms the conclusion of Subsection 2.3.2: even though singlet incompressible states try to maintain constant density, they can be fairly easily polarized.

A good example of the influence of the form of the inhomogeneity are the half-polarized states, Fig. 58. The lowest level in the $S = 2$ sector is six-fold degenerate (factor of three from the centre-of-mass and factor of two from the relative part). The two states are mirror images of each other with respect to the diagonal of the elementary cell. We split them into two groups $J = 2, 6, 10$ and $J = 0, 4, 8$ (within each group the states differ only by the center-of-mass part) and subject each group to one-stripe and two-stripe inhomogeneities, Fig. 57c.

One group ($J = 2, 6, 10$) responds strongly to the two-stripe H_{MI} and is left almost unchanged by the one-stripe H_{MI}, upper row in Fig. 58b. Nearly the opposite is true for the other group. It gives a clear picture of the structure of these states. They are spin density waves with two periods in one direction and one period in another direction. This is in full agreement with the spin-spin correlation functions, not shown here. The conclusion is also underlined by the markedly lowered energy of the $J = 2$ state when it is addressed by the two-stripe inhomogeneity, Fig. 58a. This is a practical demonstration of one spin-density-wave state selected by an impurity from a degenerate manifold.

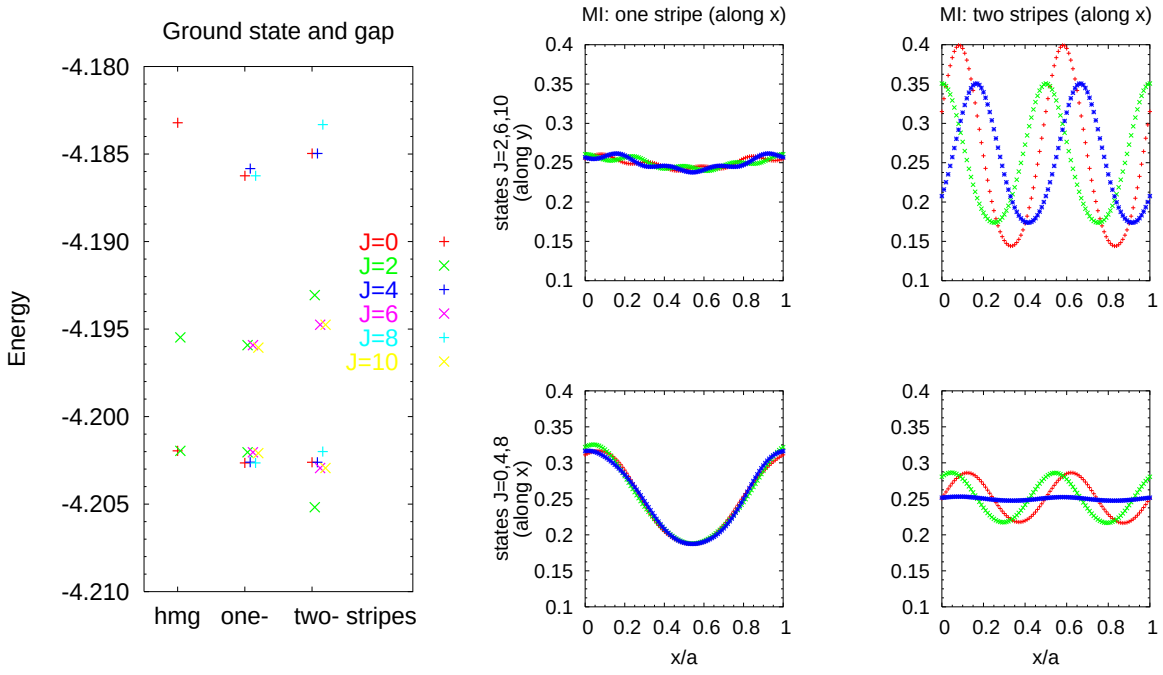

(a) Energies.

(b) Polarizations.

Fig. 58: The half-polarized states ($S = 2$) and their response to a magnetic inhomogeneity of the form of one or two stripes.

3.1.6 Transition at nonzero temperature

Regardless of how intensely we try to help an eventual domain state to become the ground state, it may still be, that it is hidden among the excitations. Therefore we may try to take the excited states into account by means of thermal averaging.

The strong impurity mode ($E_{MI} = 0.02$) was chosen for this study. Three-fold degeneracy in center-of-mass of the incompressible ground states is lifted. The level splitting is however still smaller than the incompressibility gap, compare the black and grey points in the upper plot of Fig. 56a around $B = 10$ T.

Various temperatures were considered: $kT \ll E_g$ means than we do not average even over all states of the originally degenerate triple. Knowing that E_g means the gap energy at $B \to 0$ or $B \to \infty$, the other temperatures shown in Fig. 59 are self-explaining.

Judging by polarization $n_\downarrow(x)/n(x)$, the state at the transition approaches a situation which we could call 'domain'. In the middle ($x/a \approx 0.5$), the polarization drops to zero and only spin up electrons are present. In the other region ($x/a \approx 0 \equiv 1$), polarization is about 0.5, meaning that the number of spin up as spin down electrons in this area is the same.

We should note though that an inhomogeneity which is strong enough to produce such nice 'domains' is also strong enough to change the originally incompressible singlet state completely, Fig. 59a. In other words, the response of the system at the transition is still weaker than the response of the singlet state. This manifests that spontaneous build-up of domains is not very likely within this model.

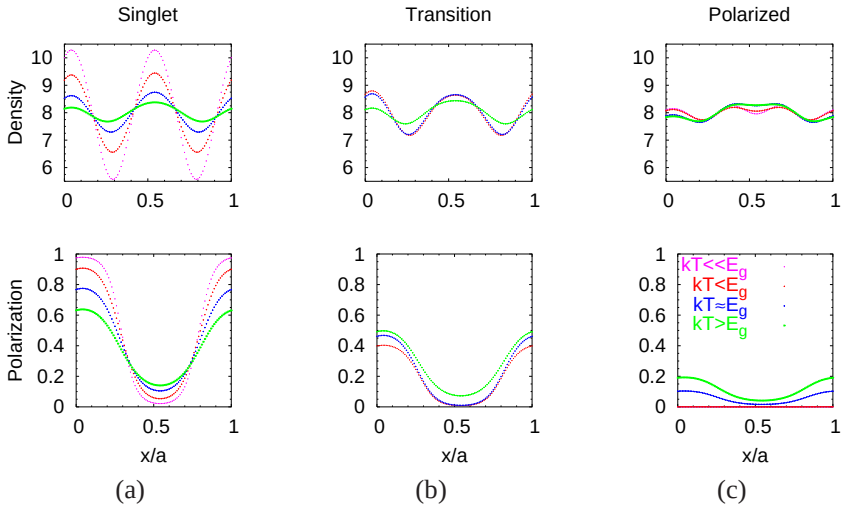

Fig. 59: Density and polarization at different temperatures: filling factor $2/3$ with magnetic inhomogeneity (corresponding to Fig. 53c). *Left to right:* before, at and after transition, i.e. $B \to 0$, $B \approx B_c$ and $B \to \infty$.

In the following Section we will try to suggest slightly different models which may put us on the trace of states which exhibit nontrivial behaviour at the transition between the incompressible singlet and polarized ground states.

3.2 Systems with short range interaction

As far as the transition between singlet and polarized ground state is concerned, the most obvious feature of the $\nu = 2/3$ Coulomb-interacting systems is the energy 'gap' which separates the two degenerate ground states from excited ones even at the very crossing, Figs. 60a, 48. In the previous section we demonstrated that this picture may change when fairly strong magnetic inhomogeneities are applied, Fig. 53. We can cause a similar drastic change by replacing the Coulomb by the short-range interaction, Fig. 60b.

Let us first concentrate on the calculated spectrum of the *homogeneous* system with short-range interaction, Fig. 60b. Again, we observe a gapped ground state with maximum spin and zero spin in the limit of $B \to \infty$ and $B \to 0$, respectively. In between, states with different spins become the absolute ground states. Aforemost, it is the half-polarized state ($S = 2$), although states with other spins ($S = 1$ and 3) are not very far. Alternatively, this can be expressed by the B-dependence of the spin of the ground state, Fig. 61a.

The half-polarized states have been extensively discussed in Sec. 2.1 where they were studied as 'zero-temperature candidates' for the ground state in homogeneous systems. However, since inhomogeneities couple the ground state to the excited states, the properties of the lowest-lying state will not be determined solely by the those of the ground state.

Spectral properties of the short-range interacting (SRI) system subjected to a 'perpendicular' magnetic inhomogeneity (58) are summarized in Fig. 61. In a similar fashion as for the Coulomb-interacting systems, states with other spins become the absolute ground state in some range of the magnetic field, Fig. 53. This is also manifested in the expectation value of spin (or S_z) of the system even at nonzero temperatures. Most significant is still the 'half-polarized' plateau $S_z(B) \approx 2$, Fig. 61d.

After this introduction let us look at the inhomogeneous states themselves. Their properties are highlighted especially in comparison to the Coulomb interacting (CI) states. When subjected to a 'rectangular cosine'

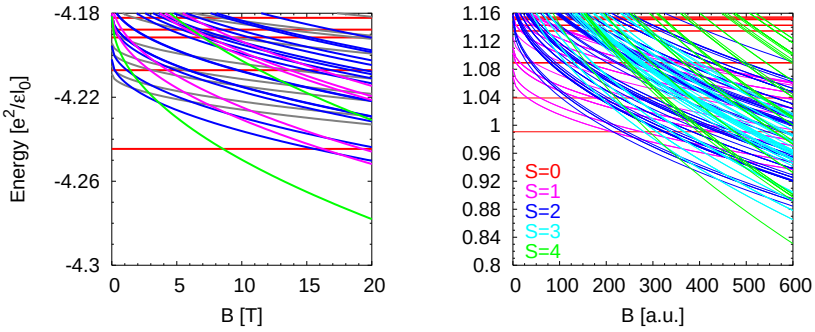

(a) Coulomb interaction.

(b) Short-range interaction.

Fig. 60: Spectrum of a homogeneous system with Zeeman splitting (8 electrons, $\nu = 2/3$).

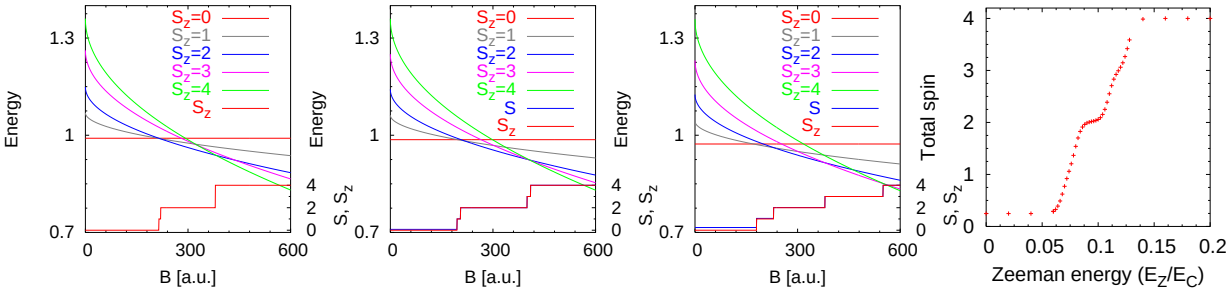

(a) Homogeneous.

(b) Intermediate inhomogeneity ($E_{MI} = 0.01$).

(c) Strong inhomogeneity ($E_{MI} = 0.02$).

(d) Spin at finite temperature, cf. Fig. 61c.

Fig. 61: Spectrum and the expectation value of the spin in the ground state in short-range interacting systems (eight electrons).

magnetic impurity, those CI states showed a smooth monotonous transition from the singlet to the polarized state. The singlet was most strongly affected by the inhomogeneity, the polarized state was not affected at all, it was frozen by its symmetry. The polarized state has all spins up, $S_z = N_e/2$. Since magnetic inhomogeneity of the form in (58) preserves S_z, it does not couple the polarized state with any states which contain spin down electrons, since such a state must have $S_z < N_e/2$. The transition state was just in the middle. This is the finding both at $T = 0$, Fig. 50b, and at temperature low enough to average only over the three degenerate states of the homogeneous system, Fig. 62a.

The SRI systems give a different view. The response to the inhomogeneity is slightly stronger at the transition than in the singlet state, Fig. 62a, inset. This is not very surprising given that there are quite many states near the ground state in the transition region. At slightly higher temperature where we average over about 10 states in the singlet and polarized limit, the distinction between Coulomb and short-range interacting systems weakens, Fig. 62b.

Regarding Figure 62, it should be stressed once again, that the 'transition states' for the Coulomb and the short-range interaction have completely different character. In the former case, this state is basically a

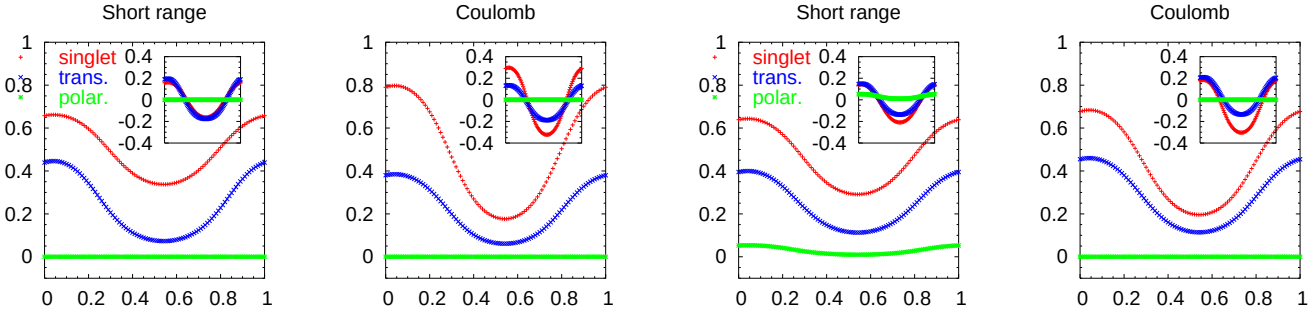

(a) 'Low' temperature.

(b) Slightly higher temperature.

Fig. 62: Short-range interacting system with strong inhomogeneity, (58), $E_{MI} = 0.02$: polarization in the singlet sector, around the transition and in the polarized sector, cf. spectrum in Fig. 61c. Insets show how polarizations fluctuate around anticipated mean values (0.5, 0.25 and 0 for the singlet, transition and polarized state).

superposition of the singlet and the polarized states, whereas it is a half-polarized state ($S_z = N_e/4$) for the SRI.

It seems we are on the track of the domain build-up here. In an ideal case, we would expect negligibly affected singlet and polarized states while the polarization of the transition state varies between 0 (polarized domain) and 0.5 (singlet domain). In real systems, we are still very far from such behaviour as the difference between polarizations of the singlet and transition state is quite small. Nevertheless, the direction seems correct, in contrast to the Coulomb interacting systems. We may therefore conclude:

(i) If nontrivial effects at the transition are expected, there must be more states involved than just the singlet and polarized ground states; (ii) it is likely that the half-polarized states play a major role; (iii) at low temperatures inhomogeneous states as in Fig. 62b can be observed simultaneously with a plateau in $S_z(B)$, Fig. 61d.

The last point is a consequence of the fact that not only the ground state but also the lowest excited states have $S_z = 2$ in a part of the transition region, Fig. 60b.

3.2.1 Comments on the form of the short-range interaction

For a short-range interaction, the form described in Subsect. 1.3.5, Fig. 2d was chosen. The basic idea there was to keep the pseudopotentials V_0 and V_1 at their normal values while setting the others to zero. V_0 and V_1 give the energy of two interacting particles in the state with angular momentum 0 and 1. These are the states with smallest and second smallest interparticle separation possible and only the latter one is accessible if the particles have the same spin.

As far as incompressible liquid states are concerned, not much happens during such 'pseudopotential engineering'. The best measure for this are directly the density-density correlation functions, Fig. 18. The good match between correlation functions of Coulomb- and short-range-interacting states agrees with the common claim that their energy is determined mostly by effects occurring at short distances. Also excitation energies remain essentially unchanged as long as 'zero momentum' states are considered (as opposed to charge or spin density waves).

What strongly changes is the energy difference between the polarized and singlet state: it is 0.0632 for Coulomb and 0.3693 for short-range interaction in an eight-electron system, with zero Zeeman energy. This happens because the average Coulomb potentials felt by electrons in a singlet state and in a spin

polarized state differ. Roughly, we take the average over set $\{V_0, V_1, 0, 0, \ldots\}$ in the former case (all m's allowed) and over $\{V_1, 0, 0, \ldots\}$ in the latter case (only odd m's allowed). This is a fundamental problem. The requirement of equal averages is not compatible with preserving the ratio of V_0 and V_1 as in a Coulomb interacting system. We would have to use higher Haldane potentials to achieve this, losing thereby the simplicity of the definition of short-range interaction. Therefore, with short-range interactions, we must be very cautious whenever we compare absolute energies of states with different spins (and thus parity properties of the wavefunction). Namely, position of the singlet-polarized transition depends directly on the energy difference of the singlet and polarized ground state, Sec. 3.

This difficulties apply to spectra in this subsection, Fig. 61, 60b. Fortunatelly, the polarizations in Fig. 62 do not suffer from this, provided that half-polarized states indeed become the absolute ground state somewhere around the transition.

3.3 Systems with an oblong elementary cell

So far in this Chapter, we have only considered square elementary cells a by a so far. If we somehow e.g. by means of a magnetic inhomogeneity, manage to split such a system into two domains of the same size, this will be $a/2$ by a, cf. Fig. 57c. Consequently, the spin singlet and spin polarized states which we expect to appear in these domains would necessarily have to be deformed as in a cell of aspect ratio $1:2$. In principle, this could even suppress the formation of such domains or at least shift them to higher excited states. The energy of any of the two incompressible ground states depends on aspect ratio (the stronger the smaller the system is), Subsect. 2.4.1. There is no reason to expect that the energy of a domain wall between two such states is constant. In the following Section we will investigate systems in a rectangular cell with aspect ratio $2:1$ which have the possibility of splitting into two square domains. All results in this Section refer to Coulomb interacting systems.

3.3.1 Overview of the transition: which states play a part

Going from square elementary cell to aspect ratio $1:2$, the overall view of the transition changes. The crossing between singlet and polarized incompressible states is no longer well separated from excited states, Fig. 63.

Similarly, as for short-range interaction, states with different spin appear near the transition: most prominently $S = 1$ and $S = 2$. Again, Figs. 53, 61, these states are promoted by the perpendicular magnetic inhomogeneities in the form of a 'rectangular wave', Fig. 64. A consequence of this is a gradual change of the spin in the ground state as we sweep magnetic field (or simply increase Zeeman energy). Here, we should point out the difference between the present case and the Coulomb interacting system in a square elementary cell, Fig. 53. For an oblique elementary cell, (i) the $S = 1$ state becomes the absolute ground state near the transition even in homogeneous systems. (ii) A much weaker inhomogeneity is needed to make the $S = 2$ state the absolute ground state in some range of the magnetic field. Fig. 64c shows that $E_{MI} = 0.004$ is sufficient for this to happen in a $2:1$ system, while $E_{MI} = 0.02$ is not strong enough for a square elementary cell, Fig. 53c.

By changing the elementary cell geometry we support possible domain states, but it is adequate to ask how much the incompressible singlet and polarized states are affected by this procedure. The inner structure of these states under elementary cell variations was addressed in Subsect. 2.4.1 and we saw indications that the states are liquid like (and very similar to the original states from square elementary cell) even at aspect ratio $1:2$. However, overlaps between the square-cell and deformed states are noticeably below unity and hence their behaviour is not representative if we are interested in infinite homogeneous systems. Recall, that the square-cell polarized state is extremely close to the Laughlin state (overlaps $\approx 99\%$).

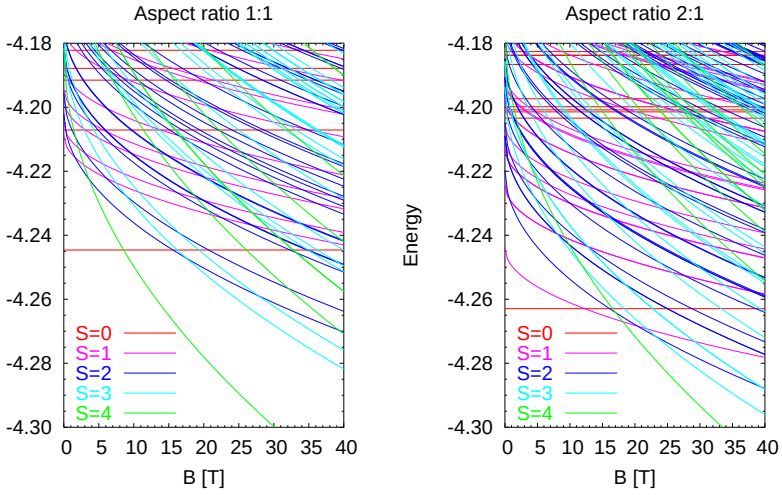

(a) Aspect ratio $1:1$.

(b) Aspect ratio $2:1$.

Fig. 63: Spectra of homogeneous eight electron systems (with Zeeman splitting) for square and oblong elementary cell.

	asp. $1:1$, hmg.	asp. $2:1$, hmg.	asp. $2:1$, $E_{MI} = 0.004$
$S_z = 0$ GS	0.713	0.976	
$S_z = N_e/2$ GS	0.750	0.9996	

Table 3: Incompressible ground states (polarized and singlet) in an eight-electron system. Overlaps between states in a square elementary cell, oblong elementary cell and oblong elementary cell with intermediate magnetic inhomogeneity.

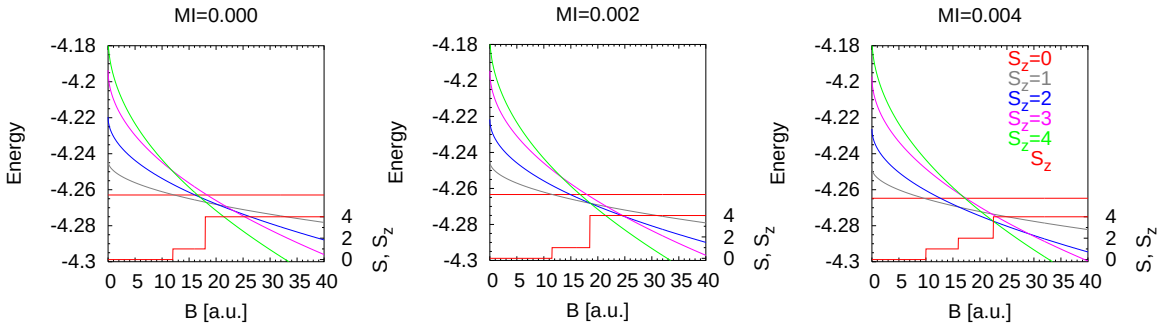

(a) Homogeneous.

(b) $E_{MI} = 0.002$ (weak).

(c) $E_{MI} = 0.004$ (intermediate).

Fig. 64: Spectra and S_z of the ground state in a system with oblique rectangular elementary cell (aspect ratio $2:1$, eight electrons). Magnetic inhomogeneities (58) of different strengths are considered.

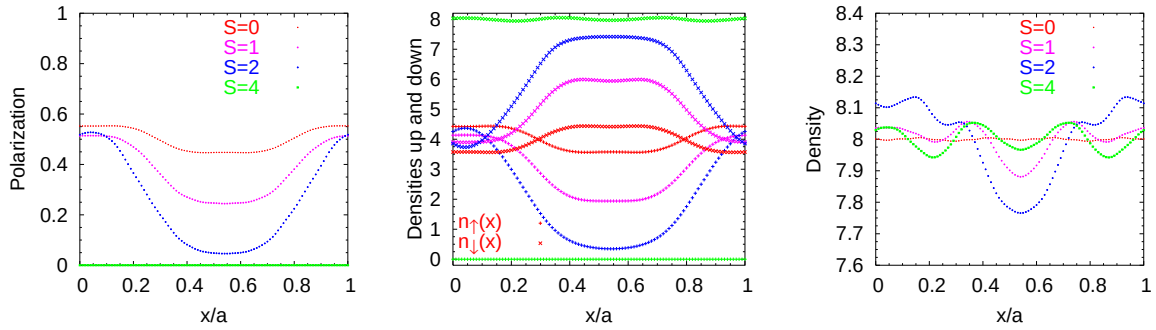

(a) Polarization.

(b) Densities of electrons with spin up (or down).

(c) Total density.

Fig. 65: 'Domains' imprinted by a magnetic inhomogeneity of type 'rectangular wave' into a system with oblong rectangular elementary cell (aspect ratio $2:1$). The strength of the inhomogeneity is about 20 % of the gap in the limit $B \to 0$ (in particular $E_{MI} = 0.004$). Plotted quantities are averaged over the three states which were degenerate in the homogeneous system (in the center-of-mass part).

3.3.2 States at the transition

The following paragraph deals with he central result of the investigations on systems with aspect ratio $2:1$. The low-energy states near the transition ($S = 1$ and $S = 2$ in Fig. 64) respond very strongly to a 'rectangular wave' magnetic inhomogeneity, Fig. 65 (the middle two lines). Already for intermediate strength of the inhomogeneity like 15% of the singlet incompressibility gap in a square cell, polarization varies between ≈ 0.5 and ≈ 0.05, Fig. 65a (values of 0.5 and 0 would mean a state with $S_z = 0$ and $S_z = N_e/2$, respectively). Equivalently, Fig. 65b shows that (a) the density of spin down electrons drops below 25% of its average value in the spin polarized region and (b) spin up and spin down densities are balanced up to 10% variations in the 'spin singlet region'. At the same time, variations of the total density remain small (less than 5%), but there is a clear deficit of electrons in the 'polarized region', Fig. 65c.

In order to check that the inhomogeneity is not too strong ('destructive') compared to the Coulomb interaction responsible for the formation of the incompressible ground states (far away from B_c), we should observe the incompressible $S = 0$ and $S = N_e/2$ states, Fig. 65. For both of them, responses are much weaker than for the transition states.

Let us now concentrate exclusively to the half-polarized states and try to analyze their nature. Observe first the homogeneous system near the transition, Fig. 66 and focus on the half-polarized sector ($S_z = N_e/4 = 2$) with one particular value of J, Subsect. 1.5.2. The low lying states show pronounced spin structures and, moreover, several distinct types of spin structures appear in the low energy part of the spectrum. This is heralded by different values of k^r which are $(0,0)$, $(\pm 1, 0)$ and $(2,0)$ for the lowest three states (`st01`,`st02+st03`, `st04`, the middle pair is degenerate) and the different spin structures can be seen best in the density-density correlation of minority spin, $g_{\downarrow\downarrow}(r)$, Fig. 67. Half-polarized states contain six spins up and two spins down here, which we choose to call majority and minority spins respectively.

The lowest state looks isotropic as far as the rectangular elementary cell allows, the other two (`st02+st03` and `st04`) are different kinds of spin density waves in the 'long direction' (x). Keeping in mind that these states are energetically close to each other as compared to incompressibility gaps at $\nu = 2/3$ in a square elementary cell, for example, we can indeed expect strongly modulated polarization in response to suitable not very strong inhomogeneities. Polarizations in Fig. 65 were a good demonstration of this prediction.

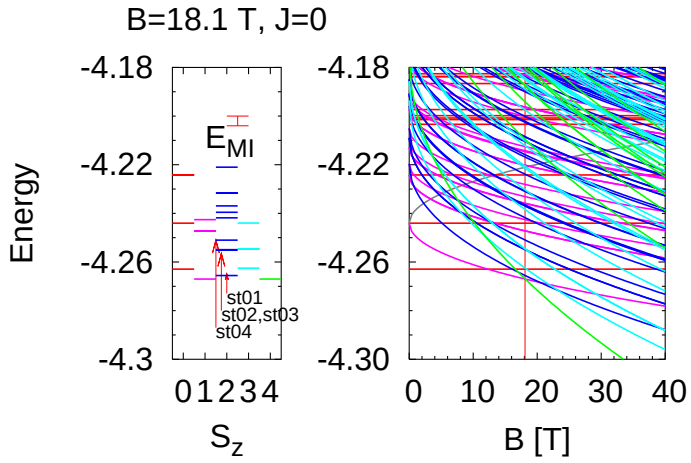

Fig. 66: Low lying states near the transition (in absence of inhomogeneity, eight electrons). The $J = 0$ sector is where (a) both incompressible ground states (singlet and polarized) occur and (b) the lowest half-polarized state occurs.

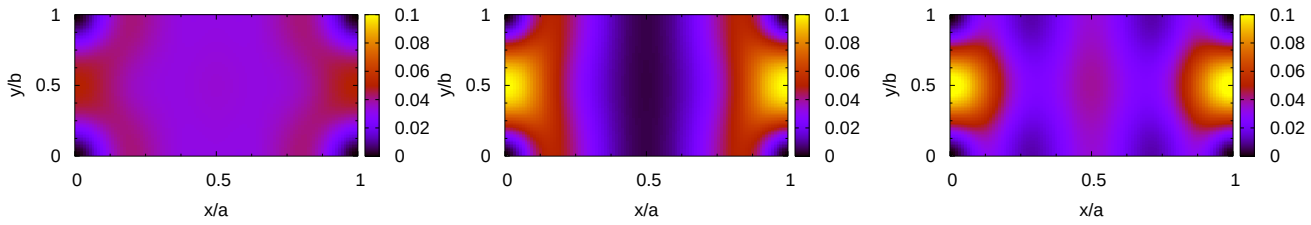

(a) The lowest state (`st01`). (b) An SDW state (`st02`, `st03`). (c) Another SDW (`st04`).

Fig. 67: Density-density correlations ($g_{\downarrow\downarrow}$, i.e. minority spin) in the lowest half-polarized states. Coulomb interaction, a homogeneous system, aspect ratio $2:1$.

This leads us to the question what types of spin structures can be imprinted into these states. Are they completely 'soft' or are some particular structures preferred? An answer is given by polarizations in response to various types of inhomogeneities, Fig. 68. Briefly summarized: a variety of spin structures is possible but 'periodic' structures are preferred. Among the 'periodic' structures, the largest period available is preferred. This means one stripe or just the 'domains' as in Fig. 65. By periodic we mean commensurate with the elementary cell period, for instance a 'rectangular wave' in contrast to a delta peak since otherwise, any structure is periodic in our system due to periodic boundary conditions.

Looking only at polarizations, Fig. 68a, responses to all types of inhomogeneities considered here seem to be the same (in strength) within a factor of two. However, a closer look reveals some differences between those which are 'periodic' and the others, Fig. 68b. The one-stripe and two-stripe inhomogeneities mix mostly only the lowest four states: (sum of squares of) projections of the inhomogeneous state to states

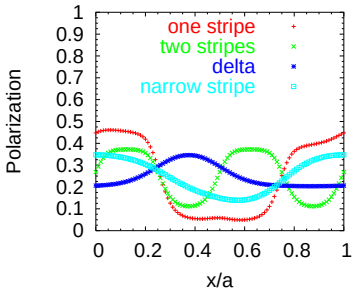

(a) Polarization. Impurity types are the same as in Fig. 57.

State	hmg.	one stripe	two stripes	δ-peak
Energy	-4.2656	-4.2713	-4.2695	-4.2439
st01	1	-0.82	-0.92	-0.04
st02	0	-0.51	0.00	0.03
st03	0	0.21	0.00	0.07
st04	0	0.03	0.22	0.64
cummul. $\Sigma(\langle\cdot\vert\cdot\rangle)^2$	1	0.98	0.90	0.41

(b) Projections of the inhomogeneous ground states to the lowest four homogeneous states (in Fig. 67).

Fig. 68: Half-polarized state and different forms of inhomogeneity. Strength of the inhomogeneity is the same in all cases, $E_{MI} = 0.004$.

st01-st04 give in these cases $\geq 90\%$. It seems that a one-stripe structure, or domain state in Fig. 65, stems from the $k^r = (\pm 1, 0)$ states (st02+st03) and the two-stripe structure comes from the $k^r = (2, 0)$ state (st04). In both cases, however, projections to the lowest state (st01) remain high.

A different situation occurs for 'non-periodic' structures like a delta peak. Inhomogeneous states are then 'constructed' in the main from states which were originally energetically higher in a homogeneous system. Such states (e.g. with a delta peak in the polarization) only have a strong projection to the $k^r = (2, 0)$ state (st04), but still more than 50% of weight comes from higher states, Fig. 68b.

This scheme, 'periodic-welcome, others-less welcome', is confirmed also in terms of energy. While the 'periodic' states (one- and two-stripes) profit energetically from the inhomogeneity, the delta-peak state is shifted to higher energy, Fig. 68b.

Finally, the following conclusion about the $\nu = 2/3$ system near the transition seems to be possible. The softening against magnetic inhomogeneities of different forms, as observed in Fig. 65a, stems not only from the spectral properties of the system (small level spacing, Fig. 66) but also from the fact that more different (inner) spin structures occur among the low lying states. States belonging to a single value of S (e.g. $S = N_e/4$) are capable of generating a response as shown in Fig. 65a.

3.3.3 What is inside the domains?

We will now only consider the 'one-stripe' inhomogeneity, in sense of Fig. 57, which has lead us to the states with polarization varying almost between zero and one half, Fig. 65. In other words, we could distinguish between two domains of about equal areas in that state: one, with only spin up electrons and another with as many spin up as spin down electrons, whereby the total density is spatially nearly constant. Now we are interested in the inner structure of these domains. One of the aims of this thesis was to find side-by-side domains comprising of the incompressible singlet and incompressible polarized states. Unfortunately, the results presented in this Subsection cannot conclusively answer whether the states discussed in the previous Subsection are of this type or not. Also, it would be surprising if they could in the view of the small systems (eight electrons) we study. One of the reasons why studies of finite systems on a torus or on a sphere were so successful was that these models contain no edges. On contrary, there are 'edges' in the state with 'domains': the domain walls. Nevertheless, these results provide at least some basis for comparing the inside of the domains to the incompressible states and, in particular, highlight some differences between these two.

As a probing tool we chose density-density correlation functions. As we are dealing with inhomogeneous states, we must use $g(r, r_0) \propto \langle \delta(r_1 - r)\delta(r_2 - r_0)\rangle$ rather than $g(r) \propto \langle \delta(r_1 - r_2 - r)\rangle$. The former quantity is the conditional probability to find an electron at r given there is an electron at r_0 and we will separately address the cases when both electrons have spin up or when they both have spin down. By convention, majority electrons are spin up (expected to be present in both domains) and minority electrons are spin down (absent in the fully polarized domain).

Roughly, we can say that the eight electrons are organized in four vertical stripes: two in the polarized and two in the unpolarized domain. For instance, if we catch a majority spin electron in the left stripe in the polarized domain, we will see another quite sharply localized (majority spin) electron in the same stripe and two delocalized electrons in the other stripe of the polarized domain, Fig. 69c. In the unpolarized domain, we will see the two majority electrons distributed nearly equally among the two stripes.

Similarly, if we pin a majority spin electron in one stripe of the unpolarized domain, Fig. 69a, we find another (majority spin) electron in the same stripe. Four electrons in the polarized domain are distributed homogeneously to the two stripes. We will see almost the same picture with minority spin electrons, if we catch a *minority* spin electron at the same place. Naturally, we will see almost nothing in the polarized domain, Fig. 69b.

Summary. In eight electron systems, the domain states comprise of four vertical stripes (i.e. parallel to the short side of elementary cell), each occupied by two electrons. In the polarized domain, each stripe contains two electrons separated by $b/2$, and the two stripes can 'freely slide' besides each other. Stripes of the unpolarized domain are preferentially occupied by electrons of the same spin and both spins (majority and minority) seem to be equivalent: schematically $\langle\uparrow\uparrow|_L\langle\downarrow\downarrow|_R + \langle\downarrow\downarrow|_L\langle\uparrow\uparrow|_R$. The domains seem to be rather independent. For instance, regardless of where, within the unpolarized domain, we pin the majority spin electron, the density of electrons seen in the polarized domain does not change much.

It should be emphasised that although the stripe structure is well pronounced in conditional probabilities, the density varies only weakly, Fig. 65c. But, even so, it contains indications of the four stripes. This structure suggests that the interior of any of the domains is rather anisotropic and this is quite distinct from the liquid states at $\nu = 2/3$ (polarized and singlet, Fig. 13) where at least the first maximum in $g(r)$ occurs for all r with $|r| = r_1$ (Subsect. 2.1.1) and not only in the x- or y-direction. The study of finite size effects comparing the averaged and non-averaged correlation functions suggests that for liquid states, the anisotropy of non-averaged correlation functions should be much smaller than what we observe in Fig. 69. On the other hand, the results shown in Fig. 69 refer to a state which is inhomogeneous and strongly influenced by the aspect ratio being far from unity. A more thorough study of the non-averaged correlation functions in systems of various aspect ratios and comparison to systems of different sizes is therefore necessary to allow more definite conclusions.

3.3.4 Comment on homogeneous half-polarized states

It should be mentioned that the half-polarized state we study here is not the same as the half-polarized states discussed in Sect. 2.2.

The lowest state here, in an elongated elementary cell, has $k^r = (0, 0)$, whereas the half-polarized ground state in a square cell has $k^r = (2, 2)$, Sect. 2.2. These are the two inequivalent points of the highest symmetry.

In the present system (aspect ratio $2:1$) all low lying half-polarized states belong to the $k^r_y = 0$ sector. States with other values of k^r_y lie well above the four discussed states `st01`-`st04`, the lowest of these other states has an energy of -4.240, cf. the spectrum on the left in Fig. 66. Being interested in the states low in energy we may therefore stay restricted to the sector $k^r_y = 0$. This is a pleasant fact since there is no need to consider inhomogeneities of very low symmetry (implying handling larger Hilbert spaces).

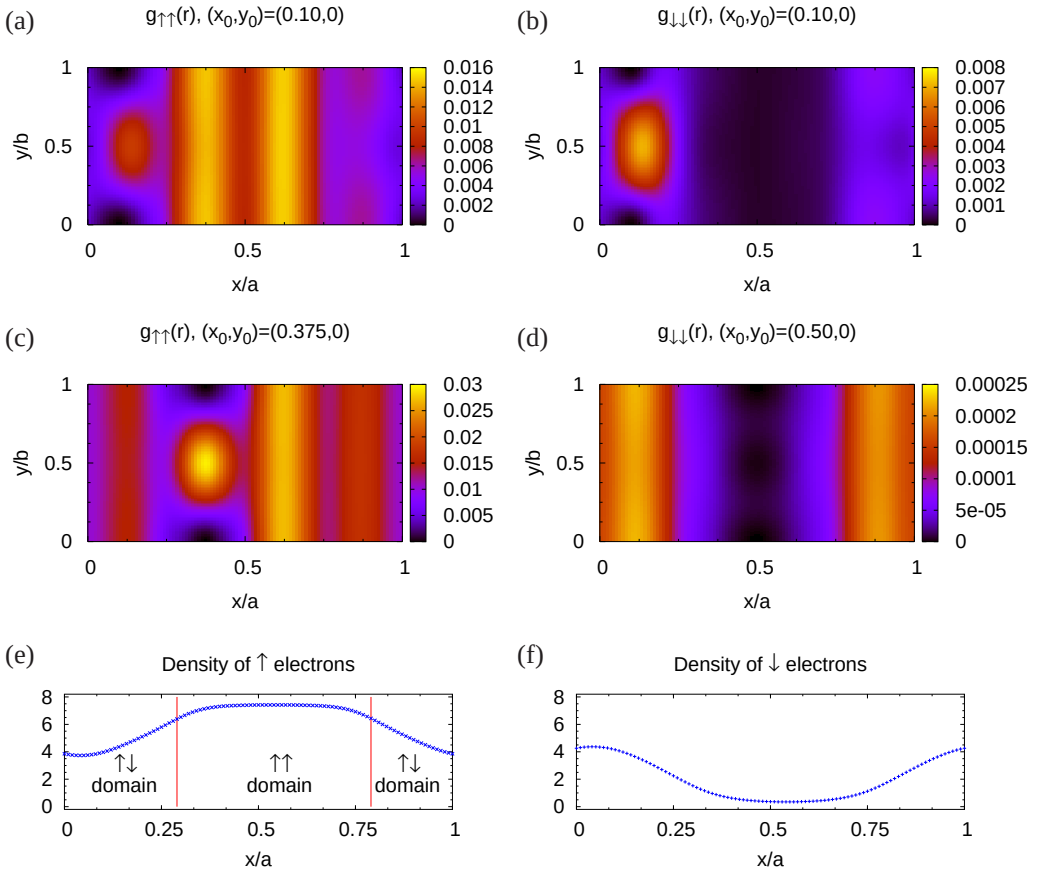

Fig. 69: Half-polarized state with intermediate magnetic inhomogeneity ('rectangular wave', $E_{MI} = 0.004$), non-averaged density-density correlation functions.

Also note that a spatially fixed inhomogeneity couples the relative and center-of-mass (CM) coordinates. At filling $\nu = 2/3$ there are three possible CM states on a torus, which however remain mutually decoupled owing to the high symmetry of the inhomogeneity. The chosen sector $J = 0$ corresponds to a combination of $k_y^r = 0$ sector and the one CM state, which leads to the lowest energy. Differences to other CM states are, however, not too large.

3.4 Summary of studies on the inhomogeneous systems

Perhaps the most important conclusion of this Chapter is that the two incompressible ground states at $\nu = 2/3$, the polarized and the singlet one, alone are not enough to create a state with 'domains', i.e. regions of polarization zero, corresponding to $S_z = 0$, existing side-by-side with regions of polarization one. We have demonstrated this in Subsection 3.1. When a 'domain-inducing' magnetic inhomogeneity is applied, the singlet ground state is more strongly affected than states near the transition. This claim remained true for different types of magnetic inhomogeneities, for different quantities used to detect the domains (apart from the polarization, also for $S_z(x)$, $S_x(x)$, etc.) and also for non-zero temperature.

Different conclusions apply when more than just the polarized and the singlet ground states are present in the low-energy sector. We have demonstrated, that near the transition, the gap could actually close in several different situations. In the present study, this happens for very strong magnetic inhomogeneities

(Subsect. 3.1.3), for systems with an elongated elementary cell (Sect. 3.3) and for short-range interacting systems (Sect. 3.2). The states which closed the gap always belong to an intermediate value of spin, most prominent are those with $S = 1$ and $S = 2$ and since we considered only eight-electron systems, the latter value of spin corresponds to the half-polarized sector $S = N_e/4$. These states are considerably softer against magnetic inhomogeneities than the incompressible singlet and polarized states. On one hand, this fact follows from a small level spacing in the low energy sector when the gap closes. However, the magnetic inhomogeneities were also found to have large (~ 0.1) matrix elements between most of the low lying states.

The states with the strongest tendency to form domains i.e. the 'softest' states, were found in systems with Coulomb interaction and an elongated elementary cell. Near the transition, even a moderately strong magnetic inhomogeneity (weaker than the incompressibility gap) was enough to make the polarization approach the values corresponding to the singlet and polarized states inside the domains. For these domain states, we have investigated the 'inside' of the domains by means of non-averaged correlation functions, Subsect. 3.3.3. We could not yet confirm that the domains comprise of an incompressible liquid but this system defintely deserves a more detailed study. Especially in this case, a comparison with larger systems would be very helpful.

4 Conclusions

Fractional quantum Hall systems at filling factors $\nu = 2/3$ and $2/5$ have been studied numerically by means of exact diagonalization techniques on a torus. In both systems, the existence of two different ground states is well established: one is fully spin polarized, another is a spin singlet and they are both strongly correlated. All four states can be visualised as composite fermion systems at integer filling factor ($\nu_{CF} = 2$). A transition between these two ground states can be induced by changing the Zeeman energy while keeping the filling factor constant, Chapter 3.

At the beginning of Chapter 2, we investigated the polarized and the singlet incompressible ground states in terms of their density-density correlation functions. First, we highlighted the fact that – even if these states were *exactly* described by some composite fermion model – the inner structures of the ground states at $\nu = 2/3$ and $2/5$ differ strongly from the inner structure of a state comprising of two fully occupied Landau levels. In other words, in a composite-fermion state (e.g. $\nu_{CF} = 2$), the correlations between the *electrons* are different than in a corresponding electronic state ($\nu = 2$). A more important result is, however, that the electronic correlations differ strongly also between the $\nu = 2/3$ and $2/5$ states themselves. This is surprising, since both filling factors map to the same filling factor of composite fermions ($\nu_{CF} = 2$) and only the orientation of the effective field is different. Study of the correlation functions allowed to suggest a new interpretation of the singlet $\nu = 2/3$ ground state. The electrons move along in pairs of opposite spins and the pairs form a state equivalent to a fully occupied lowest Landau level. This conclusion does *not* apply to the $\nu = 2/5$ singlet ground state.

The central focus of the present work was on the low-energy states occurring near the transition between the singlet and the polarized ground states. Some experimental results indicate that another ground state distinct from the two ground states already mentioned could exist near the transition [46]. In Sections 3.4 and 2.2 we found several arguments in favour of a half-polarized state ($S = N_e/4$) becoming the absolute ground state in a narrow range of the magnetic field. The systems available to exact diagonalization were however too small to allow for an unswerving prediction. Two candidates for the half-polarized ground state were identified. In Section 2.2 we concentrated on the 'isotropic candidate'. A study of its inner structure (correlation functions) combined with an investigation of the response to probing magnetic inhomogeneities (Sect. 2.3) produced results resembling both the singlet and polarized incompressible ground state. A hypothesis that both these states coexist within the half-polarized state has been presented.

Calculations with elongated rectangular elementary cells (Sect. 2.4) suggested another candidate for the half-polarized ground state: a spin-density wave along the longer side of the elementary cell. A comparison between two systems of different size indicated that this state has the shortest period allowed by the finite size of the considered system (e.g. one third of the length of the cell for a state which contains three minority spins). Based on the present calculations it is not possible to decide which of the two candidates (if any) evolves into the ground state of an infinite system.

At $\nu = 2/5$, no obvious analogue to the half-polarized state at $\nu = 2/3$ was found.

Employing magnetic inhomogeneities to enforce domains of different spin polarization near the transition at $\nu = 2/3$ (Chapter 3) we found that no signs of domain formation occur unless the energy gap closes. The loss of incompressibility could however still be compatible with the experimental observation of a plateau of polarization one half during the transition. It is enough if there are many states with $S = N_e/4$ and no (or only few) states with other values of S in the low-energy sector (Sect. 3.2).

The 'best' candidates for domain states were found to appear in systems with an elongated rectangular cell. The fundamental idea here was that the elementary cell with aspect ratio $2 : 1$ is divided by the inhomogeneity into two square parts which could be more convenient for the formation of isotropic states (the singlet and the polarized incompressible liquid). Examination of the domain state however showed that the inside of the domains does not resemble the incompressible ground states at $\nu = 2/3$. Nevertheless, a more detailed study is necessary here, since systems with aspect ratio far from unity can suffer more from finite size effects than what was demonstrated in Sect. 2.1.

At the very end, I would like to acknowledge Daniela Pfannkuche for her support during my PhD studies and many fruitful discussions, Benjamin Krüger, Philip von Ende and Ondřej Čertík for some of the calculations presented here and Matti Manninen for his hospitality in the period when this work was being completed. Finally, I am much obliged to a group of my colleaugues who carefully read the very long manuscript and helped to substantially improve both its contents and language: Frank Hellmuth, Rob Knapik, Katrin Malessa, Christian Müller, Michael Prouza, Arek Wójs and Jan Zemen.

References

[1] Going once around an s-fold vortex gives phase $2\pi s$. Exchange of two particles corresponds to one half of such a loop (for $\psi(r_1, r_2) \to \psi(r_2, r_1)$ corresponds to $\psi_{rel}(\varrho) \to \psi_{rel}(-\varrho)$ with $\varrho = r_1 - r_2$ in the relative part of the WF; $\varrho \to -\varrho$ is half the way of going around zero). Thus exchanging two particles with s attached vortices, the wavefunction acquires phase πs. For two *fermions* with s attached vortices, it is $\pi(s+1)$. Thus the wavefunction changes sign at exchange of two particles when s is even and does not change the sign when s is odd.

[2] The magnetic field described by the vector potential in (17) is proportional to electron density, $\Psi^\dagger(\boldsymbol{r}_1)\Psi(\boldsymbol{r}_1)$. In other words: the magnetic field felt by an electron at $\boldsymbol{r}$ is only non-zero if $\boldsymbol{r} = \boldsymbol{r}_1$, or, an electron at $\boldsymbol{r}$ sees magnetic field consisting of delta–functions located at positions of other electrons. However, these points in space are inaccessible to the electron by virtue of the Pauli principle.

[3] In Fig. 41b, energies of low–lying states at $\nu = 2/3$ are plotted against the aspect ratio $a : b$, assuming the short–range interaction (13). The ground state at $\nu = 1/3$ has zero energy (cf. Subsec. 1.3.3) for any value of $a : b$ and hence the energy of the $\nu = 2/3$ ground state is equal to the energy of the completely filled lowest Landau level, E_f, multiplied by $(m - 2n)/m$. The energy E_f is not completely independent on $a : b$. As long as the $a \times b$ rectangle is still large enough to be a good description of a $\nu = 1$ 2DEG, E_f is constant. As soon as b ($< a$) becomes too small (a reliable indication is that the density of the state $|1\rangle$ becomes markedly inhomogeneous) E_f starts to change (this is the case for $a : b > 4$ in Fig. 41b).

[4] Consider the action of S^- (the lowering operator for the z-component of spin) on the $\nu = 2$ (or $\nu_{CF} = 2$) ground state $|\Psi, S_z = 0\rangle$ at zero Zeeman energy ($0 \uparrow$ and $0 \downarrow$ LLs are filled). On one hand, the state $S^-|\Psi, S_z = 0\rangle$ may not contain any particles in higher LLs (up to Zeeman energy, it should have the same energy as $|\Psi, S_z = 0\rangle$). On the other hand, there is no room for an extra spin down in the lowest LL which is completely filled and therefore flipping a spin $\uparrow \to \downarrow$ (as contained in S^-) must annihilate the state. Finally, $S^-|\Psi, S_z = 0\rangle = 0$ implies that $|\Psi, S_z = 0\rangle$ is a $S^2 = 0$ state.

[5] If we were able to distinguish two particles in a state described by a single Slater determinant, even such a state would also be entangled: consider a state $\Psi(1,2) = \psi_L(1)\psi_R(2) - \psi_R(1)\psi_L(2)$ and say the states L and R are localized on the left and on the right, respectively. There is an uncertainity in whether it is the particle 1 or the particle 2 which is on the right. If we measure one particle on the right, we automatically know that it is the *other* particle which is on the left. Owing to the indistinguishability of indentical particles, however, we cannot say whether it was the particle 1 or the particle 2 which we have just caught on the right. If the particles 1 and 2 have different spin, the indistinguishability requirement is lifted and the state Ψ is entangled. In that case, Ψ is the spin–singlet state.

[6] Several lowest of these polynomials are: $L_0^1(x) = 1$, $L_1^1(x) = 2 - x$, $L_2^1(x) = \frac{1}{2}(6 - 6x + x^2)$, $L_3^1(x) = \frac{1}{6}(24 - 36x + 12x^2 - x^3)$.

[7] In fact, there are *some* analytical results. Very appealing schemes how to evaluate energy and correlation functions were suggested by Girvin [25] Takano and Isihara [72]. Interesting extension of the former work was presented by Görbig (Subsec. 1.2.2. in [28]). All these schemes however present closed formulae neither for energy nor for correlation functions.

[8] If we completely fill the lowest Landau level with spin up electrons and with spin down electrons (imagine $\nu = 2$ and zero Zeeman energy), then spin up and spin down electrons are uncorrelated, $g_{\uparrow\downarrow}(r) = 1$. It is *not* a claim of composite fermion theories that the same is true if we do the same with CF Landau levels. The attachment of flux quanta introduces correlations between the originally uncorrelated $(n = 0, \uparrow)$ and $(n = 0, \downarrow)$ levels: spin up CFs do not feel the spin down CFs (owing to LL mixing neglect) but they do feel fluxes attached to the spin down CFs.

[9] M. Allesch, E. Schwegler, F. Gygi, and G. Galli. *cond-mat*, page 0401267, 2004.
[10] V.M. Apalkov, T. Chakraborty, P. Pietiläinen, and K. Niemelä. *Phys. Rev. Lett.*, 86:1311, 2001.
[11] G. Bertotti. *Hysteresis in magnetism : for physicists, materials scientists and engineers*. Acad. Press, San Diego, California, 1998.
[12] L. Bonsall and A. Maradudin. *Phys. Rev. B.*, 15:1959, 1977.
[13] T. Chakraborty. *Adv. Phys.*, 49:959, 2000.
[14] T. Chakraborty and Pietiläinen, P. *The Quantum Hall Effects*. Springer, Berlin, second edition, 1995.
[15] H. Cho, J.B. Young, W. Kang, K.L. Campman, A.C. Gossard, M. Bichler, and W. Wegscheider. *Phys. Rev. Lett.*, 81:2522, 1998.
[16] R.G. Clark, S.R. Haynes, A.M. Suckling, J.R. Mallett, P.A. Wright, J.J. Harris, and C.T. Foxon. *Phys. Rev. Lett.*, 62:1536, 1989.
[17] S. Das Sarma and A. Pinczuk. *Perspectives in Quantum Hall Effects*. Wiley, New York, 1997.
[18] E.P. de Poortere, E. Tutuc, S.J. Papadakis, and M. Shayegan. *Science*, 290:1546, 2000.
[19] W. Dietsche and S. Kronmüller. *Physica E*, 10:71, 2001.
[20] R.B. Dunford, M.R. Gates, V.W. Rampton, C.J. Mellor, O. Stern, W. Dietsche, W. Wegscheider, and M. Bichler. Absence of the huge longitudinal resistance maxima in surface acoustic wave measurements of narrow quantum wells. In *Proceedings of the 26th International Conference on the Physics of Semiconductors*, page P143, Edinburgh, UK, July 2002. IOP.
[21] J.P. Eisenstein, H.L. Stormer, L. Pfeiffer, and K.W. West. *Phys. Rev. Lett.*, 62:1540, 1989.
[22] J. Eom, H. Cho, W. Kang, K.L. Campman, A.C. Gossard, M. Bichler, and W. Wegscheider. *Science*, 289:2320, 2000.
[23] G. Fano, F. Ortolani, and E. Colombo. *Phys. Rev. B.*, 34:2670, 1986.
[24] N. Freytag, Y. Tokunaga, M. Horvatić, C. Berthier, M. Shayegan, and L.P. Lévy. *Phys. Rev. Lett.*, 87:136801, 2001.
[25] S.M. Girvin. *Phys. Rev. B.*, 30:558, 1984.
[26] S.M. Girvin. *cond-mat*, page 9907002, 1999.
[27] S.M. Girvin, A.H. MacDonald, and P.M. Platzman. *Phys. Rev. Lett.*, 54(6):581, 1985.
[28] M.O. Goerbig. *Etude théorique des phases de densité inhomogeène dans les systeèmes à effet Hall quantique*. PhD thesis, Université de Fribourg, Switzerland, 2004.
[29] I.S. Gradshteyn and I.M. Ryzhik. *Tables of Integrals, Series, and Products*. Academic Press, New York, any edition, 1980.
[30] F.D.M. Haldane. *Phys. Rev. Lett.*, 51:605, 1983.
[31] F.D.M. Haldane. *Phys. Rev. Lett.*, 55(20):2095, 1985.
[32] F.D.M. Haldane and E.H. Rezayi. *Phys. Rev. B.*, 31:2529R, 1985.
[33] F.D.M. Haldane and E.H. Rezayi. *Phys. Rev. Lett.*, 54:237, 1985.
[34] F.D.M. Haldane and E.H. Rezayi. *Phys. Rev. Lett.*, 60:956, 1988.

[35] B.I. Halperin. *Helv. Phys. Acta*, 56:75, 1983.
[36] K. Hashimoto, K. Muraki, T. Saku, and Y. Hirayama. *Phys. Rev. Lett.*, 88:176601, 2002.
[37] M. Helias. Quasihole tunneling in the fractional quantum hall regime. Master's thesis, University of Hamburg, Germany, 2003.
[38] J.K. Jain. *Phys. Rev. Lett.*, 63:199, 1989.
[39] J.K. Jain. *Science*, 266:1199, 1994.
[40] T. Jungwirth and A.H. MacDonald. *Phys. Rev. B.*, 63:035305, 2000.
[41] T. Jungwirth and A.H. MacDonald. *Phys. Rev. Lett.*, 87:216801, 2001.
[42] R.K. Kamilla, J.K. Jain, and S.M. Girvin. *Phys. Rev. B.*, 56:12411, 1997.
[43] S. Kraus, O. Stern, J.G.S. Lok, W. Dietsche, K. von Klitzing, M. Bichler, D. Schuh, and W. Wegscheider. *Phys. Rev. Lett.*, 89:266801, 2002.
[44] S. Kronmüller, W. Dietsche, K. von Klitzing, G. Denninger, W. Wegscheider, and M. Bichler. *Phys. Rev. Lett.*, 82:4070, 1999.
[45] S. Kronmüller, W. Dietsche, J. Weis, K. von Klitzing, W. Wegscheider, and M. Bichler. *Phys. Rev. Lett.*, 81:2526, 1998.
[46] I.V. Kukushkin, K.v. Klitzing, and K. Eberl. *Phys. Rev. Lett.*, 82:3665, 1999.
[47] P.K. Lam and S.M. Girvin. *Phys. Rev. B.*, 30:473, 1984.
[48] R. Laughlin. *Phys. Rev. Lett.*, 50:1395, 1983.
[49] R. Laughlin. *Phys. Rev. B.*, 27:3383, 1983.
[50] D.R. Leadley, R.J. Nicholas, D.K. Maude, A.N. Utjuzh, J.C. Portal, J.J. Harris, and C.T. Foxon. *Phys. Rev. Lett.*, 79:4246, 1997.
[51] E. Mariani, N. Magnoli, F. Napoli, M. Sassetti, and B. Kramer. *Phys. Rev. B.*, 66:241303, 2002.
[52] R.H. Morf, N. d'Ambrumenil, and S. Das Sarma. *Phys. Rev. B.*, 66:075408, 2002.
[53] Ch. Müller. *Disorder and vortex detachment in fractional quantum Hall liquids*. PhD thesis, University of Hamburg, Germany, 2005.
[54] G. Murthy. *Phys. Rev. Lett.*, 84:350, 2000.
[55] G. Murthy. *Phys. Rev. Lett.*, 87:179701, 2001. comment.
[56] G. Murthy and R. Shankar. *Rev. Mod. Phys.*, 75:1101, 2003.
[57] K. Niemelä, P. Pietiläinen, and T. Chakraborty. *Physica B*, 284:1717, 2000.
[58] K. Nomura. *Various broken symmetries in two–component quantum Hall systems*. PhD thesis, Department of Basic Science, University of Tokyo, Japan, 2003.
[59] W. Pan, H.L. Stormer, D.C. Tsui, L.N. Pfeiffer, K.W. Baldwin, and K.W. West. *Phys. Rev. Lett.*, 90:016801, 2003.
[60] R. E. Prange and S. M. Girvin. *The Quantum Hall Effect*. Springer, Berlin, 1987.
[61] E.H. Rezayi and F.D.M. Haldane. *Phys. Rev. B.*, 32:6924, 1985.
[62] E.H. Rezayi and F.D.M. Haldane. *Phys. Rev. B.*, 50:17199, 1994.
[63] E.H. Rezayi, T. Jungwirth, A.H. MacDonald, and F.D.M. Haldane. *Phys. Rev. B.*, 67:201305(R), 2003.
[64] U. Schollwöck. *cond-mat*, page 0409292, 2004.
[65] U. Schollwöck. *Rev. Mod. Phys.*, 77:259, 2005.
[66] N. Shibata and D. Yoshioka. *Phys. Rev. Lett.*, 86:5755, 2001.
[67] N. Shibata and D. Yoshioka. *J. Phys. Soc. Jpn.*, 72:664, 2003.
[68] N. Shibata and D. Yoshioka. *cond-mat*, page 0308122, 2003.
[69] N. Shibata and D. Yoshioka. *cond-mat*, page 0403493, 2004.
[70] J.H. Smet, R.A. Deutschmann, F. Ertl, W. Wegscheider, G. Abstreiter, and K. von Klitzing. *Nature*, 415:281, 2002.
[71] J.H. Smet, R.A. Deutschmann, W. Wegscheider, G. Abstreiter, and K. von Klitzing. *Phys. Rev. Lett.*, 86:2412, 2001.
[72] K. Takano and A. Isihara. *Phys. Rev. B.*, 34:1399, 1986.
[73] R. Tao and F.D.M. Haldane. *Phys. Rev. B.*, 33:3844, 1986.
[74] S.A. Trugman and S. Kivelson. *Phys. Rev. B.*, 31:5280, 1985.
[75] A. Wójs and J.J. Quinn. *Phil. Mag. B*, 80:1405, 2000.
[76] A. Wójs and J.J. Quinn. *Phys. Rev. B.*, 66:045323, 2002.
[77] X.G. Wu, G. Dev, and J.K. Jain. *Phys. Rev. B.*, 71:153, 1993.
[78] D. Yoshioka. *Phys. Rev. B.*, 29:6833, 1984.
[79] D. Yoshioka. *The Quantum Hall Effect*. Springer, Berlin, 2002.
[80] D. Yoshioka, B.I. Halperin, and P.A. Lee. *Phys. Rev. Lett.*, 50:1219, 1983.
[81] D. Yoshioka, B.I. Halperin, and P.A. Lee. *Surf. Sci.*, 142:155, 1984.
[82] D. Yoshioka and N. Shibata. *Physica E*, 12:43, 2002.
[83] J. Zak. *Phys. Rev.*, 134:A1602, 1964.
[84] J. Zak. *Phys. Rev.*, 134:A1607, 1964.
[85] F.C. Zhang and T. Chakraborty. *Phys. Rev. B.*, 30:7320, 1984.
[86] F.C. Zhang, V.Z. Vulovic, Y. Guo, and S. Das Sarma. *Phys. Rev. B.*, 32:6920, 1985.

Spin in fractional quantum Hall systems

Dissertation
zur Erlangung des Doktorgrades
des Fachbereichs Physik
der Universität Hamburg

vorgelegt von
Karel Výborný
aus Kolín (Tschechien)

Hamburg
2005

Gutachter der Dissertation:	Prof. Dr. D. Pfannkuche
Gutachter der Disputation:	Prof. Dr. D. Pfannkuche Prof. Dr. S. Reimann
Datum der Disputation:	23.05.2005
Vorsitzender des Prüfungsausschusses:	
Vorsitzender des Promotionsausschusses:	Prof. Dr. G. Huber
Dekan des Fachbereichs Physik:	Prof. Dr. G. Huber